DOCTORAL THESIS

Agata Godula - Jopek

WETTABILITY OF SOME SOLIDS BY BINARY AND TERNARY ALKALI CARBONATE MOLTEN SYSTEMS

Doctoral Thesis

Agata Godula-Jopek

Promotor prof. dr hab. Leszek Suski

Institute of Physical Chemistry
of the Polish Academy of Sciences
Department of Molten Salts

Kraków 1999

The author is indebted to Professor Leszek Suski for his guidance in understanding some aspects of the work as well as for valuable discussions, criticism and for the formal corrections during the preparation of the manuscript.

The technical assistance of Mr. Jerzy Kołacz and of Mr. Grzegorz Mordarski during the experimental part of this work is gratefully acknowledged.

Special thanks are due to my husband, Edward Jopek, for his valuable help in designing the experimental set-up and for the moral support over all through.

CONTENTS

Introductory part

The presentation of the original results

INTRODUCTORY PART

I. Preface

This thesis in general is devoted to some problems of wettability properties of the molten carbonate fuel cell electrode materials by the molten alkali carbonate eutectics, used as an electrolyte in the Molten Carbonate Fuel Cell (MCFC). The results of investigations presented in this text have been a subject of three publications, *i.e*:

1. A. Godula-Jopek and L. Suski, *Wetting Behavior of Molten Alkali Carbonates on Au Interface under Various Gas Atmospheres. (Published in Polish J. Chem., 72, 1045-1053, 1998)*,
2. L. Suski, A. Godula-Jopek and J. Obłąkowski, *Wetting of Ni and NiO by Alternative Molten Carbonate Fuel Cell Electrolytes. I. Influence of Gas Atmosphere. (J. Electrochem. Soc. in print, Re: JES Ms. No. 98-12-066)*,
3. A. Godula-Jopek and L. Suski, *Wetting of Ni and NiO by Alternative Molten Carbonate Fuel Cell Electrolytes. II. Influence of the Electrode Overpotential. (J. Electrochem. Soc. submitted to publication, Re: JES Ms. No. 99-02-100)*.

The results of this work have also been presented during the conference in Tokyo and published in the conference materials as L. Suski and A. Godula-Jopek, *Wettability of Ni and NiO by Molten Li/Na, Li/K, Li/Na/K Carbonates Under Various Atmospheres*, International Open Seminar, Design Optimization and Advanced Material Development for Molten Carbonate Fuel Cell, MCFC Research Association, 18th March, 1999, Tokyo, Japan as well as during invited lecture in Delft as A. Godula-Jopek, *Wettability of Some Solids by Molten Alkali Carbonate Melts*, presentation of results, 9-11 Dec., 1998, Delft, the Netherlands.

In the text there is a the review of the literature data including the wettability properties of MCFC electrode materials (*i. a.* at Au as reference) by the molten alkali carbonates. In order to make more comprehensive the review of the wettability phenomena in molten carbonates, the respective literature data for other solids are also comprised, although they are not strictly related to MCFC.

This text is divided into two parts - the first, embracing the introductory part and the second, regarding the presentation of the original results.

II. The fuel cell - principles of operation, technology and fields of operation

A fuel cell is an electrochemical device, consisting in a system of an anode, cathode and an electrolyte, which continuously convert the energy of chemical reactions into the electrical one. The process is not limited by the Carnot cycle and consequently, the Carnot limit for the efficiency does not apply, so practically efficiences up to 65% are possible. The reactants are fed to the cell only when the generation of electric power is needed. Fuel and oxidant are supplied continuously from outside to the fuel cell, so it may theoretically produce electrical energy as long as the fuel and oxidant are fed to the electrodes, where the reactions take place. In order to complete the electrical circuit in the fuel cell, the charges must be transported between electrodes. In the fuel cell the electrodes are gas-diffusion ones, only partially filled with the electrolyte. They are porous for making as large as possible the contact area at three-phase boundary layer at the electrode / electrolyte / reactant interface, where the respective reactions take place. To maximize the power *per unit* mass of an electrochemical cell, the electronic and electrolytic resistances of the cell must be minimalized. Since fused salts have lower electrolytic resistances in comparison with aqueous solutions, the high temperature electrochemical cells are of special interest for practical applications.

Fuel cell technology could possibly alleviate the conflict between the increasing demand for mobility and, at the same time, the desire to reduce energy consumption. In comparison to conventional engines, fuel cells have higher efficiences, lower energy requirements and loss CO_2 emissions. Since, there is no combustion and no direct contact between the fuel and the oxygen containing gas, the emission of NO_x, SO_x, CO and others, is practically zero. Fuel cells have good part load behavior which is also an advantage compared to combustion. Using fuel cells, heat rejected in the process can be used, for example, for combined heat and power generation. The co-generation of heat and power in co-operation with the fuel cells ability of a high efficiency for wide range of output power, makes a very suitable for the on-site production.

Fuel cells offer very attractive features for in-city power generation. Some of the features include:

- high efficiency at full and partial load in small sizes,
- environmental attractiveness including low level of pollutants, audible noise and water usage,
- modularity, so incremental electrical load growth can be met locally,

- electricity & heat co-generation,
- operating flexibility, including rapid transient response and unattended operation,
- practical possibility of obtaining efficiencies of the electrical power production up to 65%,
- waste heat can be used for space heating, steam and hot water

There are five various categories of fuel cell:

- alkaline fuel cell, (**AFC**),
- proton-exhange membrane fuel cell, (**PEM-FC**),
- phosphoric acid fuel cell, (**PAFC**),
- molten carbonate fuel cell, (**MCFC**),
- solid oxide fuel cell, (**SOFC**).

More than 20 years have passed since the first well known success of a practical application of fuel cells during the space flights of the Gemini (1 kW PAFC) and Apollo (1.5 kW AFC) mission. More recently, 7 kW AFC was used in the Space Shuttle Orbiter. In the R&D of ACF for a long time has been involved Siemens AG, Germany [1]. It has developed a modular 7 kW / 20 kW fuel cell power plant initially designed for under-sea propulsion.

The PAFC is close to a commercial stage for co-generation systems. The major advantage here is the high state of development. In Japan, about 100 on-site PAFC plants have now been successfully operated for commercialization. Most of them have been operated at 50 to 200 kW power output under ambient pressure, some of them more than 30 000 hours. Large-scale PAFC demonstration plants of more than 1 MW are now under operation in Japan and Italy. An 11 MW PAFC power plant, constructed in 1993 at Goi Power Station, Tokyo Electric Power Company, is the largest fuel cell in the world [2-4].

The high temperatures of fuel cells such as MCFC (650°C) and SOFC (850-1000°C) are predominantly used for both the centralized utility power generation applications. The high operating temperatures of these fuel cells allow them to be directly used with different fuels, *e.g.* natural gas. R&D on MCFC technology was initiated in MELCO (Mitsubishi Electric Corporation) in 1981 at the Central Research Laboratory to aim at realization of its highly efficient energy conversion potential of various fuel to electricity[5]. MCFC are the most promising type of fuel cell for large scale power production. Its commercial development is also very advanced. 1 MW pilot plant is located in Kawagoe near Nagoya, 2 MW in Santa

Clara, California, smaller generators (to 300 kW) have been tested in USA, Japan, Denmark, Italy and Germany [1,2,6].

In the mid-Seventies Westinghouse Electric Corp. started work on SOFC and continued. 300 W and 3 kW field units are built today, also in connection with Japanese manufacturers[1,4]. The SOFC has the same potential for efficiency as the MCFC from higher operating temperature around 1000°C. Therefore its application is basically similar to and competitive with the MCFC [1,2-4].

The PEM-FC, low temperature fuel cell with solid electrolyte, has a high power density potential. In addition, these cells operate with air. For these reasons PEM-FC are best suited for vehicle applications. They shares several attributes, like low or even zero tailpipe emissions, low noise, modularity and reasonable shape flexibility. Lately Ford, GM, General Electric and other companies are interested in PEM fuel cell technology development for transport applications [7-9].

II.1. The Molten Carbonate Fuel Cell

The MCFC should be favored system for dispersed use in co-generation applications in the industrial, commercial and domestic sectors, in which its waste heat can be used for space heating, steam and hot water. The fuel cell for stationary application promises to be great innovator in this regard. It can be built in units, whose chemical and accoustic emissions are totally innocuous, therefore it can be used for dispersed applications, where it waste heat can be used directly. Of all the fuel cell systems which appear today, the MCFC may have the widest application. Its electrical efficiency is higher than that of any other system operating on a hydrocarbon fuel, such as natural gas. A lower current density internal reforming version could have 25% electrical efficiency, though available high-quality waste heat might them only be 25%.

The MCFC operates at working temperature of *ca* 650° at which the carbonate mixture forms a highly conductive molten salts and therefore are considered as a high-temperature fuel cell electrolyte. A mixture of lithium and potassium or, alternatively, lithium and sodium carbonates is retained in a porous, ceramix matrix, made from $LiAlO_2$. In the state-of-the-art fuel cell, the anode is made from porous nickel and the cathode from porous nickel oxide. In order to avoid sintering and creep of the nickel anode, its material is often alloyed with few percent, *ca* 10%, of aluminium or chromium. The cathode mounted in the MCFC as a porous

nickel oxide electrode doped with lithium. In order to distribute electrolyte effectively, the porosity of the different components have to match each other. This is important for achieving high ionic conductivity and to prevent gas cross-over [10]. A schematic representation of the Molten Carbonate Fuel Cell is presented in Fig.1.

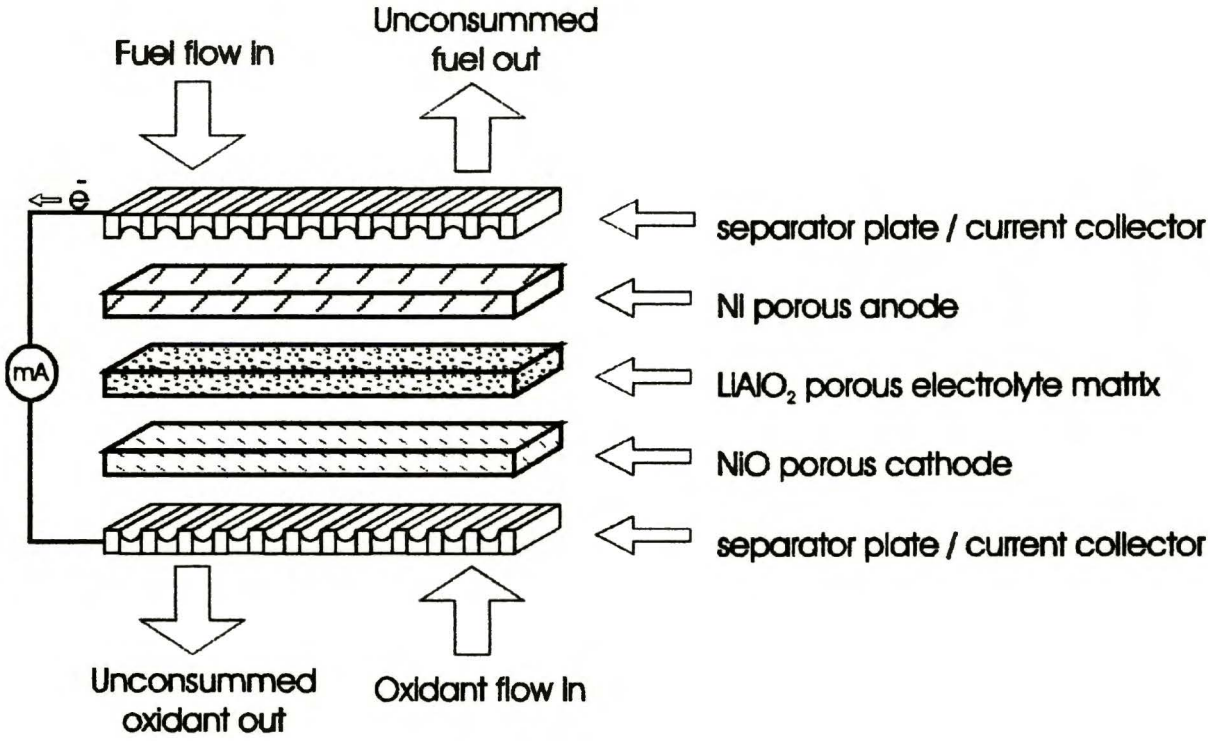

Fig.1. Schematic view of the Molten Carbonate Fuel Cell.

The electrochemical reactions, which take place in the cell are as follows:

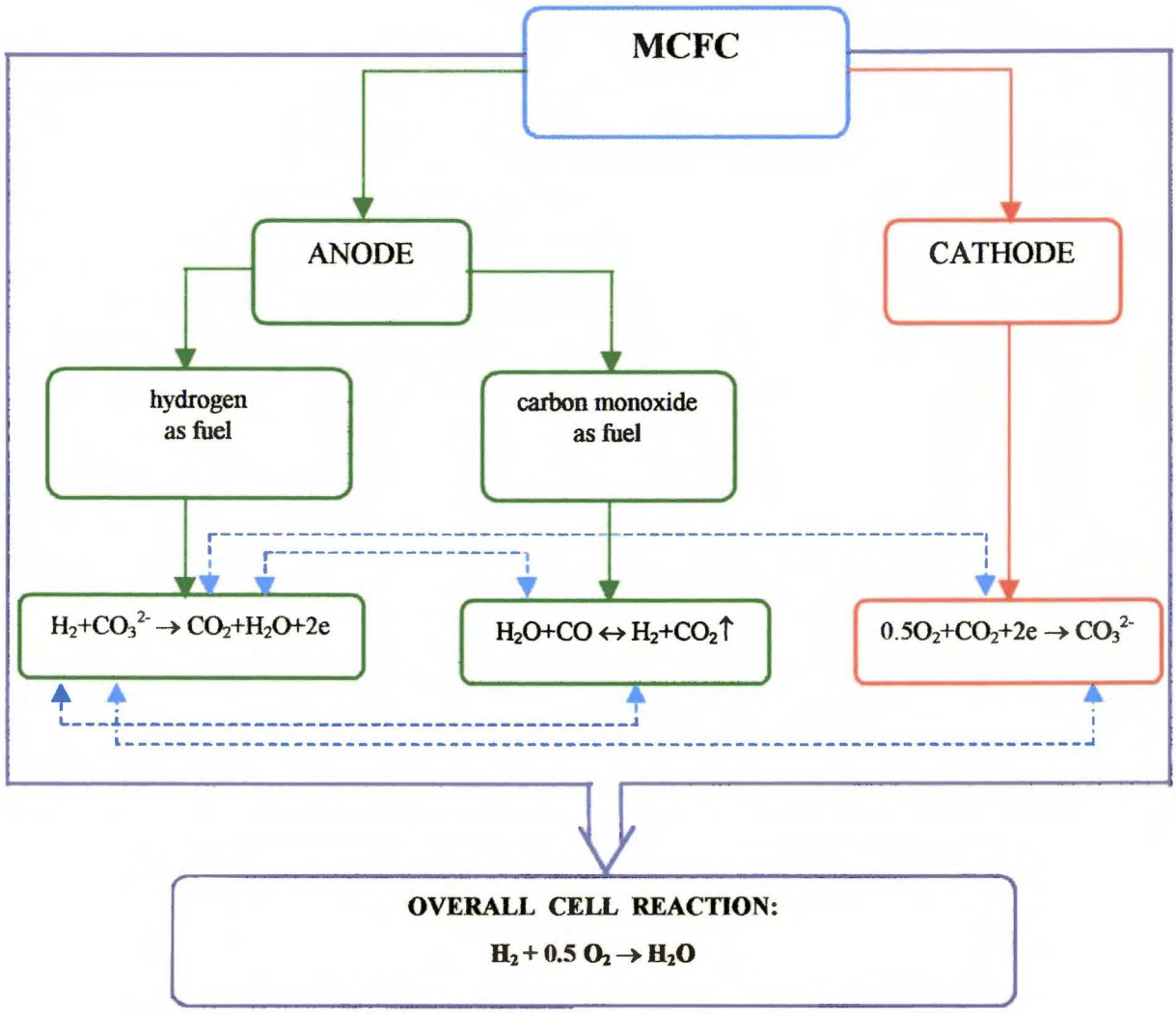

Fig.2. Scheme of the electrochemical reactions occuring at the MCFC anode and cathode and overall MCFC balance-reaction.

II.2. Role of the surface phenomena in MCFC

Capillary phenomena, *i.e.* wettability and surface tension at metals or oxides / molten electrolyte interface, under respectively gas atmospheres, are very important parameters if one wants to optimize the molten carbonate fuel cell. The carbonate melt penetrates into the porous structure of the electrodes and make contact with the solid over large areas. The reactant is a gas and the reaction takes mainly place near there-phase boundary layer at the electrode / electrolyte / reactant interface. If flat electrodes would be used in the cell, the surface area of the electro-catalyst might be too small or the fuel cell would become unreasonably large. To overcome such a problem, that the surface area of the catalyst is too small, porous electrodes were developed, so that the surface area increased without increasing the size of the electrodes. The porosity has to secure the complete fulfillment of the electrolytic matrix and a partial of the electrodes and it cannot be changed during the fuel cell work. A thin film covers the electrodes, when the molten carbonates effectively wet the solid plates. For the short path of the diffusion, the whole filmed surface will contribute to the overall current. The efficiency of the fuel cell will increase due to a higher current density. The wetting of electrodes by molten alkali carbonates and their structure are also an important parameter for describing the electrolyte distribution between porous electrodes and the porous, ceramic matrix containing the electrolyte. After my study has been completed, I have received a preprint of work by M. Kawase, Y. Mugikura and T. Watanabe " *An electrolyte distribution model accounting for the electrode wetting by molten carbonate in the molten carbonate fuel cell* ", where the authors have developed an electrolyte distribution model to account the wettability and the pore distribution within the electrode. They have calculated the electrolyte distribution by taking into account:

- the wettability of the electrode,
- the temperature distribution,
- the effect of the pore distribution of the electrode.

It is found that the difference between the electrolyte fill ignoring and accounting for the wettability is in the range from 6 to 18%. This difference affects the cell performance and the electrolyte loss. It is also found that the electrolyte fill is lower at the fuel gas inlet side and is increased along the fuel gas stream.

III. Some fundamental aspects of the solid/liquid contact angle phenomena

III.1. Basic principles of wetting the solids by the liquids

The wetting property of a given liquid consists in the liquid drop ability to have various stable contact angles at various solid surfaces, so the contact angle is a common and useful measure of wettability. It gives information about surface energetics, surface roughness and surface heterogeneity. Also it is a sensitive measure of surface contaminations and it controls many technical processes where mass transport is important. A free liquid drop takes the shape which minimizes the free energy of the system. In the absence of gravity, this is equivalent to minimizing the surface area of the drop. The equilibrium drop shape is spherical. When a drop is in contact with either a solid or liquid substrate, it still takes the shape which minimizes the free energy of the system[11]. The contact angle of a liquid drop on a solid surface is the result of a balance between the cohesive forces in the liquid and the adhesive forces between solid and liquid. Basic to the subject of "*wettability*" is Young's concept of the contact angle Θ between a drop of the liquid and a plane solid surface. The contact angle is measured through the liquid from a tangent to the liquid surface at the point of contact with the solid to the plane of the solid surface. In the case where there is no wetting, the contact angle is 180°. In the case of complete wetting the contact angle is 0°. All angles other than 180° or 0° indicate partial wetting. However, some distinction should be made between contact angles that are greater or less than 90°, for contact angles less than 90° will cause a capillary rise and angles greater than 90° will cause a capillary depression[12]. Fig. 3 presents degrees of wetting.

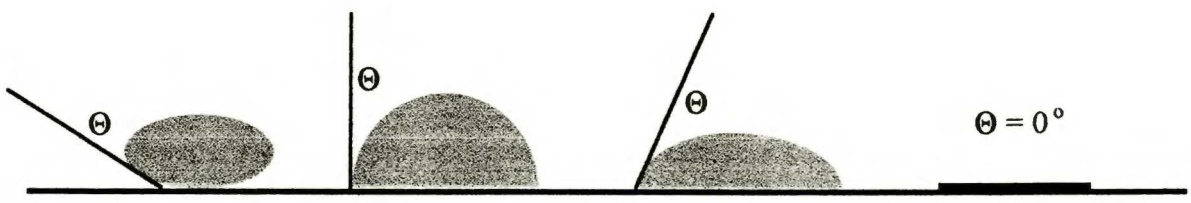

Fig 3. Contact angle illustrating degrees of wetting.

On a homogeneous solid surface contact angle is independent of the volume of the liquid drop as long as the hydrostatic pressure remains a minor factor. Since, the tendency for the liquid to spread increases as Θ decreases, the contact angle is a useful inverse measure of spreadability or wettability.

III.2. Basic thermodynamic relationships

The thermodynamics of the solid/liquid interface is based on two equations, that of Young for the contact angle and of Dupré defining the work of adhesion (W_{SL}). Young described the trigonometric relations between the contact angle and the forces acting on a drop in mechanical equilibrium on a solid surface, as it may be seen in Fig.4.

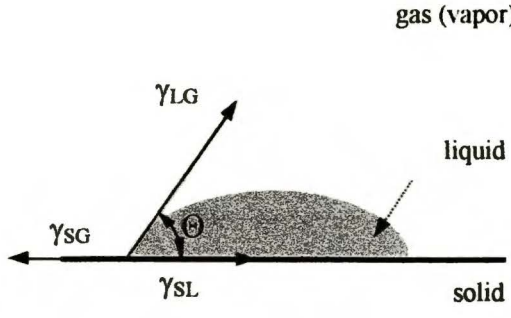

Fig.4. Contact angle between a drop of liquid and a solid surface

The surface free enthalpy (ΔG^s) resulting of a change of solid surface covered by the liquid is [13]

$$\Delta G^s = \Delta A\,(\gamma_{SL} - \gamma_{SG}) + \Delta A\,\gamma_{LG}\cos(\Theta - \Delta\Theta), \qquad \text{(III.2.1)}$$

where : ΔA denotes the change of the solid surface covered by the liquid, γ is the surface tension at the given interface, sl, sg, lg - indexes for solid/liquid, solid/gas, liquid/gas interfaces, respectively, Θ - the angle between the tangent to the liquid surface at the triple phase boundary.

Equilibrium condition requires

$$\lim_{\Delta A \to 0} \frac{\Delta G^s}{\Delta A} = 0, \qquad \text{(III.2.2)}$$

so the relationship between the surface tensions of the solid, the liquid, the solid/liquid interface and the contact angle may be expressed as

$$\gamma_{SL} - \gamma_{SG} + \gamma_{LG}\cos\Theta = 0, \qquad \text{(III.2.3)}$$

or after simple transformation as

$$\gamma_{SG} - \gamma_{SL} = \gamma_{LG}\cos\Theta, \qquad \text{(III.2.4)}$$

This relationship is known as Young's equation.

Several conclusions about wetting result from Young's relationship[14]:

(1), when the contact angle is equal to 90°, the solid surface energy is equal to the interfacial energy,

(2), when the interfacial energy is less than the surface energy of the solid, the contact angle will be less than 90°,

(3), when the interfacial energy is greater than the surface energy of the solid, the contact angle will be greater than 90°,

(4), when $\Theta = 0$, the surface energy of the solid must be equal to or greater than the interfacial energy plus the surface energy of the liquid,

(5), if the contact angle is equal to 180°, the surface energy of the solid must be equal or less than the interfacial plus the liquid surface energy.

According to the Dupré definition of adhesion work (W_{SL}), following relationship is generally accepted

$$W_{SL} = \gamma_{LG} + \gamma_{SG} - \gamma_{SL}, \qquad \text{(III.2.5)}$$

It results from eq. (III.2.4) and (III.2.5) that

$$W_{SL} = \gamma_{LG} (1 + \cos \Theta), \qquad \text{(III.2.6)}$$

The last relationship is usually called the Young- Dupré formula.

This model posesses one serious defect which was first considered by Harkis and Dahlstrom (1930) and by Bangham and Razouk (1937); it neglects the presence on the free solid surface of an adsorbed film of vapor in equilibrium with the saturated vapor pressure p_o of the liquid[15]. This film exerts a spreading pressure π_{SG} which reduces the free surface energy of the solid surface from γ_S to γ_{SG} and is defined by

$$\pi_{SG} = \gamma_S - \gamma_{SG}, \qquad \text{(III.2.7)}$$

where γ_S is the surface tension of the solid against its own vapor, γ_{SG} is the surface tension of the solid in equilibrium with the vapor of the wetting liquid.

In such a case the following equation for W_{SL} is derived

$$W_{SL} = \pi_{SG} + \gamma_{LG} (1 + \cos \Theta), \qquad \text{(III.2.8)}$$

Also, when Θ is the equilibrium contact angle, the equlibrium relation becomes as

$$\gamma_{SG} = \gamma_S - \pi_{SG} = \gamma_{SL} + \gamma_{LG} \cos \Theta, \qquad \text{(III.2.9)}$$

Schrader says[16], that the work of adhesion has generally been identified with the free energy of adhesion. He has shown, that it constitutes the total work of adhesion only under

artificial condition that the sessile drop retains its shape after detaching from the solid surface. Under "real" conditions, the work of adhesion represents only one component of the total free-energy change taking place when drop is separated from, or attached to, a vapor-equilibrated smooth solid surface. An alternative formulation, *the Net Free Energy of Adhesion*, ΔF_N, is defined to describe the reversible work required to separate a sessile drop from a smooth surface (in presence of the vapor of the liquid p_o) to form of a sphere. If the final state of the detached drop could have the same shape as the sessile drop, ΔF_N would reduce to the classical Young- Dupré equation. This restriction, however, requires that the sessile drop separate from the surface without having change its shape, *i.e.* it must exist in the strange form of free spherical section. But, of course, a free drop with its shape is not in mechanical equilibrium. It would seem that the most convenient equilibrium configuration for the sessile drop, when it separates from the surface, would be its equilibrium shape, when free, *i.e.* a sphere. It is presented in Fig.5.

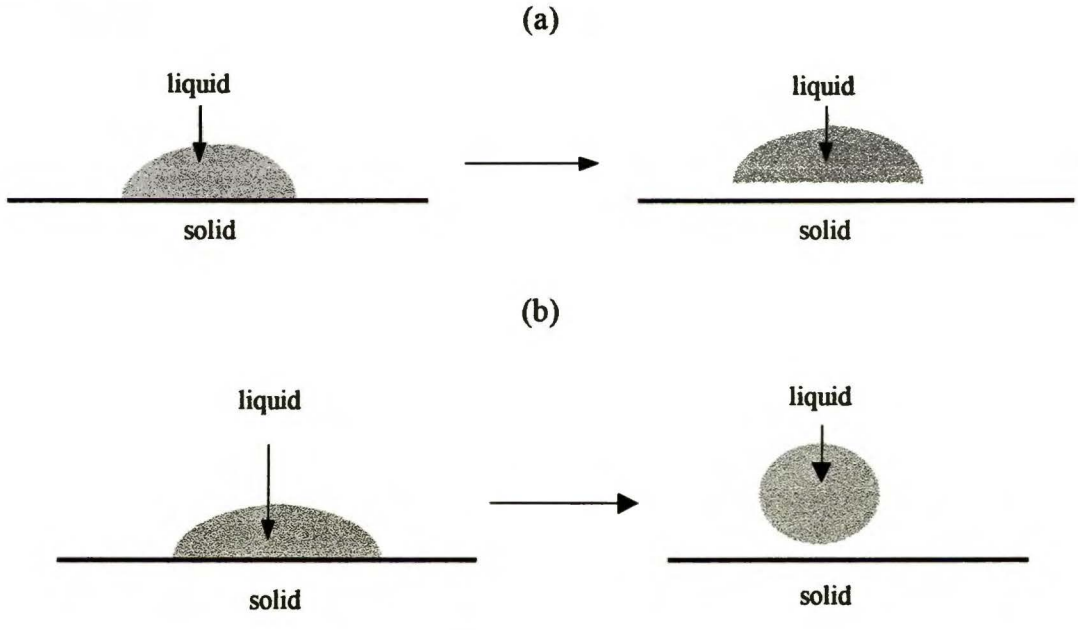

Fig.5. Models for free energy of adhesion,
(a) - Young-Dupré work of adhesion, (b) -Net free energy of adhesion

A free energy difference for the initial (bonded) state of sessile drop and final (separated) state of spherical drop can than be obtained from the surface free energy of the sphere and of the sessile drop. This is the Net Free Energy of Adhesion, ΔF_N, and is given by :

$$\Delta F_N = F_{V,D} - F_{SV,D} \qquad \text{(III.2.10)}$$

where $F_{V,D}$ is the free energy of formation of the free spherical drop from its saturated vapor, $F_{SV,D}$ is the free energy of formation of the sessile drop on a surface previously equilibrated with the vapor of the drop at p_o.

Another quantity is *the adhesion tension A*, which may be defined as :

$$A_{SLV} = \gamma_{SG} - \gamma_{SL} = \gamma_{LV} \cos \Theta, \qquad \text{(III.2.11)}$$

where the subscript $_{SLV}$ reminds that the work of adhesion and the adhesion tension involve γ_{SG} rather than γ_S.

The work of cohesion, Wc, is defined as the work of adhesion when both phases are the same. In this case $\gamma_{SL} = 0$ and

$$Wc = 2\,\gamma_{LG}, \qquad \text{(III.2.12)}$$

Bangham and Razouk[13] also pointed out that if the surface concentration of the adsorbed vapor from the liquid is Γ and the chemical potential is μ, then :

$$\Gamma = -\left(\frac{\partial \gamma}{\partial \mu}\right), \qquad \text{(III.2.13)}$$

or

$$\gamma_S - \gamma_{SG} = \int_{p=0}^{p=p_o} \Gamma d\mu, \qquad \text{(III.2.14)}$$

where p is the vapor pressure, p_o is the saturated vapor pressure.

In the special case where the vapor behaves like a perfect gas,

$$d\,\mu = RT\, d \ln p, \qquad \text{(III.2.15)}$$

so that :

$$\pi_{SG} = \gamma_S - \gamma_{SG} = RT \int_{p}^{p_o} \Gamma d \ln p = RT \int_{p}^{p_o} \frac{\Gamma}{p} dp, \qquad \text{(III.2.16)}$$

Hence, for π_{SG} will always have a positive value. This makes it evident that in general

$$W_{SL} > \gamma_{LG}(1 + \cos \Theta), \qquad \text{(III.2.17)}$$

For practical purposes, if the contact angle is greater than 90°, the liquid does not wet the solid; in such a case drops of liquid tend to move on the surface and not to enter capillary pores. On the other hand, a liquid is considered to wet a solid only if the contact angle is zero. In this last case, the imbalance of surface free energies is given by a "*spreading coefficient*", $S_{L/S(G)}$. Cooper and Nuttall[12] found the well-known conditions for the spreading of a liquid substance "b" on a solid (or liquid) substance "a" :

- for spreading : $S > 0$,
- for non-spreading : $S \leq 0$,

where $S = \gamma_a - (\gamma_b + \gamma_{ab})$ or in the above notation for a solid,

$$S_{L/S} = \gamma_{SG} - \gamma_{LG} - \gamma_{SL}, \qquad \text{(III.2.18)}$$

γ_{SL} and γ_{LG} should be made as small as possible if spreading is to occur. From a practical point of view, this is best by adding to the liquid phase a surfactant that is adsorbed at both the solid/liquid and the liquid/gas interfaces and therefore lowers these interfacial tensions.

Harkis developed and applied these relations more fully, identified S "*the initial spreading coefficient*" and derived the relations :

$$S = W_{SL} - W_C, \qquad \text{(III.2.19)}$$

and $$S = -\frac{\partial F}{\partial \sigma}, \qquad \text{(III.2.20)}$$

where F is the free energy of the system, σ is the surface area.

Assuming there is no surface electrification, the Young and the last equations are the basic equilibrium thermodynamic relations for wetting and spreading phenomena.

III.3. Physical factors influencing the solid/liquid contact angle

For physically and chemically homogeneous surfaces, wetting characteristics are well defined, whereas the wetting characteristics of the heterogeneous surfaces which are present in various laboratories, industrial and natural setting, are still a matter of investigation. There is widespread misunderstanding about the effect upon the contact angle of the physical conditions existing during its measurements and about the effect on it of the constitution of liquid and solid. The factors which determine the magnitude of the contact angle are as follows :

- the composition of the solid, of the melt and of the gas atmosphere,
- the temperature,
- the electrocapillary effect,
- the surface roughness of the solid and the hysteresis.

The composition of the solid, liquid and gas phases have a strong and direct influence on the energies of the surfaces and thus on the values of the contact angle. Due to the electrochemical processes which take place at the metal / solution interface[17] the initial contact angle changes, becouse it depends on chemical composition of the solid/liquid interfaces.

Weewer *et al.*[18-21] have found that the contact angles increase with the nobility of the

substrate composition in order: Cr - Ni/Al - Ni/Cu - Cu and to decrease with carbonate composition in the order: Li/Na - Li/K - Li/K/Ba. Some authors say that the effect of temperature on contact angle is not usually very great, as a practical observation. In the literature both positive and negative temperature effects on the contact angle values have been reported. Adamson[13] presents a table included some data on the temperature dependence of contact angle.

W. A. H. Peelen *et al.* [22], Kamping[23] , Y. Mugikura and J. R. Selman[24-26] have notice that with the increasing temperatue the contact angle values also increase. On the other hand Lundblad and Bergman[27] have found the opposite relation. Such a discrepancies among authors possibly might be explained by differences in the surface characteristics, which are known to have a large effect on the wetting behavior.

It is obvious that if the potential difference over the interface is changed the contact angle is change, too. According to Peelen *et al.*[22], J. M. Fisher[21], Mugikura and Selman [24,25] the contact angle increase with increasing cathodic potential, applied to the solid.

According to A. W. Neumann and R. J. Good[28,29] heterogeneous surfaces and rough surfaces are well known to exibit hysteresis of contact angle and wetting. Solid surfaces may be heterogeneous in two ways:

1. There may be patches or areas in which the atomic or molecular composition differs in other areas. If they are more than one or two orders of magnitude larger than ultimate resolving power of a light of microscope, than it is often easy to observe that a liquid forms different contact angles on different region of the surface. A drop of liquid on such a surface has a ragged-looking, contorted boundary when viewed from above, so the contact angle exibit hysteresis.
2. Different crystallographic planes of a pure, single crystal are known to have different densities of matter and energy and the contact angle of a liquid on two different planes will be different. Also the surface of a single crystal is seldom truly planar. Many conductive solids can be brought close to planarity by electropolishing, however such surfaces can contain facets, *i.e* etch-pits and points where dislocations intersected the surface. This authors also studied the hysteresis on an idealized rough surface which is energetically homogeneous, so the surface made up of small areas of smooth, homogeneous solids is taken into consideration.

The oldest experimental problem in the contact angle measurements is the occurence of large differences between the contact angle observed, when a liquid boundary advances for

the first time over a dry clean surface and the value of Θ observed, when the liquid recedes from the previously wetted surface[12,13]. They are called " *the advancing angle*", Θ_A, and " *the receding angle*", Θ_R, respectively and get their names from the fact that the advancing angle is often measured by advancing the periphery of a drop over a surface and the receding angle is measured by pulling it back. The difference, $\Theta_A - \Theta_R$, is called " *the hysteresis*". The most common cause of the differences observed is the effect of pores and crevices in the surface of the solid in trapping some of the liquid, as it is made to flow over the surface of the solid. When the liquid is forced to recede over that area at a latter time, the surface uncovered usually includes wet area, hence the receding contact angle is always lower than the advancing one, *i.e.* $\Theta_R < \Theta < \Theta_A$. Whenever sufficient care has been exercised in preparing and handling smooth, clean surfaces and whenever sufficiently pure liquids have been used, no significant differences have been found between the slowly advancing and receding contact angles. However, such a perfection may be obtained for easy workable simple systems, but in case of systems like Au/molten carbonates, Ni/molten carbonates, where the process of the recrystallization of metal surfaces occures or NiO/molten carbonates because of process of lithium incorporation, is practically inevitable.

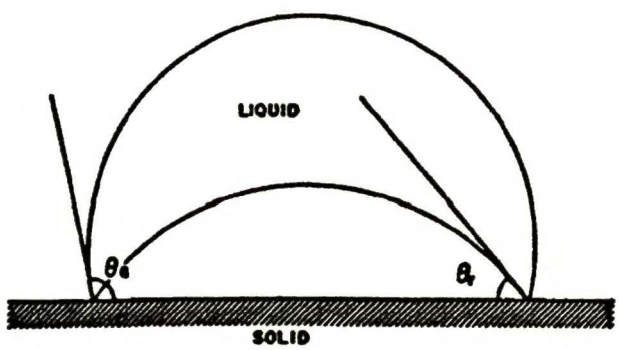

Fig.6 Advancing and receding angles of a drop on a surface (acc. to Johnson and Dettre[11]).

Wenzel showed[12,13] that the gross or macroscopic roughness of a solid surfaces as measured by the "*roughness factor*" r (the ratio of the true area of the solid to the apparent one) is related to the apparent or measured contact angle Θ′ between the liquid and the envelope to the surface of the solid and also to the true contact angle Θ between the liquid and the surface at the gas/liquid/solid contact boundary.

$$r = \frac{\cos\Theta'}{\cos\Theta}, \qquad \text{(III.3.1)}$$

Wenzel relation is especially valuable, because surfaces having r = 1 are rarely encountered. Surface roughness can also make difficult the problem of accurate determination of Θ, therefore in the experimental methods is often assumed that $\Theta' = \Theta$. In order to make accurate measurements of small contact angles, the solid surface must be much smoother than when measuring large contact angles.

The influence of the surface roughness on the contact angle measurements showed also D. Y. Kwok in his doctoral thesis [30] , as well as M. Miyama, Y. Yang, T. Yasuda *et al.*[31] who emphasized many factors influencing the discrepancy of contact angle measurement, such as surface roughness, deformation, surface chemical heterogeneity and configuration change during the process of the contact angle measurements.

III.4. Some experimental methods of the contact angle measurements

A variety of methods for the measurement of the contact angle have been described in the literature.

1. The most commonly used method is that of measuring the contact angle directly for a drop of liquid resting on a flat surface of the solid. The contact angle is determined by constructing a tangent to the profile at the point of the contact with the solid surface. The drop can be simply viewed directly through a microscope filled with a goniometer scale and the contact angle may be obtained from a photograph of the drop profile either by measuring the angle or by calculating from the entire of drop profile[12,18,19].

F. M. Fowkes, M. S. Kaczinsky and D. W. Dwight described[32] the contact angle measurement by using a Ramé-Hart apparatus with environmental control chamber and averaging the contact angles on each side of the drops.

M. Miyama, Y. Yang *et al.* [31] measured the static advancing and receding contact angles of sessile drop with increasing and decreasing droplet volume. A drop was placed on the surface and a picture of the droplet was taken by a camera. The contact angle was measured using an enlarged image of the developed film. The diameter of contact area which was the surface area under the sessile droplet was also measured on the enlarged image of the developed film and the actual contact area was calculated.

M. J. de Ruijter, J. de Coninck *et al.*[33] used a method where the needle of a syringe containing the liquid was just above the substrate, so that a drop of liquid falling from the tip of the needle immediately touched the solid surface and began to spread. The spreading of the

drops were captured, from the moment they detached the needle by a video-recorder connected to a CCD cammera and a microscope. The contact angle was determined at the point where the fit of the drop and its reflection intersected.

Also D. Y. Kwok *et al.* [30] described in his Ph. D. thesis the contact angle measurements by axisymmetric drop shape analysis and goniometer sessile-drop technique. The sessile drop contact angle measurement were performed dynamically by using a motor- driven syringe to pump liquid steadily into the sessile drop from below the surface. The drop increased axisymmetrically in the center of the image field when liquid was supplied from the bottom of the surface. A conventional goniometer equipped with eye-piece was also used. A syringe connected to a Teflon capillary was used to supply liquid into the sessile drop. The three-phase contact line of the drop was then slowly advanced by supplying more liquid from above through the capillary was always kept in contact with a drop.

2. A classic method for obtaining contact angles is known as the tilting-plate method. A several centimeter wide plate of the solid dips into the liquid and its altered until the angle is such, that the liquid surface appears to remain perfectly flat right up to the surface of the solid. The contact angle is determined from the slope of the solid surface at the boundary line. The method has limited use becouse both a large, smooth sample of solid and a large volume of liquid are required.

3. A. W. Neumann[34,35] has used vertical glass-plates submerged in different organic liquids and observed that the meniscus at a partially immersed plates rises to definite height h, if Θ is finite (as it may be seen in Fig.7). This method, using a cathetometer, is capable of giving contact angles to 0.1° precision. An equation, describing this relation has been experimentally determined and firstly given by V. Hagen in 1845 as:

$$\sin\Theta = 1 - \frac{\rho g h^2}{2\gamma_{LV}}, \qquad \text{(III.4.1)}$$

where ρ is the density of the liquid, g - gravity acceleration, h - the meniscus height, γ_{LV} - liquid surface tension, respectively.

Selman in series of his work [24-26] has adapted this method to determine the contact angle values for Li/K eutectic mixture at Au, Ni and NiO surfaces.

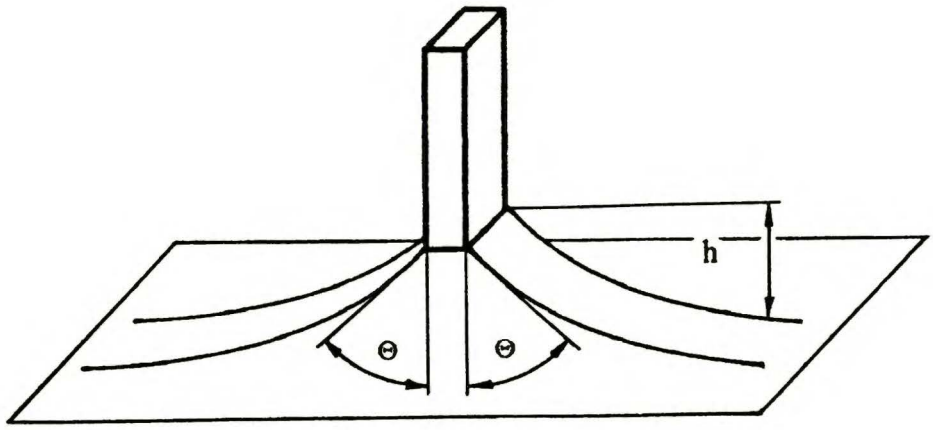

Fig.7. The meniscus rise of a liquid of a partially immersed vertical-plate.

4. In the Wilhelmy-balance method, the "pull" on the balance arm is noted by the balance as detachment occurs. From the weight changes and the dimension of the plate, the contact angle can be calculated.The weight of meniscus is equal to the wetting force F_w. At equilibrium, the measured force over the flag electrode is given by Wilhelmy:

$$F_w = P\,\gamma_{LV}\cos\Theta, \qquad \text{(III.4.2)}$$

where P is the perimeter of the sample, γ_{LV} is the surface tension.

The weight of the meniscus depends on the contact angle at the top of the meniscus. The smaller is the contact angle the higher is the meniscus height and hence its weight will be. Peelen[22] has adapted the Wilhelmy - balance method to determine the ellectrocapillary effect of gold in molten carbonates and to estimate the wetting as a function of the overpotential applied to the solid.

J. A. M. Sondag-Huethorst and L. G. Fokking[36] used for the electrode potential-dependent contact angles the apparatus placed on a vibration-isolated table. It consisted of a Wilhelmy plate suspended with a nonconducting tread from a bottom-leading balance. The Wilhelmy place also constituted the gold working electrode of a standard three-electrode cell. The cell rested on a micrometer-controllable lifting table and was connected to a potentiostat and a frequency response analyzer. The setup enables a simultaneous measurement of the force on the Wilhelmy plate electrode by measurement of the change of mass associated with the electrolyte meniscus rise, the current and the differential capacitance as a function of the overpotential applied to the solid under investigation.

A. Miyama, Y. Yang *et al.*[31] used the Wilhelmy-balance technique for the measurements of the surface force and made a comparative study of the sessile-drop and the

Wilhelmy-balance method, using samples from the same bath. Immersion and emersion of the glass plate coated by the plasma polymer were accomplished by raising and lowering the beaker stage. Data points, including depth and force of the measuring point were collected and stored in the computer memory. The immersion depth was calculated from the time and speed of immersion and emersion.

E. L. Decker and S. Garoff [37] also used the Wilhelmy-plate geometry of a partially immersed vertical plate for determining the wetting characteristics of various surfaces, *i.e* for contact line and contact angle measurements. They determined contact angles by measuring the rise (or depression) height of the meniscus of a liquid against the solid surface. The rise height was measured with the contact line in the recede or advance condition and the plate moving to keep the contact line with the flicker regime for the measurements. They also used a reflection geometry to image the contact line. This geometry incident light propagates along the optical axis of the camera toward the sample. Light was reflected off axis by the liquid meniscus, so the light region of the image (the reflective backing) and the dark region (the liquid meniscus).

5. The contact angle may also be obtained indirectly from the measurements of the dimensions of a sessile drops. For a very small drops, the distorting effect of gravity is negligible and the drop can be considered to be a segment of a sphere. Thus, if a spherical shape is assumed, the contact angle is calculated from the drop height h and the diameter of its base, d, using the following equation

$$\tan\frac{\Theta}{2} = \frac{h}{r}, \qquad \text{(III.4.3)}$$

This procedure requires the measurements of the diameter of the drop of known volume[11,13].

6. For larger sessile drops, where distortion due to gravity is not negligible, the contact angle can be calculated from drop dimensions, if the drop profile is known.

Bashworth and Adams[38-42] derived the differential equation describing the profile and numerically integrated this equation, as well as compiled tables, which permitted one to determine contact angle from drop dimensions.

III.5. Selected problems embracing some contact angle and wettability phenomena

A lot of significant modern advances in the field of wettability have been described in the latest literature.

E. L. Decker and S. Garoff [42] give background description and analysis of contact angles, as well as contact line structure and dynamics using the Wilhelmy-plate geometry of a partially immersed vertical plate. The authors observed the extreme complexity of wetting with chemical heterogeneity. On heterogeneous solid surfaces, the local contact angle varies spatially across the surface. This is observed in the deformations of the contact line from the ideal, smooth shape that the contact line would have a perfectly homogeneous surface with one value of contact angle at all point of the surface. On typical heterogeneous surfaces, the value of contact angle depends on the motion of the bulk liquid relative to the solid surface. In such a case, the motion of the solid surface or bulk liquid can move the liquid/vapor interface with no motion of the pinned contact angle. This can increase or decrease the contact angle. If such motion increases the contact angle, then the maximum angle attained just before the contact angle lines unpins and advances further across the solid, displacing solid/vapor interface by new solid/liquid interface, is called the advancing contact angle. The minimum value, *i.e* the receding contact angle occurs for thr opposite motion.

A. Marmur[43] presents the effect of the equilibrium conditions of constraints imposed on the motion of the contact line. The discussion is limited to two dimensional (cylindrical) solid/liquid fluid interfaces. In general, equilibrium is achieved when the internal energy of an isloated system reaches its minimum. When the motion of the contact lines is constrained, the actual and intrinsic contact angles differ each other, whereas they are identical in the absence of constraints.

M. Miyama, Y. Yang, T. Yasuda *et al.*[31] have performed comparative study of the sessile-drop method and the Wilhelmy-balance one using samples from the same bath. The contact angle which is measured in a static condition is referred to as "*static contact angle*" and the contact angle which is measured under the condition that the three-phase contact line is moving with the respect to the surface is referred to as "*dynamic contact angle*". When the volume of the sessile-drop is increased, the three-phase contact line advances to dry the surface. For this situation, the contact angle measured on the volume increasing process is customarily referred to as "*the advancing contact angle*". The contact angle measured on the

droplet-volume withdrawing process is referred to as "*the receding contact angle*" with the assumption that the three-phase contact line recedes, indeed. The authors notice that the contact line in the receding process often does not recede from the contact line, developed on the last step of the advancing process. The hysteresis (discrepancy) of contact angles in the advancing and receding processes is a common phenomena and there are many factors influencing the hysteresis effect like surface roughness, surface chemical heterogeneity, surface deformation, adsorption and desorption, as well as surface configuration change during the process of the contact angle measurement. The dynamic advancing and receding contact cngles were calculated from the immersion and emersion lines in the Wilhelmy force loop. The authors remarked that a single volume of dynamic receding contact angle and its difference from the dynamic advancing contact angle can be obtained from the Wilhelmy force measurement, which is a strong contrast to the case of the sessile-drop measurement. In general, they concluded that: $\Theta_{D,a}$ (dynamic advancing contact angle) > Θ_s (static contact angle) > $\Theta_{D,r}$ (dynamic receding contact angle). The three contact angles are related by:

$\cos \Theta_s = (\cos \Theta_{D,a} + \cos \Theta_{D,r}) / 2.$

C. D. Dushkin, P. A. Kralchevsky, V. N. Paunov *et al.*[44] have described interesting particle-particle and particle-wall capillary interactions measured as a function of the separation distance. The "particles" were vertical thin glass cylinders and/or small glass spheres, protruding from an air/liquid interface and they attracted each other due to the overlaping of the menisci formed around each of them. The force of interaction was detected by a sensitive torsion balance, based on counterbalancing the moment of a couple of forces, acting between two pairs of particles by the torsion moment of thin platinum wire. As a result, the smallest force was measured with two cylinders. For two spheres the authors have obtained difference in the forces corresponding to different heights of protrusion from the liquid surface, whereas for interacting sphere and glass cylinder the force followed similar trends as the forces between two spheres or cylinders. In a case of sphere and glass wall, the force first increased with decreasing the distance and then decreased close to the wall through a maximum. Such forces play a role for aggregation of particles in two-dimensional arrays on substrate.

P.A.Kralchevsky and K.Nagayama[45] have described a special kind of capillary interaction, which differs from the common lateral capillary forces between floating particles and have compared the magnitudes of the capillary interactions taking place at two different boundary conditions on the particle surfaces: fixed contact angle and fixed contact line. The

authors have demonstrated the difference between floation and immersion lateral capillary forces. The former originated from the particle weight, whereas the latter was generated by the particle wettability (position of the contact line and magnitude of the contact angle). Both these forces appeared when a liquid interface was deformed due to a presence of attached particles.

IV. Review of the literature concerning the wettability properties of the molten carbonates

Wetting of the solid electrode materials by the molten alkali carbonates in the MCFC stacks is of great importance if one wants to optimize the MCFC processes, therefore a possibility of comparing wetting properties at MCFC electrodes is of first interest for these devices. Several authors have studied this problem, but there are large discrepancies among results obtained by various research-teams. Selman[46] and Weewer[20] have summarized investigations of different researchers, concerning the contact angles of solid materials (Ni, NiO, Au) wetted by three alkali carbonate melts, *i.e* $Li_2CO_3 + K_2CO_3$, $Li_2CO_3 + Na_2CO_3$ and $Li_2CO_3 + Na_2CO_3 + K_2CO_3$ under hydrogen and oxygen containing atmospheres, which is presented in Tab.1.

This review shows also rather large discrepancies among results obtained in various laboratories at Ni in Li/K carbonate melt under hydrogen containing gas atmosphere and at NiO under oxidizing one. Analogous investigation performed at Au/molten carbonates interface as reference material show some discrepancies. Also in this case one can notice that the study has been limited to the Li/K carbonate electrolyte[47]. It should be mentioned that some researchers have carried out wettability studies relating the contact angle values of different solid materials in the molten alkali carbonates, using the sessile-drop method. The review of the obtained results is presented in Tab.2.

Taking the results both from Tab.1 and Tab.2 into consideration, it should be remarked that the reproducibility of these contact angle measurements, from one investigator to another, are quite different and that there is a lack of data for Li/Na carbonate electrolyte. In view of the fact that these measurements are very sensitive to the method of preparation of the surface and to trace impurities in the electrolyte, some studies ought to be performed and repeated in one laboratory, by the same research team, under the same conditions and technique of measurements.

Hydrogen containing atmosphere, Ni			**Oxygen containing atmosphere, NiO**		
Li/Na carbonate eutectic	Li/K carbonate eutectic	Li/Na/K carbonate eutectic	Li/Na carbonate eutectic	Li/K carbonate eutectic	Li/Na/K carbonate eutectic
	Fisher, Bennett [47] ~ 50°	Moiseev, Stepanov [48] ~ 33°		Mugikura, Selman [24] ~ 0°	
	Lessing, Johnston [46] ~65°			Lessing, Johnston [46] ~0 °	
	Mugikura, Selman [24] ~ 50°				
Weewer *et al.* [19] ~ 50°	Weewer *et al.* [19]~ 40°				
	Eberhart – non wetting [46]				
Hydrogen containing atmosphere, Au			**Oxygen containing atmosphere, Au**		
Li/Na carbonate eutectic	Li/K carbonate eutectic	Li/Na/K carbonate eutectic	Li/Na carbonate eutectic	Li/K carbonate eutectic	Li/Na/K cacrbonate eutectic
	Fisher, Bennett [47] ~ 65°			Matsumura, Selman [26] ~ 60° (in CO_2)	
	Mugikura, Selman [24] ~ (55°-70°)			Mugikura, Selman [24] ~ 65°	
				Kamping *et al.*[22,23] ~ 65° (in air)	
				Eberhart 0° [46]	

Tab.1. Contact angle values at the MCFC electrode materials and at Au as reference / molten alkali carbonate interfaces under hydrogen and oxygen containing gas atmospheres.

Hydrogen containing atmosphere			Oxygen containing atmosphere		
Li/Na carbonate eutectic	Li/K carbonate eutectic	Li/Na/K carbonate eutectic	Li/Na carbonate eutectic	Li/K carbonate eutectic	Li/Na/K carbonate eutectic
Tseung [46] C gr~ (100°-150°), BN – non wetting, $BaO{\cdot}6Fe_2O_3$ - wets	Fisher, Bennett [48] Rh~ 43° Ru~ 92° Ag~ 63° Pd~ 41° Cu~ 88° Pt~ 49°	Moiseev, Stepanov [49] Pt~ 53° C gr~ 70° BN ~ 90°	Tseung [46] $PbO{\cdot}6FeO_3$ ~ (60°- 70°) (in air/CO_2)	Lundblad, Bergman [27] $LiCoO_2$ (in air) (~14°-40°), using a method of capillary	Moiseev, Stepanov [49] Pt~ 0°(in CO_2), C gr~ 85° (in CO_2), BN ~ 90°(in CO_2)
	Fisher, Bennett, Pignon, Makkus, Weewer, Hemmes [21] NiAl~ 10° NiCr~ 10° NiAl~ 35° (in H_2/CO_2), NiCr~ (40°- 50°) in H_2/CO_2	Cobb, Aebright [46] Pt ~ 90°		Fisher, Bennett, Pignon, Makkus, Weewer, Hemmes [21] $LiFeO_2$-wetted, Si_2N_3- wetted, NiAl- wetted, NiCr- wetted	Cobb, Aebright [46] Pt ~ 0° (in air /CO_2)
	Weewer *et al.* [19] NiAl~ 10° (in Li/K/Ba), Cu~ 0°(Li/K/Ba)				
	Lessing, Johnston [46] GG 321~ 18° (in fuel), Inconel 671 ~ 19° (in fuel 500°C), ZrO_2(+Y+Cr) ~ 0° (in fuel), γ - $LiAlO_2$ ~ 0° (in fuel)				

Tab.2. Contact angle values at different solids / molten alkali carbonate interfaces under hydrogen and oxygen containing gas atmospheres.

V. The aim of the work

Although today Li/Na alkali carbonate eutectic is thought to be an alternative electrolyte for the MCFC and is a subject of increasing interest, the researchers have been focused on Li/K carbonate electrolyte, because for a long time this system has been considered as the most appropriate as the MCFC electrolyte. Therefore it is a lack of respective data for Li/Na carbonate electrolyte, which at present is even more taken into account as main electrolyte[52,53].

It is an essential difficulty in the investigation of wetting phenomena that only few solid materials are chemically stable in very agressive molten carbonate media. For this reason a lot of studies in molten carbonates have been carried out on gold, which of course is not used in MCFC devices, but it is the most corrosion resistant and chemically stable pure metal in molten carbonates. Investigations of the wettability at gold/carbonate melts interface, mostly have been limited also to Li/K carbonate electrolyte and show some discrepancies [Tab.1]. Moreover, the contact angle values at Ni and NiO as main MCFC electrode components, have been extensively determined by several authors and limited generally to Li/K carbonate eutectic, but also in this case the review of the literature concerning the wettability properties in MCFC proves the lack of data for Li/Na carbonate electrolyte [Tab.1]. Even more ambiguous and doubtful are the reported data for NiO under oxidizing atmosphere. In general, an opinion has been accepted, that the wettability of this solid is perfect and the contact angle is 0^{o}. Contemporaneously, the researchers claim the difficulties in obtaining smooth, continuous and uniform surface of this compound, stable in molten carbonates. Therefore, a perfect consistency of the contact angle values for the same solid/carbonate melt interface, when done by various research-teams cannot be expected. It has to be obtained in one investigation program, carried out by the same research-team. This data should not only be limited to Li/K carbonate electrolyte but, according to increasing interest, also to Li/Na carbonate.

Taking into account above observation, the aim of this work was to gather data embracing the contact angle values for the main MCFC electrode materials, *i.e* Ni and NiO under both reducing and oxidizing gas atmospheres, as well as for Au as a reference material in three alkali carbonate eutectic melt compositions. Very important and ambitious was to determine the contact angle values at the NiO / molten alkali carbonate interfaces under oxidizing atmosphere using two forms of this compound, *i.e* NiO single crystal doped with 0.7

at.percent of Li and NiO smooth, continuous layer deposited on Au using the ion-sputtering method. The investigations embraced also the influence of the electrode anodic and cathodic overpotential, applied to the metallic Ni and lithiated NiO single crystal, respectively. Moreover, using the contact angles data obtained in this work, the optimal ratio of anodic to cathodic pore size values for porous MCFC electrodes have been calculated, as well as the adhesion work parameters for Au/molten carbonate interfaces have been determined.

The original results are presented in the two chapters VIII and IX in order which correspond to the three publications. References are listed at the end of every chapter. Some details of the experimental procedure and references may overlap and repeat.

VI. Investigation program performed in the contact angle measurements

Experimental determination of the contact angle values at the solid/molten alkali carbonate interfaces creates serious difficulties. Some of the contact angle determination methods are not feasible in these circumstances. Methods, which in our investigations have been applied[49-54] and have been considered as appropriate to the alkali carbonate melts under study are two optical ones:

- the sessile-drop method, consisting in direct contact angle measurements from the profile of the liquid,
- the meniscus-rise-on-vertical-plate method, consisting both in the meniscus height and the contact angle measurements at the vertical plate, immersed in the melt.

In general, as the most reliable it has been considered the sessile-drop method of measurements, however this configuration does not permit to apply the electrode overpotential to the solids under investigations. Such a possibility is given by using the vertical position of the solid plates.

Taking this remarks into consideration, in the preliminary part of this work, some investigations have been performed at Au both by the sessile-drop method and by the vertical-plate one in order to ascertain the consistency of both methods and the correctness of the vertical-plate configuration. As a result it has been found good conformability between the contact angle values determined by using both methods. Consequently, this observation allow us to realise the contact angle determination at Ni and NiO under two forms as well as the influence of the overpotential applied to these solids, using the vertical-plate method. Mentioned below scheme approximately presents the idea of the investigations program performed in this work in the temperature range from the molten carbonates melting point to 923 K, *i.e* the scope of the MCFC operating temperature.

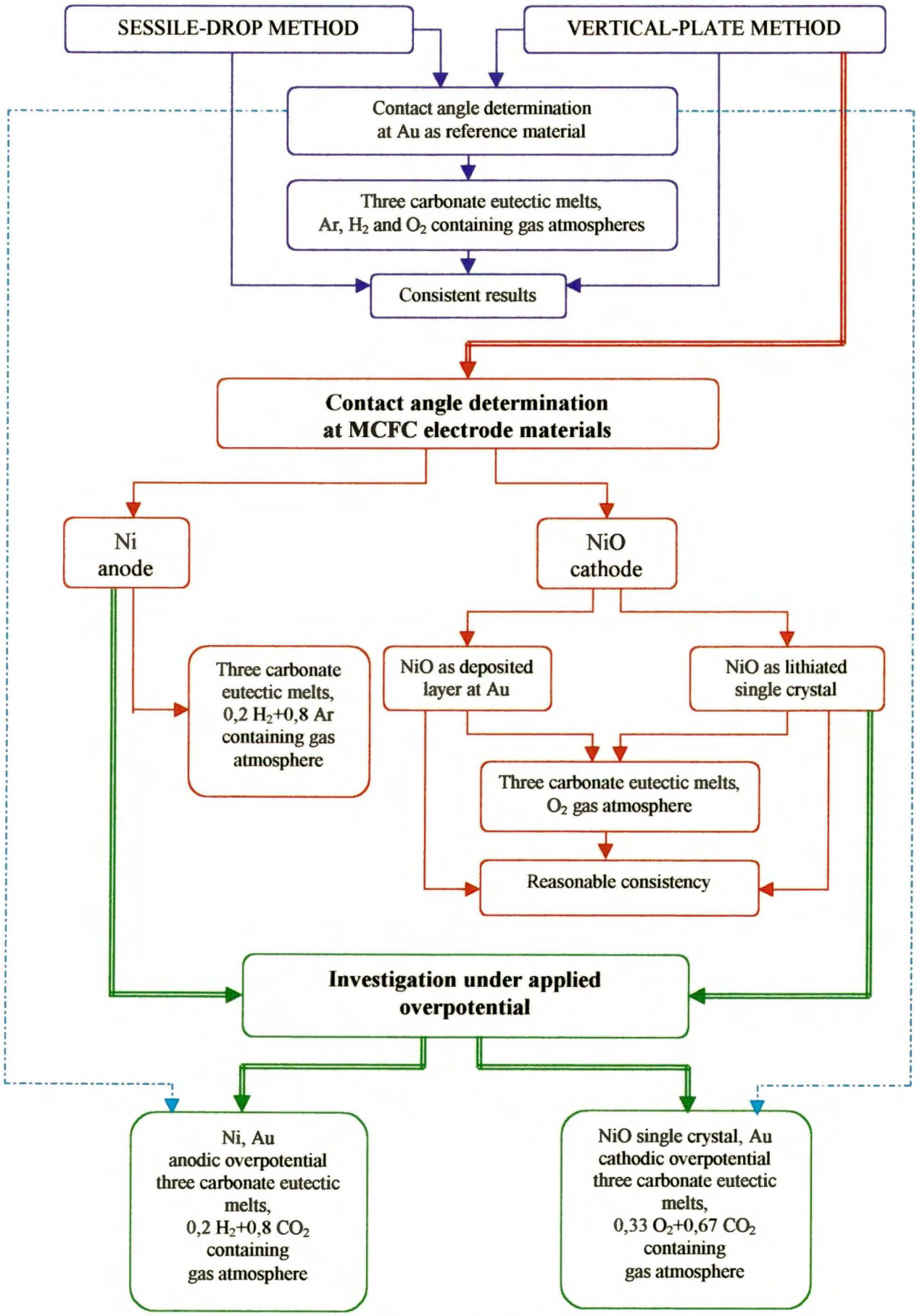

Fig. 7. Investigation program performed in this work.

VII. References

1. K. Kordesch, *Ber. Bunsenges. Phys. Chem.*, 94, 902, 1990.
2. Y. Watanabe, M. Matsumoto, K. Takasu, *J. Power Sources*, 61, 53, 1996.
3. Y. Watanabe and A. Nakaoka, *The Market for Utility Scale Fuel Cell Plant*, Fourth Grove Fuel Cell Symposium, London, 1995.
4. J. O'Bockris, S. U. M. Khan, *Surface Electrochemistry, A Molecular Level Approach*, Plenum Press, New York and London, 1993.
5. K. Kishida, *Ber. Bunsenges. Phys. Chem.*, 94, 941, 1990.
6. P. B. Tarman, *J. Power Sources*, 61, 87, 1996.
7. Ch. E. Borroni-Bird, *J. Power Sources*, 61, 33, 1996.
8. Th. Klaiber, *J. Power Sources*, 61, 61, 1996.
9. PEM-Fuel Cell Technology, *Discover the commercial and technical implications for the automobile, stationary and portable power industries*, 27-28th April 1999, Frankfurt.
10. L. Suski, *Thermochim. Acta*, 245, 57, 1994.
11. R. E. Johnston, Jr. and R. H. Dettre [in] *Surface and Colloid Science*, Vol. 2 ed. by E.Matijević, John Wiley & Sons, Inc., New York, 1969.
12. W. A. Zisman [in] *Adhesion and Cohesion, Proceedings of the Symposium on Adhesion and Cohesion*, General Motors Laboratories, Warren, Michigan, 1961.
13. A. W. Adamson and A. P. Gast, *Physical Chemistry of Surfaces*, sixth edition, John Wiley & Sons, Inc., New York, 1997.
14. D. J. Harvey [in] *Adhesion and Cohesion, Proceedings of the Symposium on Adhesion and Cohesion*, General Motors Laboratories, Warren, Michigan, 1961.
15. D. D. Eley and D. Tabor, *Adhesion*, Oxford University Press, 1961.
16. M. E. Schrader, *Langmuir*, 11, 3585, 1995.
17. O. Teschke, M. A. Tenan, F. Galembeck, *J. Colloid Interface Sci.*, 1,127, 1999.
18. R. Weewer, *Study of electrochemical processes and wetting phenomena at the molten carbonate fuel cell anode*, Doctoral thesis, Delft Technical Universitety, Delft, 1991.
19. R. Weewer, J. F. Vente, K. Hemmes and J. H. W. de Witt, *Ber. Bunsenges., Phys. Chem.*, 94, 967, 1990.
20. R. Weewer, J. F. Vente, K. Hemmes and J. H. W. de Witt, *Proceedings of the Second Symposium on Molten Carbonate Fuel Cell Technology*, J. R. Selman, I. Uchida, D. A.

Schores eds., *The Electrochemical Society*, Inc., Proceedings Volume 90-16, Pennington, N.J., 1990, p.281.

21. J. M. Fisher, P. S. Bennett, J. F. Pignon, R. C. Makkus, R. Weewer and H. Hemmes, *J. Electrochem. Soc.*, 137, 1493, 1990.
22. W. H. A. Peelen, K. Hemmes, H. Kamping, M. Bos and J. H. W. de Witt, *J. Solid State Electrochem.*, 2, 334, 1998.
23. H. Kamping, *Electrocapillary Effect of Gold in Molten Carbonate Measured by Wilhelmy Balance*, Delft University of Technology, Delft, 1994.
24. Y. Mugikura and J. R. Selman, *J. Electrochem. Soc.*, 143, 2442, 1996.
25. Y. Mugikura and J. R. Selman, *Denki Kagaku*, 64, 491, 1996.
26. M. Matsumura and J. R. Selman, *J. Electrochem. Soc.*, 139, 1255, 1992.
27. A. Lundblad and B. Bergman, *J. Electrochem. Soc.*, 144, 984, 1997.
28. A. W. Neumann, R. J. Good, *J. Colloid Interface Sci.*, 38, 341, 1972.
29. A. W. Neumann, R. J. Good, *J. Colloid Interface Sci.*,53, 235, 1975.
30. D. Y. Kwok, T. Gietzelt, K. Grundke, H. J. Jacobasch and A. W. Neumann, *Langmuir*, 13, 2880, 1997.
31. M. Miyama, Y. Yang, T.Yasuda, T. Okuno and H. K. Yasuda, *Langmuir*, 13, 5494, 1997.
32. F. M. Fowkes, M. S. Kaczinsky and D. W. Dwight, *Langmuir*, 7, 2464, 1991.
33. M. J. de Ruijter, J. De Coninck, T. D. Blake, A. Clarke and A. Rankin, *Langmuir*, 13, 7293, 1997.
34. A. W. Neumann, *Z. Phys. Chem., Neue Folge*, 41, 339, 1964.
35. A. W. Neumann and D. Renzow, *Z. Phys. Chem., Neue Folge*, 68, 11, 1969.
36. J. A. M. Sondag-Huethorst and L. G. Fokking, *Langmuir*, 8, 2560, 1992.
37. W. Missol, Energia powierzchni rozdziału faz w metalach, Wyd. "Śląsk", Katowice, 1975.
38. Y. Rotenberg, L. Boruvka and A. W. Neumann, *J. Colloid Interface Sci.*, 93, 169, 1983.
39. C. Huh and R. L. Reed, *J. Colloid Interface Sci.*, 91, 472, 1983.
40. L. M. Coucoulas and R. A. Dave, *J. Colloid Interface Sci.*, 103, 230, 1985.
41. S. H. Anastasiadis, J. K. Chen, J. T. Koberstein, A. F. Siegel, J. E. Sohn and J. A. Emerson, *J. Colloid Interface Sci.*, 119, 55, 1987.
42. E. L. Decker and S. Garoff, *Langmuir*, 13, 6321, 1997.
43. A. Marmur, *Langmuir*, 13, 6321, 1997.
44. C. D. Dushkin, P. A. Kralchevsky, V. N. Paunov, H. Yoshimura and K. Nagayama, *Langmuir*, 12, 641, 1996.

45. P. A. Kralchevsky and K. Nagayama, *Langmuir*, 19, 23, 1994.

46. R. J. Selman, *Wetting and oxidation of metals by molten carbonates*, Workshop on MCFC - Stockholm - February 20-22, 1995, documentation from the lecture, Kungl Tekniska, Stockholm, 1995.

47. J. M. Fisher and P. S. Bennett, *J. Mater. Sci.*, 26, 749, 1991.

48. G. K. Moiseev and G. K. Stepanov, *Trudy Inst. Elektrokhim. Akad. Nauk SSSR, Ural'sk. Filial*. N° 8, 103, 1966.

49. A. Godula-Jopek and L. Suski, *Zjawiska zwilżalności w modelowym układzie ogniwa paliwowego z elektrolitem ze stopionych węglanów alkalicznych*, XXV Szkoła Inżynierii Materiałowej, Kraków-Rabka, 7-10 Październik 1997.

50. A. Godula-Jopek and L. Suski, *Zwilżalność powierzchni ciał stałych przez układy stopionych węglanów alkalicznych*, XXVI Szkoła Inżynierii Materiałowej, Kraków-Zakopane, 6-9 Październik, 1998.

51. A. Godula-Jopek and L. Suski, *Wettability of Gold, Nickel and NiO by Molten Alkali Carbonate under Oxidant and Reducing Atmospheres as Relevant to Molten Carbonate Fuel Cell*, XV th Physical Metallurgy and Materials Science Conference, Advanced Materials & Technologies, 17-21 May, 1998, Kraków-Krynica, Poland.

52. A. Godula-Jopek and L. Suski, *Wetting Behavior of Molten Alkali Carbonates on Au Interface under Various Gas Atmospheres*, Polish J. Chem., 72, 1045, 1998.

53. L. Suski and A. Godula-Jopek, *Wettability of Ni and NiO by Molten Li/Na, Li/K, Li/Na/K Carbonates Under Various Atmospheres*, International Open Seminar, Design Optimization and Advanced Material Development for Molten Carbonate Fuel Cell, MCFC Research Association, 84-89, 18th March, 1999, Tokyo, Japan.

THE PRESENTATION OF THE ORIGINAL RESULTS

VIII. Wetting behavior of molten alkali carbonates on Au interface, under different gas atmospheres

VIII.1. Introduction

In last two decades, fuel cells operating with molten alkali carbonates as electrolyte (molten carbonate fuel cell – MCFC), have been extensively developed. Demonstration of pilot plants, which produce electrical current up to 2 MW of power on the principle of those devices, , is now in course. Up to now, in the majority of projects, the electrolyte composed of 0.62 Li_2CO_3 + 0.38 K_2CO_3 eutectic melt has been applied, however, in some recent models of MCFC, the melt 0.53 Li_2CO_3 + 0.47 Na_2CO_3 is being used. Gas electrodes in a fuel cell operate under determined conditions of solid electrode materials, wetted by the electrolyte. In MCFC case, those wetting properties depend on the work of adhesion at the electrode metals (Ni) or oxides (NiO) and the carbonate melt interface, under reducing (H_2 containing, anodic gas) or oxidizing (O_2 and CO_2 containing, cathodic gas) atmospheres. As relevant to MCFC optimization, wetting phenomena have been studied for $(Li/K)_2CO_3$ eutectic electrolyte in [1,2,3], as well as in [4] and [5]. Only few data exist for the alternative $(Li/Na)_2CO_3$ melt. A possibility of comparing wetting properties (adhesion work) at MCFC electrode materials and both alternative electrolyte interfaces, is of great interest for these devices [6].

It is commonly known, that very agressive molten carbonates are difficult to handle in all kind of experiments. Only few solid materials are chemically stable in these media. Even NiO, commonly used as cathodic materials, and solid matrix materials in the electrolyte plates, $LiAlO_2$, exhibit residual solubility in molten carbonates, what implicates low wetting angles (low adhesion work values) at the alkali carbonate melt / solid phase interfaces. This is the essential difficulty in the investigation of wetting phenomena in those systems. Gold is the only material considered as chemically stable in these media. Therefore, most of investigations have been carried out at Au surfaces. Transition metals: iron, nickel, cobalt, chromium, manganese might be studied only in highly reducing atmosphere. Those investigations may give information concerning the influence of carbonate melts composition on the adhesion work at this surface, under different gas atmospheres. Such an information might be useful for deducing the differences in wetting of other solid materials, *e. g.* metal oxides, by carbonate melts of various compositions. One of the simplest method of studying adhesion work on the solid / liquid interfaces, is the determination of the contact angle between both phases. This may be done using the so-called sessile-drop method, not the most precise, but the most feasible in molten melts.

In this chapter, the results of liquid – solid adhesion on the interfaces: Au/$(Li+Na)_2CO_3$, Au/$(Li+K)_2CO_3$ and Au/$(Li+Na+K)_2CO_3$ eutectic melts are presented. The contact angles between both phases have been determined by the sessile-drop method, in temperatures between the melting points of the above eutectics and 650°C, *i. e.* for the temperature range of MCFC operation, under both oxidizing and reducing atmospheres.

VIII.2. Experimental

Experimental set-up. Contact angles have been measured by sessile-drop method in a device presented in Fig. 8. The sample (0.02 – 0.08 g) (1) was placed on a golden plate (2), carefully polished. The plate and the electrical heating element (3), have been closed in a gas tight stainless steel chamber, permitting to use a controlled gas atmosphere. The temperature required, up to 650° C, has been obtained due to a silver radiation screen (4). Temperature of the sample was measured by two Pt-PtRh10 thermocouples (5a, 5b). For a good heat transfer from the golden plate to the thermocouples, the two lasts were fixed to the plate by a thin layer of alundum cement. The shape of the sample (sessile drop) was visible through a synthetic leuco-sapphire window. The sample under investigation has been illuminated by the heating element, supplementary it might be shined from an external light source through lateral leuco-sapphire windows (6). Pictures of the sample have been stored in computer memory through the MST 131 optical stereomiscroscope (PZO, Poland), with MS-468P CCD camera.

(a)

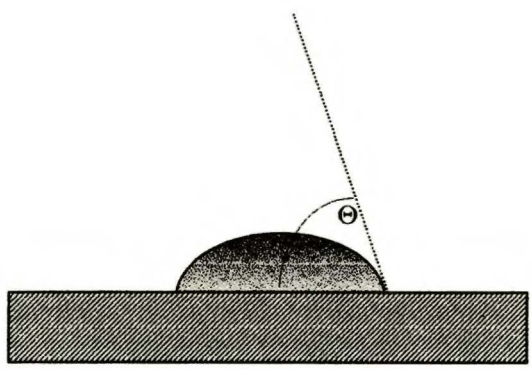

Fig. 8a. Definition of liquid/solid contact angle ("sessile drop").

(b)

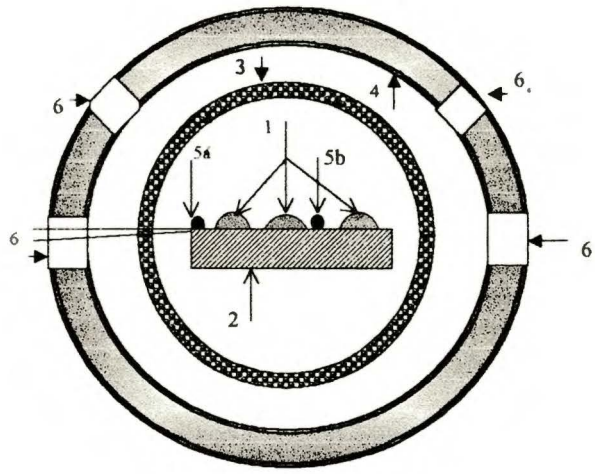

Fig. 8b. Schematic frontal cross-section of the heating chamber for contact angle measurements by the sessile-drop method. 1, three samples of melts under investigation; 2, golden plate; 3, heating coil; 4, silver radiation screen, 5a and 5b, thermocouples in alundum cement gains; 6, synthetic leuco-sapphire windows.

Reagents and gases. Li_2CO_3, Na_2CO_3 and K_2CO_3 (Aldrich Chemie GmbH & Co., A.C.S. reagents) have been used for preparing binary (0.53 Li_2CO_3 + 0.47Na_2CO_3 and 0.62 Li_2CO_3 + 0.38 K_2CO_3) and ternary (0.43 Li_2CO_3 + 0.32 Na_2CO_3 + 0.25 K_2CO_3) eutectic mixtures. Weighted amounts of these reagents were fused in an alundum crucible and bubbled by CO_2 for few hours, in order to establish the acid – base equilibrium in the melt. Gases (O_2, CO_2, Ar and H_2) were dehydrated in absorbers containing molecular sieve A5 and P_2O_5. The gas flows were controlled by electronic valves of the F-201C-FA-22 type, (Bronkhorst Hi-tech Co, The Netherlands).

Experimental procedure. Three samples of the given eutectic were placed on the golden plate, in the observation field. The chamber has been tightly closed and the given gas flowed through it during 1 hour, in order to remove air and to obtain the gas atmosphere required. Then, the heating started with a mean heating rate of *ca* 10°/min. The first sessile-drop shape was stored at the melting temperature and after it, the observations were continued every 25°, up the upper limit of the temperature range applied. Due to the reflection on polished golden plate, the shape of the sample was observed together with its reverse reproduction. This effect permitted a very precise determination of the point, at which the tangent to the meniscus curve should be drown.

At the beginning of this investigation, the following parameters were controlled: (i) The accuracy of temperature measurements has been verified by comparing the readings of

the thermocouple – temperature indicator systems in the moment of sample melting, with the melting points of the given eutectic, recommended in the physical and chemical data source [7]. (ii) It has been shown, that the contact angle values determined were independent of the sample mass (of the sessile-drop mass) within 0.02 – 0.08 g range. (iii) It has been shown, that the determined contact angle values were time independent when keeping the sample at constant temperature for 30 min. (iv) It has been shown, that with decreasing the temperature (after reaching its upper limit), the contact angles do not return to their previous values, obtained during the increasing temperature run. With increasing temperature contact angles decrease – wettability is improved. However, the solid surface, once wetted, retains the liquid, when the temperature decreases. This effect is considered as typical for sessile-drop method [8]. Therefore, only contact angle values determined in the increasing temperature run, have been taken into consideration. (v) A series of measurements has been carried out in order to establish the accuracy and the reproducibility of this method of contact angle determination. The contact angle values, measured on both sides of the sessile-drop, were identical inside of the limits of the experimental accuracy. These parameters and their standard deviations have been calculated as average values for 6 independent experimental runs with 3 samples in each experiment, for each eutectic melt, temperature and atmosphere.

VIII.3. Results and discussion

The wetting angles, in O_2, CO_2, Ar and $0.8Ar+0.2H_2$ atmospheres, for three eutectic carbonate melts, are presented in Table 3. These parameters are characteristic for the liquid state. Therefore, in order to compare among three melts under study, the contact angle values are reported as dependent on a temperature parameter (T^*), which is defined by

$$T^* = T - T_f \ , \qquad \text{(VIII.3.1)}$$

(where T_f is the melting point of given eutectic melt), determining the temperature range of existence of the liquid phase, and not as dependent on the absolute temperature.

Differences among these parameters for three melts under study, are evident. In all gas atmospheres used, temperature dependencies of contact angle are quite identical for two eutectics containing K^+ ions, but significantly lower than those for (Li+Na) carbonate melt. This difference is distinct especially for CO_2 atmosphere. Contact angles of (Li+K) and (Li+Na+K) carbonate eutectics, under different atmospheres, do not change much with temperature. Very characteristic is the evident shift of the dependence for (Li+Na) melt to

lower values of the contact angle, with changing of atmosphere, in the sequence $CO_2 \rangle O_2 \rangle Ar \rangle H_2(Ar)$. In the last, reducing atmosphere, the curves corresponding to three different melts, are near each other, nevertheless they are different in the limits of experimental error.

Table 3. Wetting angles at the Au/(0.53 Li_2CO_3 + 0.47 Na_2CO_3), Au/(0.62 Li_2CO_3 + 0.38 K_2CO_3) and Au/(0.43 Li_2CO_3 + 0.25 K_2CO_3 + 0.32 Na_2CO_3) interfaces, as dependent of temperature parameter T*, under different atmospheres. T_f - melting points of the eutectic melts, ref. [7].

T*=T-T_f K	Wetting angle / °											
	0.53 Li_2CO_3 + 0.47 Na_2CO_3; T_f= 769 K				0.62 Li_2CO_3 + 0.38 K_2CO_3; T_f=761 K				0.43 Li_2CO_3 + 0.25 K_2CO_3 + + 0.32 Na_2CO_3; T_f=670 K			
	O_2	CO_2	Ar	0.8Ar+ 0.2H_2	O_2	CO_2	Ar	0.8Ar+ 0.2H_2	O_2	CO_2	Ar	0.8Ar +0.2H_2
	Stand. dev. ± 0.8	Stand. dev. ± 0.6	Stand. dev. ± 0.5	Stand. dev. ± 1.8	Stand dev. ± 0.9	Stand. dev. ± 1.4	Stand. dev. ± 1.3	Stand. dev. ± 1.0	Stand. dev. ± 2.5	Stand. dev. ± 2.2	Stand dev. ± 2.8	Stand. dev. ± 1.0
0	54.2	60.5	50.2	48.8	37.9	45.3	40.2	40.3	38.2	42.8	37.8	39.1
25	52.5	58.5	48.3	48.0	-	-	-	-	-	-	-	-
37	-	-	-	-	36.5	38.7	38.2	39.0	-	-	-	-
50	50.3	57	46.6	44.5	-	-	-	-	-	-	-	-
53	-	-	-	-	-	-	-	-	36.4	40.4	37.5	38.6
62	-	-	-	-	33.6	35.8	36.0	38.0	-	-	-	-
75	43.8	56.4	45	42.5	-	-	-	-	-	-	-	-
87	-	-	-	-	32.8	34.8	34.4	36.6	-	-	-	-
100	42.0	55.0	43.6	40.8	-	-	-	-	-	-	-	-
103	-	-	-	-	-	-	-	-	35.2	38.5	34.6	37.0
112	-	-	-	-	31.1	31.5	32.7	35.2	-	-	-	-
150	40.6	54.8	40.6	39.7	-	-	-	-	-	-	-	-
153	-	-	-	-	-	-	-	-	34.4	34.7	33.8	35.5
162	-	-	-	-	30.0	30.7	31.3	34.5	-	-	-	-

One can conclude qualitatively, that (Li+Na) carbonates electrolyte, in an oxidant gas atmosphere and in the lower part of the experimental temperature, exhibit a lower wettability, than the (Li+K) carbonates. Of course, assuming, that these trends, identified on the Au surface, may be extended for surfaces of other solid materials. However, wettability should be

described not only in terms of contact angle parameters, but rather in terms of work of adhesion on the liquid / solid interface. According to the Young-Dupré equation, the effect of adhesion on the liquid / solid interface may be represented approximately by the W_{sl}, parameter, defined as

$$W_{sl} = \gamma_{lg}\,(1 + cos\Theta), \qquad \text{(VIII.3.2)}$$

where γ_{lg} is the surface tension on the liquid/gas interface, Θ – liquid/solid contact angle. As it may be easily shown, the dimension of the W_{sl} parameter is the work to surface ratio, therefore it signifies the adhesion work per surface unit, with the dimension identical to those of the surface tension parameter for liquid / gas interface.

For calculating the W_{sl} parameter from the obtained contact angle values, data of the respective surface tensions, reported in recommended physical and chemical data source (Janz *et al.* [7,8]), have been used. The respective, linear temperature dependencies for $(Li+Na)_2CO_3$ and $(Li+Na+K)_2CO_3$ eutectics are shown in Fig. 9. For 0.38 Li_2CO_3+0.62 K_2CO_3 system, Selman and Maru in their monograph [9] report also data calculated by interpolation of parameters for pure components, assuming the Guggenheim's rule of additivity. These values are, within the limits of accuracy, equal to the recommended experimental data and have not been presented in Fig. 9. However, as Selman and Maru have emphasized, the above surface tension values have been measured without taking into account the influence of gas atmosphere on this property. Recently, Yamamura *et al.* have measured the surface tensions of 0.38Li_2CO_3+0.62 K_2CO_3 eutectic melt by bubble pressure method, using CO_2, O_2 and Ar, respectively [10]. Also the respective surface tension data of these authors, as dependent on T* parameter, are presented in Fig. 9. As it might be seen from surface tension - temperature dependencies, presented in Fig. 9, the highest values of these functions correspond to (Li+Na) carbonate melt. All (Li+K) carbonate dependencies, considered there, are distinctly lower. Differently, than in respect to contact angle – temperature dependencies, the ternary system of carbonates shows the intermediate values of the surface tension parameters.

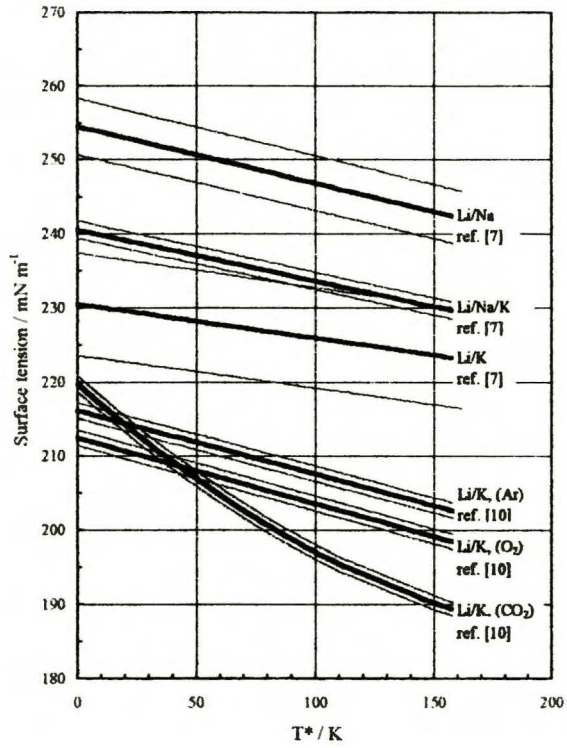

Fig. 9. Dependence of the surface tension of three carbonate eutectic melts, calculated using data reported in refs. [7] and [10], as dependent on the temperature parameter T*. Data from ref. [10] correspond to three different gas atmospheres.

The calculated values of adhesion function W_{sl}, as dependent on T^* parameter, under four different atmospheres, are presented in Figs. 10 – 13, respectively. As it results from diagrams in these figures, such a trend is not reproduced in W_{sl} – T* dependencies. The results of W_{sl} for (Li+K) carbonate eutectic, calculated using surface tension data regarding different gas atmospheres [9], are in all cases lower than all other ones. It should be emphasized, however, that in order to calculate exact values of W_{sl}, one should use surface data appropriate for the given atmosphere. Unfortunately, such data are lacking for Li/Na and Li/Na/K carbonate melts. However, in spite of this indigence of data, one might conclude from Figs. 10-13, that the adhesion parameters are the highest in case of (Li+Na+K) carbonate eutectic melt. Under all gas atmospheres this eutectic shows the same, temperature independent, value of this parameter ca 420 $mN.m^{-1}$. It can not be neglected that, at melting point, this melt shows the lowest basicity among three systems under study. At melting temperatures, the logarithms of equilibrium constant value of thermal dissociation of (Li+Na+K), (Li+K) and (Li+Na) carbonate eutectic melts, according to reaction

$$CO_{3(l)}^{2-} \leftrightarrow O_{(l)}^{2-} + CO_{2\,g}\,, \qquad \text{(VIII.3.3)}$$

(where indexes l and g signify liquid and gas phases, respectively), are –13.44, -11.38 and –9.65, respectively [11], *i. e.*, that, at melting temperatures, O^{2-} ion activities increase in the following sequence: (Li+Na+K) < (Li+K) < (Li+Na) carbonates. Adhesion work parameter values do not repeat this sequence. The respective dependencies for (Li+Na) carbonate melt under inert and reducing atmospheres, are nearly identical with the (Li+Na+K) carbonate ones. In O_2 the same dependence lies also near to the last one, however, its unusual S – shape probably results from the superposition of both experimental functions, Θ and σ - temperature dependencies, in [2]. Differently, in CO_2 the W_{sl} - T* dependence for (Li+Na) carbonates exhibit much lower values, near to those corresponding to (Li+K) carbonate eutectic melt.

Recapitulating the discussion of the results of contact angles measurements and adhesion parameters determination, it may be preliminary concluded that, on Au, the wetting properties of K^+ ion - containing carbonate eutectic melts, are rather not sensible to changes of the gas atmosphere. On the contrary, in molten (Li+Na) carbonates, the electrolyte nowadays considered as very promising in MCFC technology, these properties are influenced distinctly by the gas phase. It may be expected that, under conditions of the fuel cell, even at open-circuit-potentials of the electrodes, the wetting of solids by the last electrolyte is different on the anodic and cathodic sides of the cell.

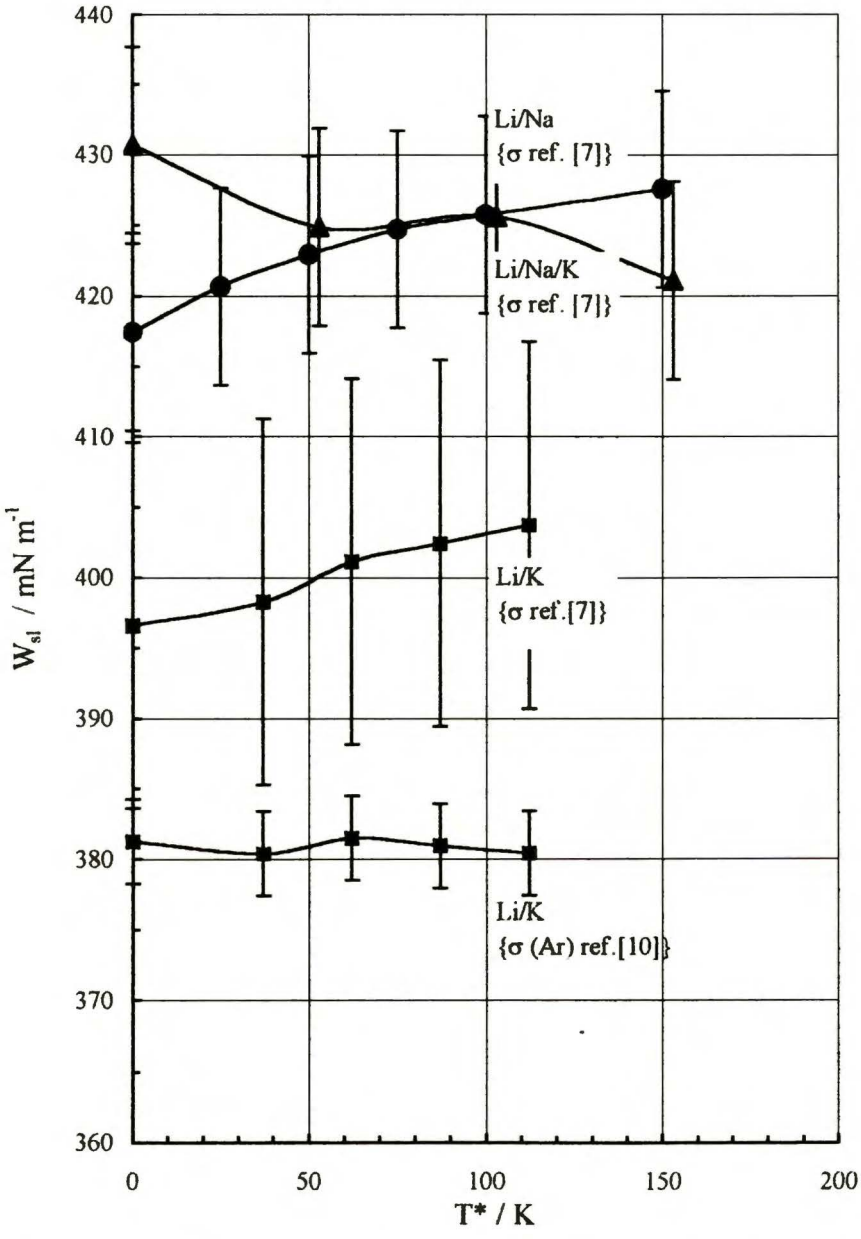

Fig. 10. Dependence of W_{sl} values for three carbonate eutectic melts / Au interfaces, on the temperature parameter T*, in Ar atmosphere.
Calculated according eq. (VIII.3.2), using Θ values from Table 3, and γ values from Fig. 9.

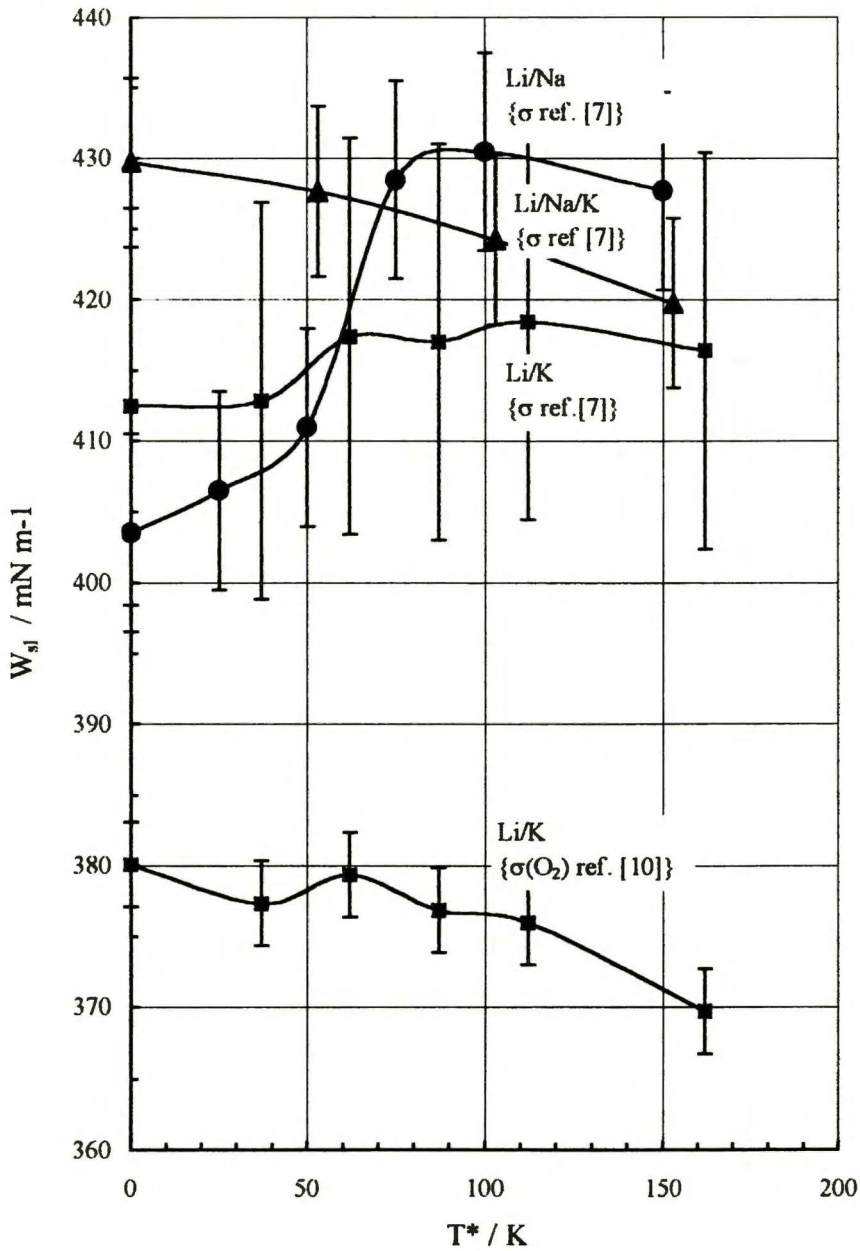

Fig. 11. Dependence of W_{sl} values for three carbonate eutectic melt / Au interfaces, on the temperature parameter T*, in O_2 atmosphere.
Calculated according eq. (VIII.3.2), using Θ values from Table 3, and γ values from Fig. 9.

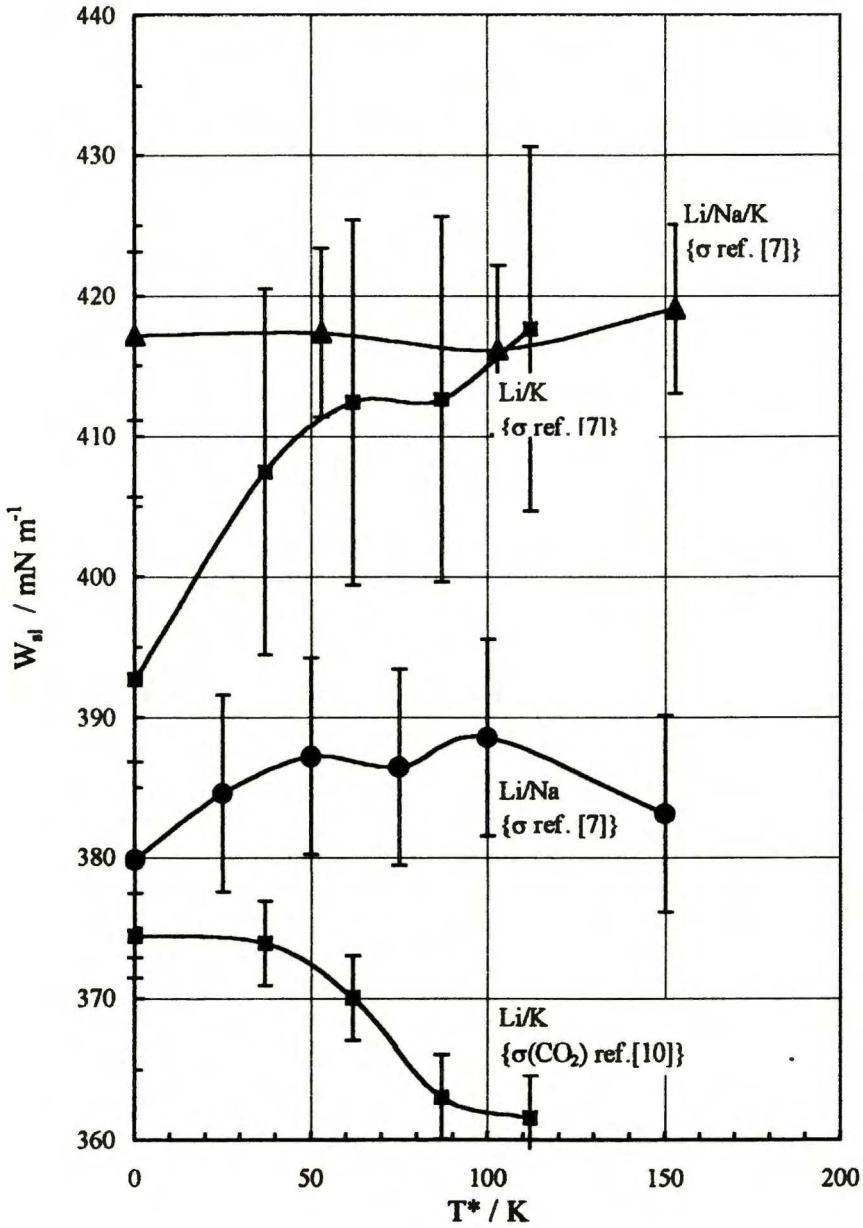

Fig. 12. Dependence of W_{sl} values for three carbonate eutectic melt / Au interfaces, on the temperature parameter T*, in CO_2 atmosphere.
Calculated according eq. (VIII.3.2), using Θ values from Table 3, and γ values from Fig. 9.

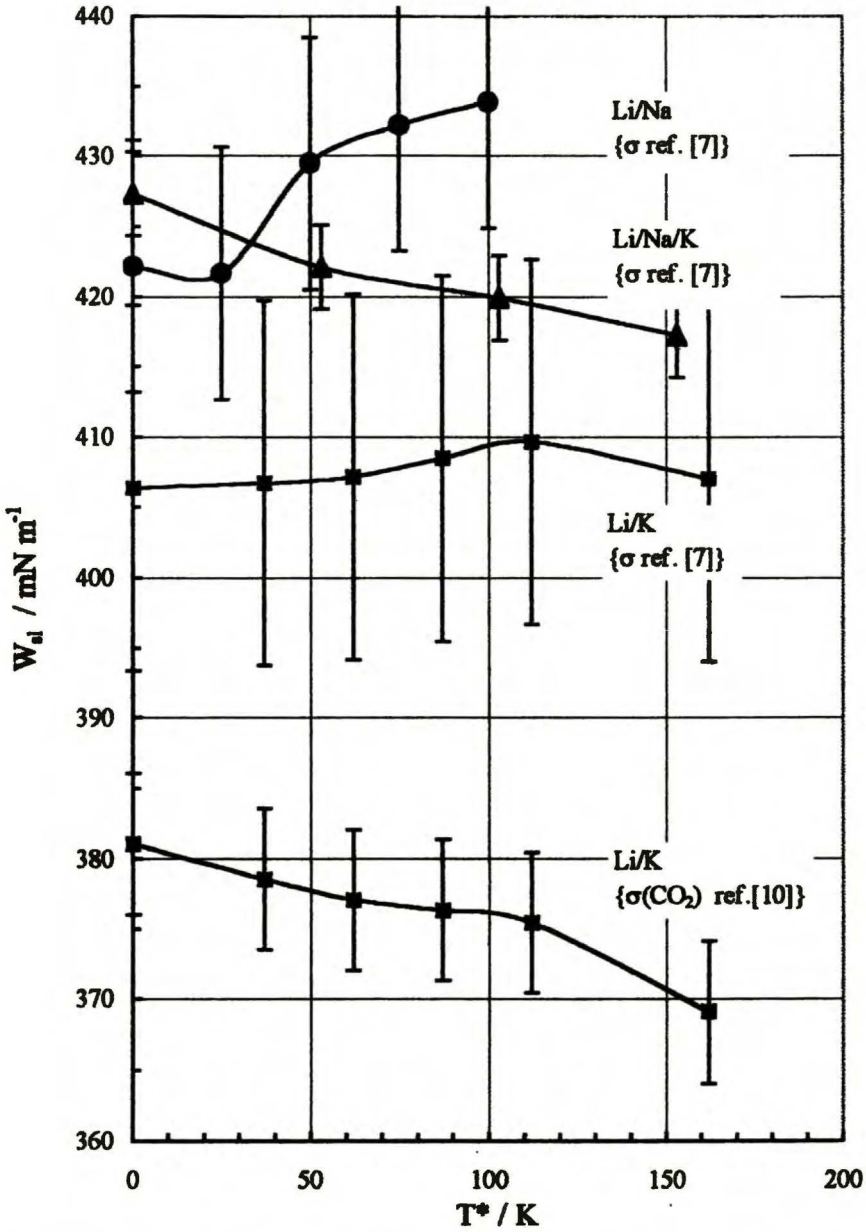

Fig. 13. Dependence of W_{sl} values for three carbonate eutectic melt / Au interfaces, on the temperature parameter T*, in (0.2 H_2 + 0.8 Ar) atmosphere. Calculated according eq. (VIII.3.2), using Θ values from Table 3, and γ values from Fig. 9.

VIII.4. References

1. Matsumura M. and Selman J. R., *J. Electrochem. Soc.*, **139**, 1255 (1992).
2. Mugikura Y. and Selman J. R, *J. Electrochem. Soc.*, 143, 2442 (1996).
3. Mugikura Y. and Selman J. R., *Denki Kagaku*, 64, 491 (1996).
4. Weewer R., Vente J. F., Hemmes K. and de Wit J. H. W., *Proceedings of the Second Symposium on Molten Carbonate Fuel Cell Technology*, Selman J. R. Uchida I., and Shores D., eds., The Electrochemical Society, Inc., Proceedings Volume 90-16, Pennington, NJ, 1990, p. 281.
5. Lundblad A. and Bergman B., *J. Electrochem. Soc.*, 144, 984 (1997).
6. Sishtla C., Donado R., Ong E. and Remick R., *Proceedings of the Fourth International Symposium on Carbonate Fuel Cell Technology*, Selman J. R., Uchida I., Wendt H., Shores D. A. and Fuller T. F., eds, The Electrochemical Society, Inc., Proceedings Volume 97-4, Pennington, NJ, 1997, p. 315.
7. Janz G.J., Allen C. B., Bansal N. P., Murphy R. M. and Tomkins R. P. T., *Physical Properties Data Compilation Relevant to Energy Storage*, II. Molten Salts: Data on Single and Multi-Component Salt Systems, US Department of Commerce, National Standard Reference Data Systems G1, Part II, (Apr. 1979), Washington, DC., 1979.
8. Adamson A. W. and Gast A. P., *Physical Chemistry of Surfaces*, Intersc. Publ., N. Y., 1997.
9. Selman J. R. and Maru H. C., *Physical Chemistry and Electrochemistry of Alkali Carbonates Melts*, Advances in Molten Salt Chemistry, Vol. 4., Mamantov G. and Braunstein J., Eds., Plenum Press, N. Y,. 1981, p. 159.
10. Yamamura T., Sato Y. and Tomczyk P., unpublished results. See also: Tomczyk P., *Oxygen Electrode Reaction in Molten Carbonates*, Institute of Physical Chemistry of the Polish Academy of Sciences, Warsaw, 1996.
11. Andersen B. K., *Doctoral Thesis*, Technical Univ. of Denmark, Lyngby Denmark, 1975.

IX. Wetting of Ni and NiO by alternative molten carbonate fuel cell electrolytes

IX. I. Influence of gas atmosphere

IX.1.1. Introduction

For modeling of processes in the molten carbonate fuel cell (MCFC) stacks, of first importance is a good knowledge of wetting of solid electrode materials by the molten electrolytes. Therefore, several authors have studied this problem, but there are large discrepancies between the results obtained by various research teams. Most of the researches have been focused on Li/K carbonates binary eutectic, because, for long time, this system has been considered as the most appropriate as MCFC electrolyte. Recently, an alternative Li/Na binary molten carbonate eutectic system has become subject of increasing interest. Selman [1] and Weewer [2] have summarized investigations of various authors, concerning wettabilities of solid materials by three alkali carbonate eutectic melts, Li_2CO_3+Na_2CO_3, Li_2CO_3+K_2CO_3 and Li_2CO_3+Na_2CO_3+K_2CO_3.

Most of researches have been carried out on smooth surfaces of solids, which are candidate materials for MCFC porous electrodes. Moiseev and Stepanov [3,4] have studied the wettability of the basic MCFC anode material, Ni, by the molten ternary Li/Na/K carbonate system, Eberhart [1] – by binary Li/K carbonate electrolyte, Johnston *et al.* [1] – by Li/Na, Li/K and Li/Na/K carbonates eutectic melt. In series of investigations by Weewer *et al.* [2,6,8], wettabilities by Li/Na and Li/K electrolytes of some Ni alloys, used in MCFC technology, have been also studied.

Analogous investigations for Li/K carbonates eutectic melt at NiO (lithiated *in situ*) have been carried out by Lessing and Johnston [1] and by Mugikura and Selman [8]. One attempt to determine the wettability of $LiCoO_2$ porous MCFC cathode by Li/K electrolyte has been done by Lundblad and Bergman [11].

Consistency of the results reported in the publications cited above is not satisfactory. Reported contact angles (CA) on Ni and on its alloys, determined under atmospheres containing hydrogen, lie within a large range of values: 10° [5] – 60° [1]. Reported parameters for NiO, in oxidant atmosphere are even more scarce and doubtful. Lessing and Johnston claim 0° CA value at this material [1]. Mugikura and Selman [8], who have had difficulties in observing carbonate meniscus on this dark material, have obtained the same result. Both results refer only to Li/K carbonate system. Summarizing the data reported above, one could conclude, that, (1), in reducing, H_2 containing atmosphere, CA at Ni/molten carbonate interfaces are

within 10-35° [2,5-8], however values as high as 65° are also reported [1]; (2), in oxidizing atmospheres, in case of NiO/molten carbonate interfaces, the zero value of CA is reported by most of authors [1,9,10]. This would indicate a perfect wettability of NiO surface. However, taking into account the impossibility of obtaining a smooth, uniform surface of NiO sample for wettability measurements, one can doubt of the reliability of the diffused opinion, that at the NiO/carbonate interfaces the wettability is perfect.

Influence of solid surface smoothness on the CA values, determined at the given solid/liquid interface, is commonly recognized [12,13]. On the other hand, the smoothness depends strongly on the polishing technique, applied by the experimenter. Therefore, a perfect consistency of CA values for the same solid/melt interface, when reported by various authors, cannot be expected. In order to compare the wettability parameters, corresponding to alternative electrolyte systems, one should dispose of results obtained by the same methods under the same, consistent experimental conditions. Evidently, a comprehensive investigation of wettability of the basic MCFC electrode materials by both alkali carbonate systems, considered as the alternative MCFC electrolytes, performed by the same research team, is still needed.

Experimental determination of CA values at solid/molten alkali carbonate interfaces creates serious experimental difficulties. Some of CA determination methods are not feasible in these circumstances, *e. g.* the capillary-rise method, because do not exist the transparent materials resistant to these ambiences. Methods which have been applied up to now, and which may be considered as appropriate to these melts, are two optical ones: (1), the sessile – drop method, consisting in direct CA measurements from the profile of a drop of the liquid, (2), the meniscus-rise-on-vertical-plate method, consisting in the meniscus height measurement on vertical plate, immersed in the melt, and, (3), the method of direct determination of interfacial forces, consisting in weighting of a solid plate with the Wilhelmy balance, immersed in the melt.

Many investigations in carbonates have been done on gold, which of course is not used in MCFC devices, but it is a pure metal, the most corrosion resistant in molten carbonates. For this reason, Au is used in many investigations in these melts, as reference material. That is also the reason of numerous wettability measurements, performed at Au/molten carbonate interfaces, by three methods mentioned above: by the sessile drop method [1,2,5-8,14], by the method of meniscus rise determination on a vertical plate [9,10,15], and by the Wilhelmy balance methods[16,17]. According to most of the authors, in all gas atmospheres the CA values at Au / carbonate interfaces, cover 50-70° range. However, also at this point

there are some differences among the authors, (*e.g.* Eberhart claims O° CA value!). Nevertheless, for proving the reliability of the experimental methods used, the results on Au should be considered, as reference data. In spite of all possible sources of error [12], the sessile-drop method may be considered as basic one for investigations in molten carbonates media.

Throughout this chapter, an attempt has been done to apply the vertical plate method in determination of CA values at Ni and NiO, in three molten alkali carbonates eutectic systems, because this solid/liquid interface configuration is the only one, which may be adapted to the future, analogous measurements under an electrode overpotential. However, the vertical plate method is not so commonly used and verified as the sessile drop one. The reliability of the data determined by the former method would be considered doubtful, if not confirmed by the last one. Therefore, in order to obtain a consistent set of CA results, characterizing three carbonate eutectic electrolytes, under various gas atmospheres, in this investigation the vertical-plate method has been used for comparative measurements, carried out by simultaneous determination of meniscus heights and/or of CA both on the plate of solid under investigation, and on the Au plate as reference. The meniscus rise and the CA values on the material investigated were determined in every experiment, together with the same parameters for Au. This procedure permitted me a comparison of CA values on Au, determined on vertical plate (both calculated from meniscus rise and directly measured), with those reported in the previous chapter [14], determined by the sessile-drop method.

IX.1.2. Experimental

Principles of both optical methods of CA determination: of the sessile-drop and of the meniscus-rise-on-vertical plate ones, and configurations of solid/liquid interfaces in these both methods, are schematically presented in Fig. 8a and 14, respectively. On vertical plate two parameters may be measured: meniscus height and, directly, the contact angle, as well. Details of the sessile-drop measurement procedure are described in chapter VIII. For direct determination of CA on vertical plates only external menisci have been used (as indicated in Fig. 14) because those between two plates were deformed by superposition of different capillary forces [18].

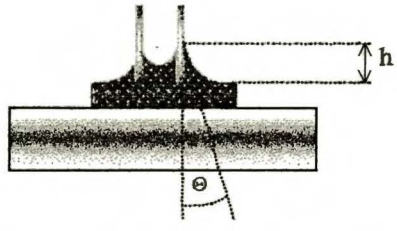

Fig.14. Schematic principle of the contact angle determination by meniscus rise at vertical plate . Θ - contact angle, h - meniscus height.

Experimental set-up. – For observation of the meniscus rise on vertical plate the experimental set-up has been used, schematic cross section of which is presented in Fig. 15. This set-up was composed of a heated chamber and of an optical observation system. The heating system of the chamber permitted of getting the temperature range up to 700° C in 20 min, due to the heating element, supplied by electrical current of varying frequency, and to the silver radiation screen, inserted around the heating space. Special attention has been devoted to the insertion of the Pt-PtRh10 thermocouples in such manner, that the measured temperature corresponded perfectly to the one of the sample under investigation. The chamber was gas tight, what permitted the control of the supplied gas atmosphere. Observation windows have been fabricated from synthetic leuco-sapphire, showing a perfect molten carbonate corrosion resistance in these conditions, and an excellent transparency for visual observations.

The gold crucible (Ø 0.65 cm, 0.17 cm height), filled with the melt under study, in which vertical solid plates (Au 0.7x0.25x0.03 cm and Ni 1.0x0.25x0.03 cm or NiO single crystal 0.75x0.2x0.17 cm) have been immersed (Fig. 14), was placed on Au plate (2.0x1.6x0.1 cm). The shape of the sample was photographed or directly observed through the MST –131 optical stereomicroscope (PZO, Poland) and through the MS-486P CCD camera, on a TV monitor screen, and stored in the computer memory. Due to an appropriate computer program, both CA and meniscus height values have been measured from the computer picture of the sample and stored in digital form.

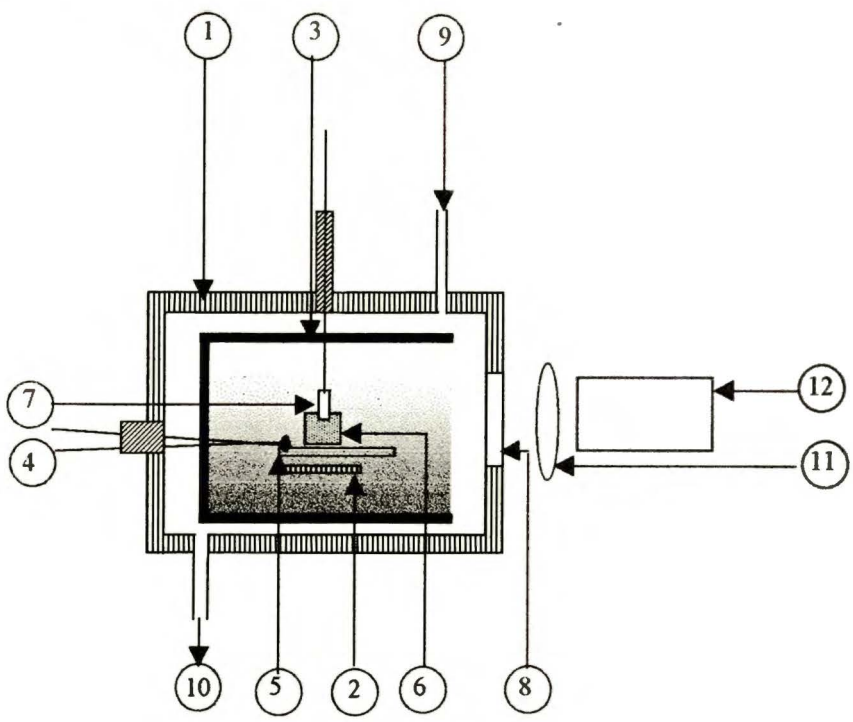

Fig. 15. Schematic cross-section of the chamber for contact angle measurements, (vertical-plate option). 1, steel chamber case; 2, heating element; 3, silver radiation screen;4, Pt-PtRh 10 thermocouple; 5, Au plate; 6, Au crucible; 7, vertical plate under investigation; 8, synthetic leuco-sapphire window; 9, gas inlet; 10, gas outlet; 11, stereomicroscope; 12, CCD camera.

Reagents and gases. – Li_2CO_3, Na_2CO_3 and K_2CO_3 (Aldrich Chemie GmbH & Co., A.C.S. reagents) have been used for preparing binary (0.53 Li_2CO_3 + 0.47Na_2CO_3 and 0.62 Li_2CO_3 + 0.38 K_2CO_3) and ternary (0.43 Li_2CO_3 + 0.32 Na_2CO_3 + 0.25 K_2CO_3) eutectic mixtures. Gases (O_2, CO_2, Ar and H_2) were dehydrated in absorbers containing molecular sieve A5 and P_2O_5.

Preparation of the Au surface for CA measurements. – Au plates for both sessile-drop and vertical-plate measurements were prepared by mechanical polishing using, successively, Alumina Polishing Powder 3 μm and Alpha-Alumina-Suspension 0,3 μm (Polysciences, Inc., Warrington, PA, USA).

Preparation of the Ni and NiO surfaces for CA measurements. – Ni plates, for both sessile-drop and vertical-plate measurements, were prepared by mechanical polishing using, successively, Alumina Polishing Powder 3 μm and Alpha-Alumina-Suspension 0,3 μm (Polysciences, Inc., Warrington, PA, USA).

Properties of the NiO scale on Ni are commonly known. It is evident, that one cannot obtain a continuous, smooth surface of this oxide by simple oxidation of this metal. Probably this is the main source of experimental difficulties in determination of CA at NiO. In this investigation, such a continuous and smooth NiO surfaces have been applied under two forms: (1), as a layer deposited by ion-sputtering on Au, (2), as NiO single crystal. The NiO single crystals, doped with 0.7 mole percent Li_2O, prepared by Verneuil method, has been kindly supplied by Mr. J. Obłąkowski (The Technical University of Mining and Metallurgy, Material Science Faculty). The samples of this material have been used in this Laboratory in a series of electrochemical researches in molten carbonates [19,20].

A set of investigations have been carried out in order to elaborate deposition of NiO layer on Au, using ion-sputtering method in oxygen atmosphere, under 1500 V voltage, by current of 35 mA. Two alternative gas atmospheres under 0.15 hPa pressure have been used in the ion-sputtering procedure: O_2, permitting a direct deposition of NiO layer, or Ar+H_2, giving a deposited layer of Ni, which next has been oxidized in O_2, at temperature of 500° C during 2 hours. Layers of *ca* 400 nm thickness were obtained after 4.5 hours. Adherence of the deposited layers to the Au background, has been tested by mechanical bending and elution by carbonate melts during 2 hours at 650° C, as dependent on ion-sputtering time. The NiO layers obtained directly by ion-sputtering in O_2 have shown insufficient corrosion resistance, and the Au background appeared in X-ray analysis throughout them. Therefore, these layers have been considered as not appropriate for wettability study.

In Figs. 16-18 there are presented results of proofs of the adhesion properties, performed at the NiO layer, obtained by ion-sputtering of Ni on Au in reducing atmosphere, and then oxidized in O_2, as described above. In Fig. 16 it may be seen, at the left side of the SEM picture, a layer of frozen Li/K carbonate melt, deposited there in order to proof the resistance of the NiO layer on Au to corrosion and erosion by molten carbonates. The corrosion resistance test consisted in subjecting of NiO layer surface to molten carbonates during 2 hours at 650° C, and then, after solidification, in removing of the carbonate layer. The uncovered NiO surface may be seen at the right side of this picture. At the left one, which corresponds to the surface covered by molten carbonates, one can see the starting point of the linear scan of X-rays microanalysis performed through both parts of the surface under investigation. In Fig. 17, one can see the result of this scanning. In the middle of the 1st scan, signed SE, is shown the boundary of the investigated surface in two parts, the covered by solid carbonates and the uncovered one. In the "CKa" scan, the X-ray signal for carbon is reported, proving that carbonates have been completely removed from the right part of the surface. This is even better visible in the potassium, "KKa" scan. The oxidation of the surface is proved by oxygen partition, which is practically the same in both parts of the surface (scan "OKa"). The scans, which are crucial in this test, are the "AuMa" and "NiKa" ones. The signal due to the Au background must be visible, even if the covering layer of the sputtered metal is thick. Very thick layers are not feasible by the procedure described, moreover, such a layer would be not well adhesive to the Au background. Sufficient covering by NiO of this background is proved, first of all, by the last, "NiKa" scan. These conclusions are well supported by the results of X-ray surface qualitative analysis, presented in Fig. 18, where the fields corresponding to the elements determined are denoted by the same symbols, as in Fig. 17. These results indicate that the NiO layers obtained by ion-sputtering in reducing atmosphere and then oxidized, have shown a satisfactory chemical stability in molten carbonate ambiences, as well as their good adherence to the surface of Au. Therefore, layers prepared by the last procedure have been considered as appropriate for wettability measurements.

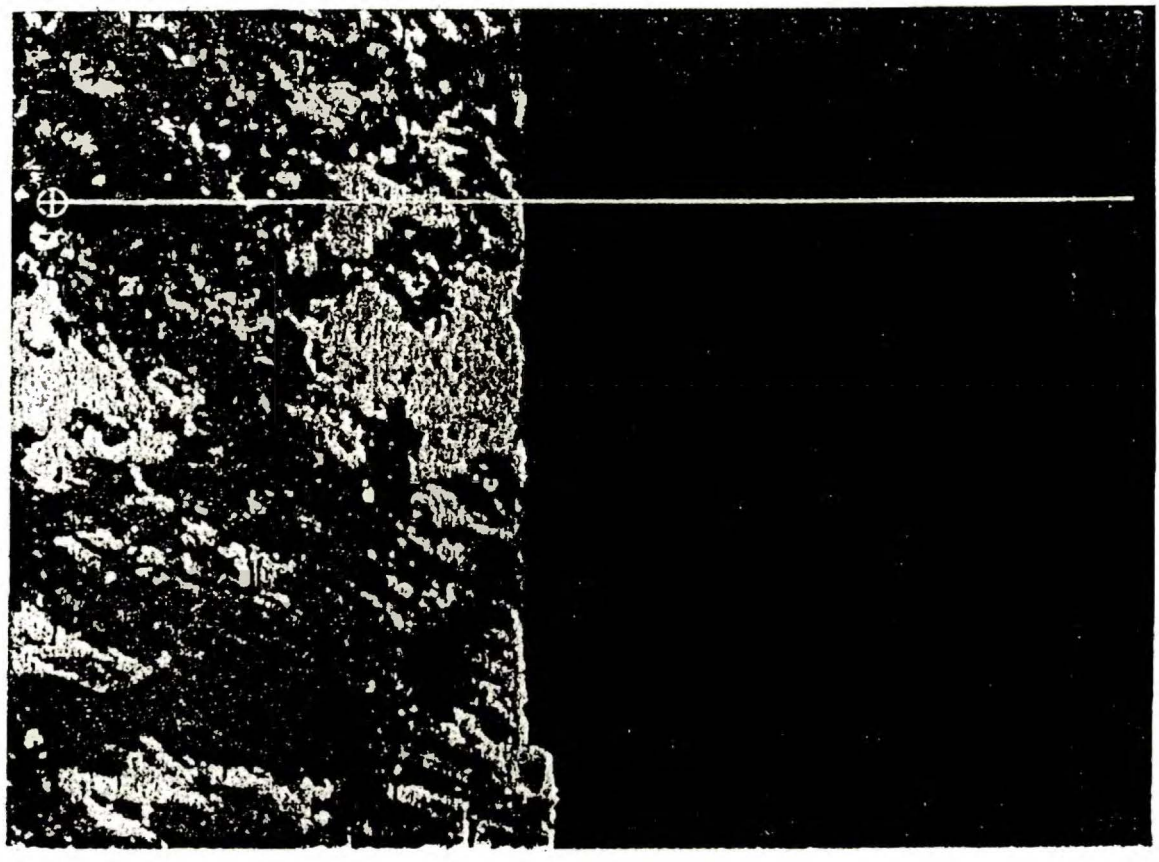

Fig. 16. SEM picture of the NiO layer on Au, obtained by ion-sputtering of Ni in H_2 atmosphere and oxidation (right side of the picture) and of the solidified layer of Li/K carbonate, deposited for testing the resistance of NiO layer to carbonate corrosion (left side of the picture). (⊕ - Starting point of the X-ray linear analysis scan (see Fig. 17). Magnification 1000x.

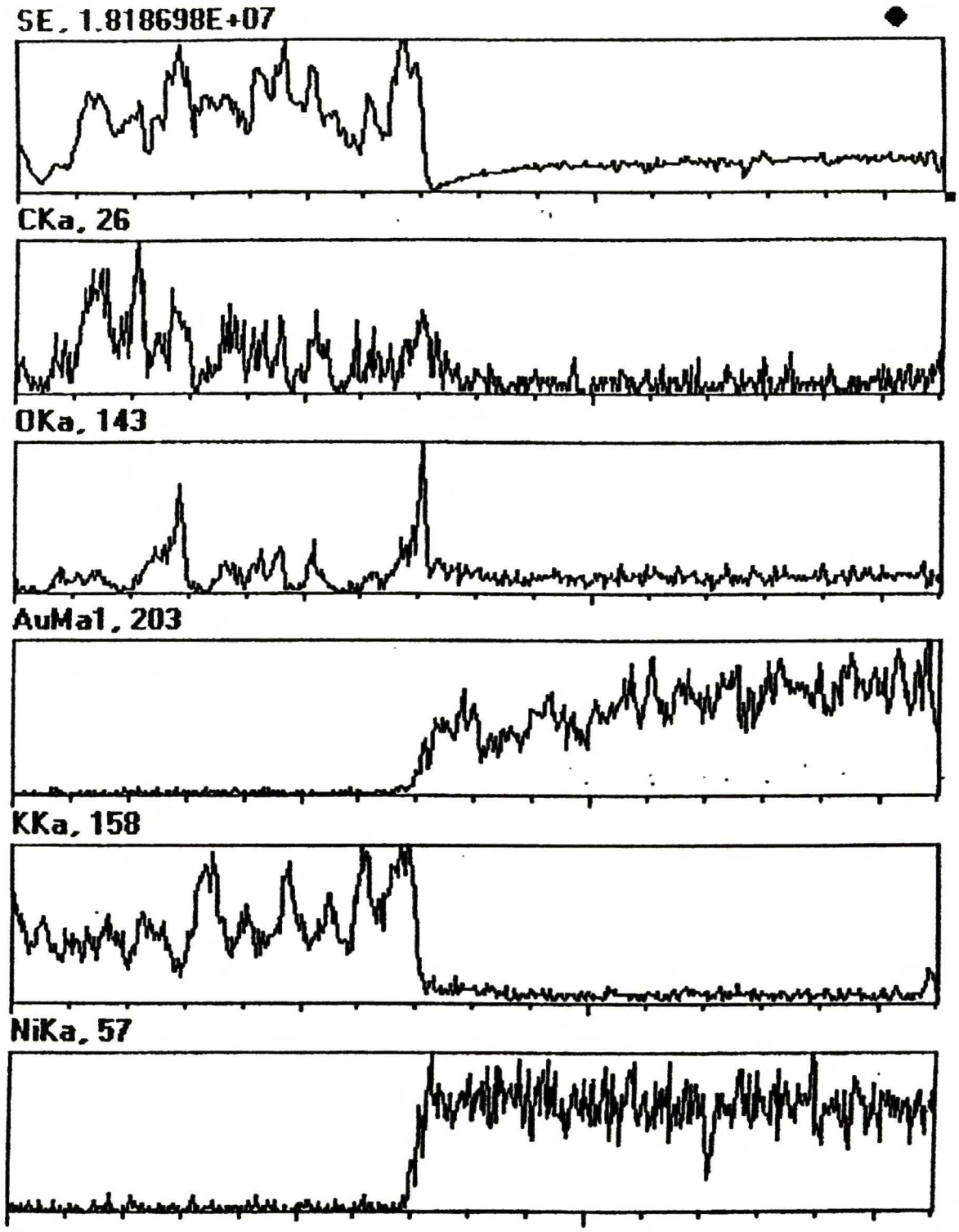

Fig. 17. X-ray linear analysis of the NiO layer deposited on Au, partially covered by solid carbonates. Symbols of scans: SE – division of the sample in two fields; CKa – carbon signal; OKa – oxygen signal; AuMa – gold signal; KKa – potassium signal; NiKa – nickel signal.

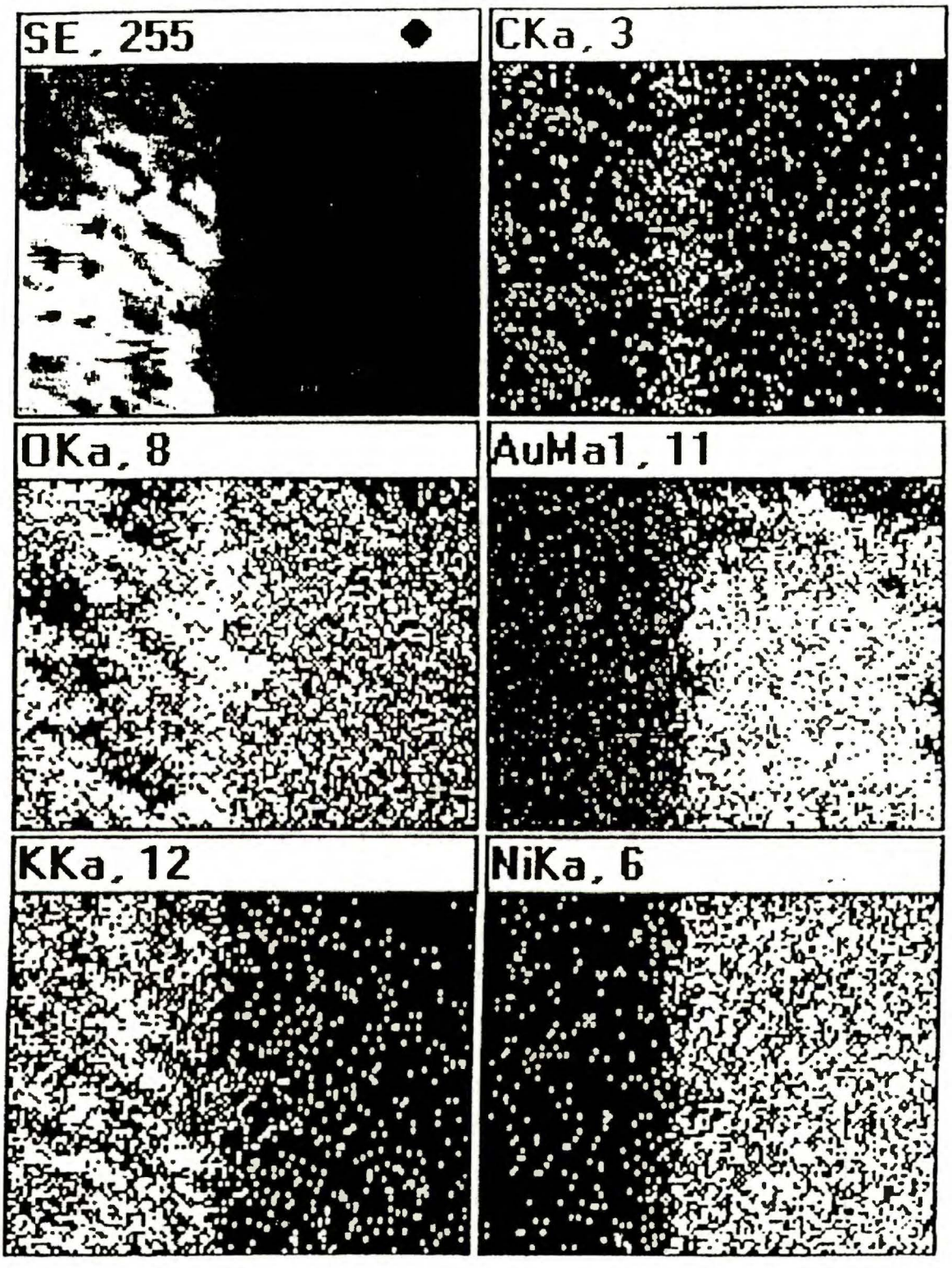

Fig. 18. X-ray surface analysis of the NiO layer deposited on Au (right sides of pictures), partially covered by solid carbonates (left sides of pictures). Symbols of pictures: SE – partition of the sample in two fields; CKa – carbon signal; OKa – oxygen signal; AuMa – gold signal; KKa – potassium signal; NiKa – nickel signal.

Experimental procedure. – Before the CA measurements, weighted amounts of alkali carbonates were fused in an alundum crucible and bubbled by CO_2 for few hours, in order to establish the acid – base equilibrium in the melt. Solid plates under investigation were placed in the chamber, in the observation field. Then samples of prepared melts were placed in the gold crucible, and inserted in the chamber, under controlled gas atmosphere. The chamber has been tightly closed and the given gas flowed through it during few hours (oxidizing atmosphere), or during 24 hours (H_2 atmosphere), in order to remove air and to obtain the gas atmosphere required. Then, the heating started with a mean heating rate of *ca* 10°/min. After fusing carbonates, the lower parts of the investigated plates were submerged in the melt. Parameters investigated were determined at increasing temperature [14].

IX.1.3. Results and Discussion

Comparison of CA on Au determined by the sessile-drop and vertical-plate methods. Both meniscus height and directly CA have been measured by the vertical-plate method, giving two independent possibilities of determination of this parameter, as presented in Fig. 14. The CA determination by the second way is analogous to the sessile-drop method, with only difference, that in the last case the meniscus of the liquid is convex, whereas the meniscus of liquid rising on the vertical solid plane is concave. Therefore, one should expect that the CA values determined by both methods must be consistent.

Another is the problem of CA determination from the height of liquid meniscus rising on the smooth solid plate, partially immersed in the liquid. The formalism of this height determination is known for the case of a capillary of circle cross-section, which is not directly applicable to the plate surface. To the last case Neumann has applied the Hagen formula [21,22]

$$\sin\Theta = 1 - \frac{\rho g h^2}{2\gamma_{lg}}, \qquad \text{(IX.1.3.1)}$$

which should permit me calculation of the CA value, as dependent on the meniscus height, h, when density of the liquid, ρ, gravity acceleration, g, and liquid surface tension, γ, are known. The validity of Hagen-Neumann formula, however, has been verified only for the case of various liquids wetting the same solid surface. This formula has been applied by Selman *et al.* to the electrocapillary curves determination on Au, Ni and NiO, in molten Li/K carbonates [8-10].

My preliminary intention was to use this formula in determination of CA values for two parallel vertical plates, one of which ought to be Au, whereas the second one – Ni or NiO, respectively. In such a case of two different solids, immersed in the same liquid, the

ρ, g, γ, parameters cancel, and, from ratio of two different h parameter values, the wetting angle on one solid plate may be determined directly, when the CA value for the second solid plate is known. All the vertical-plate measurements on Au have been carried out in parallel with the respective determinations on Ni or NiO, inserted in the same crucible, in order to calculate the CA values from the meniscus height ratios. Unfortunately, for two different solids in the same liquid – what is our case -, the way of determination the CA using the Hagen-Neumann formula in this reduced form, has been shown not reliable. The differences in meniscus heights between two different solid plates were too high and the values of *sin* of the CA to be determined, calculated according to formula (IX.1.3.1), are out of the limits of ±1. On the other hand, comparison of the CA values for Au in three eutectic melts, under both oxidizing (O_2) and reducing (0.2 H_2 + 0.8 Ar) gas atmospheres, measured directly from the meniscus shape on the vertical plate, to the ones determined by the sessile-drop method, show satisfying consistency. This one can see in Fig. 19, where the respective results are presented as dependent on temperature. The consistency of both set of values obtained in O_2 atmosphere is perfect, however, also in H_2+Ar it is satisfying.

As conclusion of this part of the investigation, one can consider the direct method of CA determination from the profile of the carbonate melt meniscus, wetting a vertical plate, as accurate and reliable as the sessile-drop method. Therefore, this method has been used in further part of this investigation, to Ni and NiO.

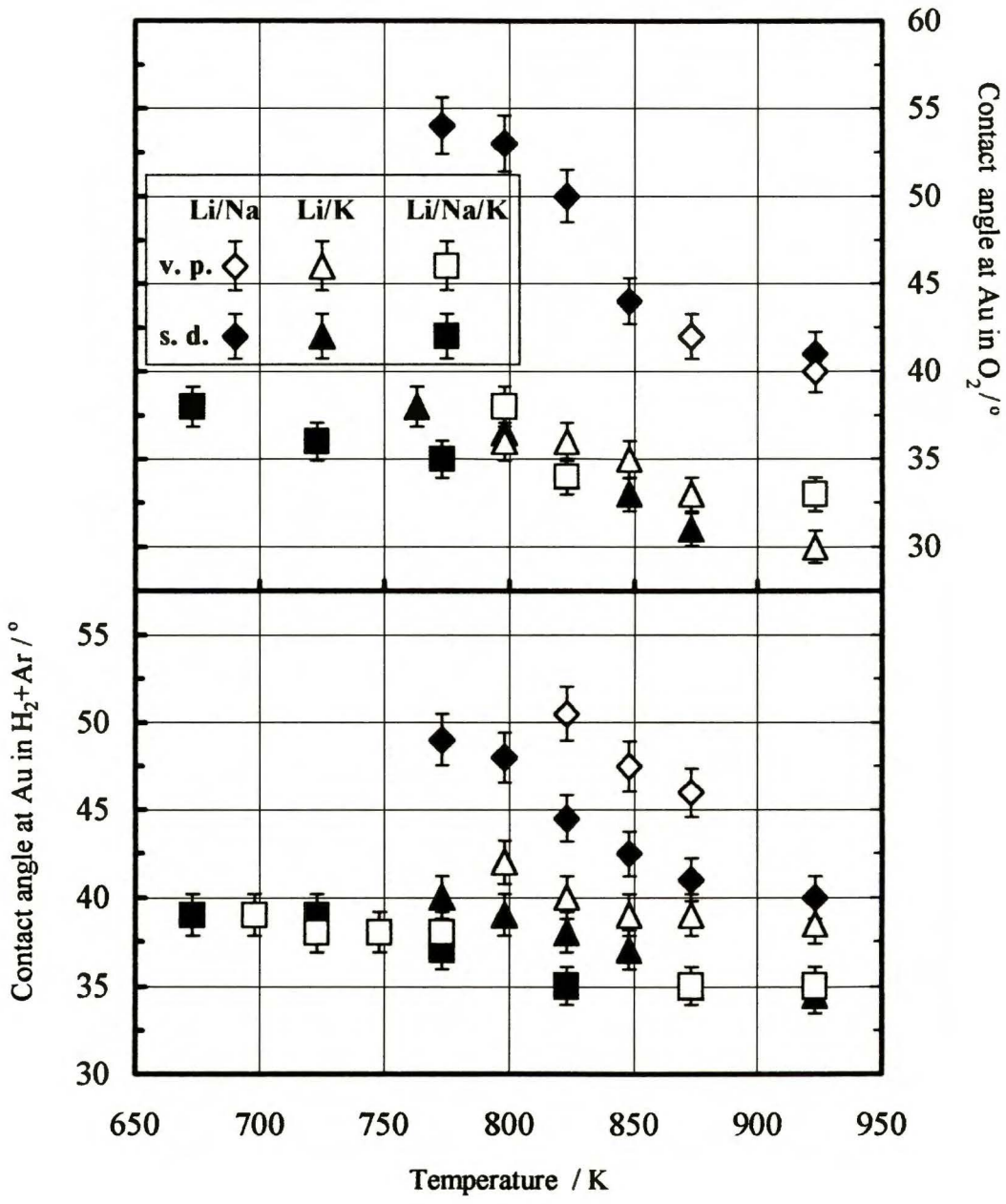

Fig. 19. Comparison of CA - temperature dependencies, determined on Au by the sessile drop method, (s. d.), with those determined by the vertical plate method, (v. h.), under O_2 (upper diagrams) and 0.2 H_2 + 0.8 Ar atmospheres (lower diagrams), in three carbonate eutectic melts.

CA on Au in three carbonate electrolytes, under O_2 and H_2+Ar atmospheres. A complete set of respective data has been reported in the previous chapter [14], however, for comparison, some essential conclusions are to be repeated here. It has been shown there that the CA values on Au are distinctly dependent on the carbonate eutectic melt compositions and only slightly dependent on the gas atmosphere. In both gas atmospheres investigated, the CA are quite identical for two eutectics containing K^+ ions, but significantly lower, than those for

Li/Na carbonate melt. The former two melts show also a quite identical and very small decrease of contact values with temperature, whereas for the last melt such a decrease is much more distinct. On base of CA measurements, one can conclude, that Li/Na carbonates electrolyte, in oxidant gas atmosphere, especially in lower temperature range, show lower wettability, than the Li/K carbonates one. The CA on Au of K^+ ion - containing carbonate eutectic melts are less dependent on gas atmosphere than those of molten Li/Na carbonates.

In respect to the CA temperature dependencies, our results differ essentially of those obtained recently by Kamping *et al.* [16,17], on Au / Li/K melt interface in air, using Wilhelmy balance, who have found an opposite wettability on temperature dependencies.

CA on Ni under H_2+Ar and on NiO under O_2 atmosphere, in three eutectic melts. In view of future electro-capillarity studies, as mentioned above, on base of the consistency between both methods of direct CA determination – of the sessile-drop and of the vertical-plate ones-, all the respective measurements at Ni and NiO surfaces have been carried out in the vertical-plate configuration. The results of the CA determinations on Ni are presented in Fig. 20, and on NiO – in Fig. 21, respectively.

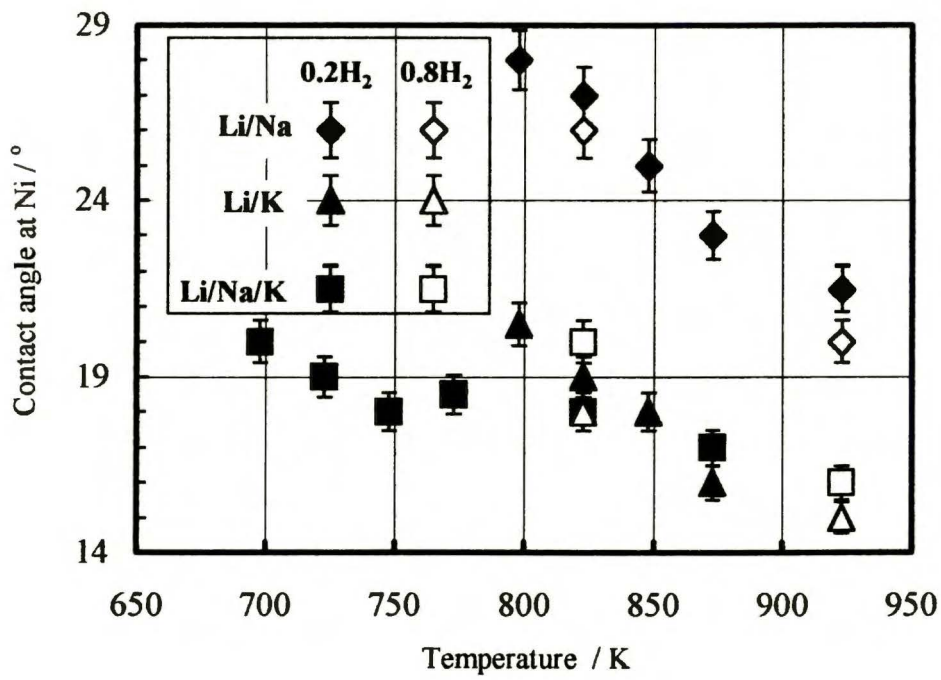

Fig. 20. CA. - temperature dependencies, determined by the vertical plate method on Ni, under 0.2 H_2 + 0.8 Ar and 0.8 H_2 + 0.2 CO_2 atmospheres, in three carbonate eutectic melts.

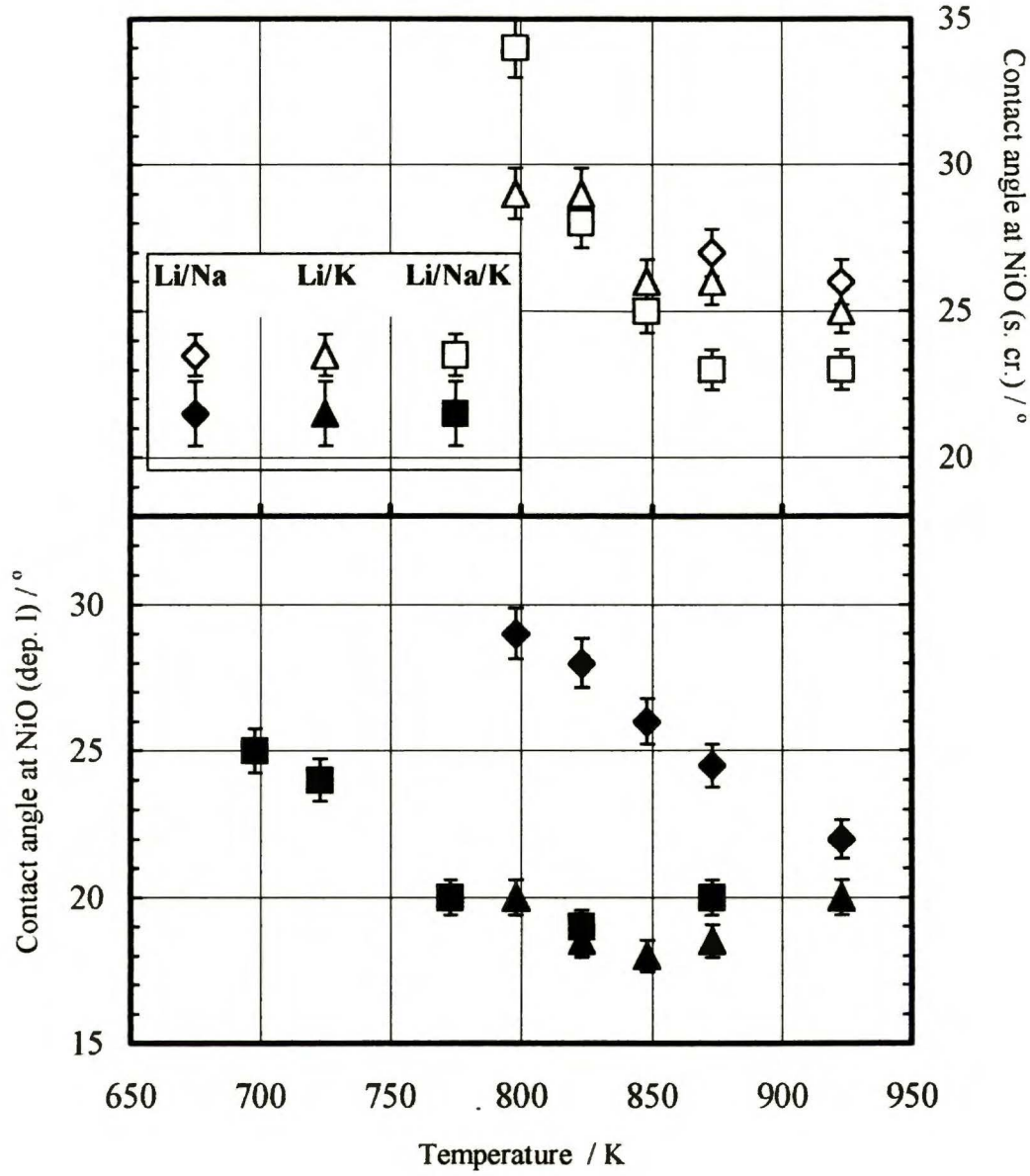

Fig. 21. Comparison of CA - temperature dependencies, determined on NiO single crystal (s. cr. - upper diagrams), with those determined on NiO deposited layers (dep. l. - lower diagrams), under O_2 atmosphere, in three carbonate eutectic melts.

In measurements on Ni under H_2 atmosphere, well reproducible CA results have been obtained, however, only when a perfect reduction of metal surface had been reached, after 24 hours of flashing of the chamber by the reducing gas. Some experiments have been carried out under 0.8 H_2 + 0.2 CO_2 atmosphere, similar to the fuel gas mixture, used in MCFC. Respective points are also reported in Fig. 20. The results obtained are very well consistent with the basic set of experiments, in spite of differences in hydrogen concentration. Depending on the melt composition, the CA values at Ni lie within 15 – 30°, which is well consistent with the results of Weewer [2] and Moiseev and Stepanov [3].

A perfect consistency of carbonate melt composition effect on CA values for Ni and Au, has been found in 0.2 H_2 + 0.8 Ar atmosphere. This may be seen when comparing data in Figs. 19 and 20. In Table 4 there are reported ratios of the CA value at Au, to the one at Ni, for three eutectic melts, at temperatures of 25° above the melting points, and at 600° C. First values in the column have been calculated using sessile-drop results for Au, whereas the second - using the vertical-plate ones. Reasonable constancy of these ratios proves that the influence of the melt composition on the CA at both metal surfaces is practically the same. As it may be seen in Fig. 20, the same differences in wettability of Ni, like this of Au, have been shown between Li/Na carbonate electrolyte on one side and on both melts, containing K^+ ion on the other. CA of Li/Na carbonate eutectics are higher and show a higher decrease with temperature, whereas both Li/K and Li/Na/K eutectics behavior is practically identical and CA of these melts only slightly decrease with temperature.

Table 4. Ratios of contact angle value on Au to the one on Ni under 0.2 H_2 + 0.8 Ar atmosphere. Contact angles on Ni by vertical-plate method, contact angle on Au by sessile-drop method (1st values) and by vertical-plate method (2nd – values); m. p. - melting point.

Temperature °C	Li/Na carbonate	Li/K carbonate	Li/Na/K carbonate
m. p + 25	1.7; 1.9	2.0; 2.2	2.0; 2.3
600	1.8; 2.0	2.3; 2.5	2.1; 2.1

As concerns wettability of NiO, application of two forms of this compound in our investigation should be emphasized. CA on both investigated forms of NiO, on the NiO layer deposited by ion sputtering and on NiO single crystal, determined in three eutectic melts, under O_2 atmosphere, are reported in Fig. 21. In this case, experimental points are more dispersed than those corresponding to Ni in hydrogen atmosphere, however, one can conclude that CA values lie within 18 - 35° what is evidently inconsistent with the 0° value (a perfect wettability) reported by in the literature [1,9] for NiO in molten Li/K carbonates. My result could be disputable in view of the possible non-homogeneity of the NiO layer on Au, in which some contents of Au cannot be excluded by X-rays analysis. However, on NiO single crystal, values of CA within 23 – 35° have been obtained, even higher, than those on NiO deposited layers, what should be considered as an appropriate consistency. This conclusion could not be formulated on base of results obtained on NiO, prepared by simple oxidation of Ni plates submerged in carbonate melt, under oxidizing atmosphere [9].

However, the differences among wettabilities of NiO by the studied melts may be reasonably evaluated only using data obtained on NiO deposited layers. CA on NiO single crystal are scarcer and less reproducible. The thin Au foil covered by a thin layer of NiO has a heat capacity much lower than those of the NiO single crystal sample. Using this second, chemically purest form of NiO, has enabled me to verify the range of respective CA values at its surface, because some contribution of Au base to the properties of NiO deposited layers cannot be excluded. However, at given temperature of all the optical observation space, temperature measured by the thermocouple may differ from the one really corresponding to the surface of the sample investigated, much more in case of single crystal, than in case of the NiO deposited layers. Therefore, in order to establish the influences of melt compositions on CA on NiO, measurements carried out on deposited layers of this compound are more appropriate.

A proof of the consistency of the melt influence on contact angles, determined on NiO deposited layer and on Au, in O_2 atmosphere, is presented in Table 5. Parameters reported there have been calculated by the same way, as values reported in Table 4. On base of these CA ratios one can see that the wettability of NiO is influenced by O_2 in a very similar manner by all three carbonate eutectic melts. These CA ratios show that like in Au case, Li/Na melt wets the NiO smooth surface better than two other carbonate melts and that the respective temperature dependencies are also similar to those for Au surface.

Table 5. Ratios of contact angle value on Au to the one on NiO (deposited layer) under O_2 atmosphere. Contact angles on NiO by vertical-plate method, contact angles on Au by sessile-drop method (1st values) and by vertical-plate method (2nd – values); m. p. - melting point.

Temperature °C	Li/Na carbonate	Li/K carbonate	Li/Na/K carbonate
m. p + 25	1.8; 1.6	1.8; 2.1	1.4; 1,5
600	1.7; 1.6	1.7; 2.0	1.6; 1.7

CA on Au and on NiO in three eutectic melts, under CO_2 atmosphere. – Both oxygen and hydrogen atmospheres used as oxidant and fuel gases in MCFC, give rise to the formation of new ionic entities in molten carbonates, *i. e.* of superoxide ions in the first atmosphere, and of hydroxide ions in the second one. Special attention should be paid to the CO_2 atmosphere, where no new ionic components are formed in the melt, and where oxide ion concentration is the lowest possible.

A set of CA measurements have been carried out on Au in CO_2 as well as on both forms of NiO in this gas and in standard mixture 0.33 O_2 + 0.67 CO_2. These results are presented in Figs. 22 and 23, the first of which is a comparison of data obtained on Au and on NiO in CO_2, whereas the second is a comparison of data for NiO in both CO_2 and O_2+CO_2 atmospheres.

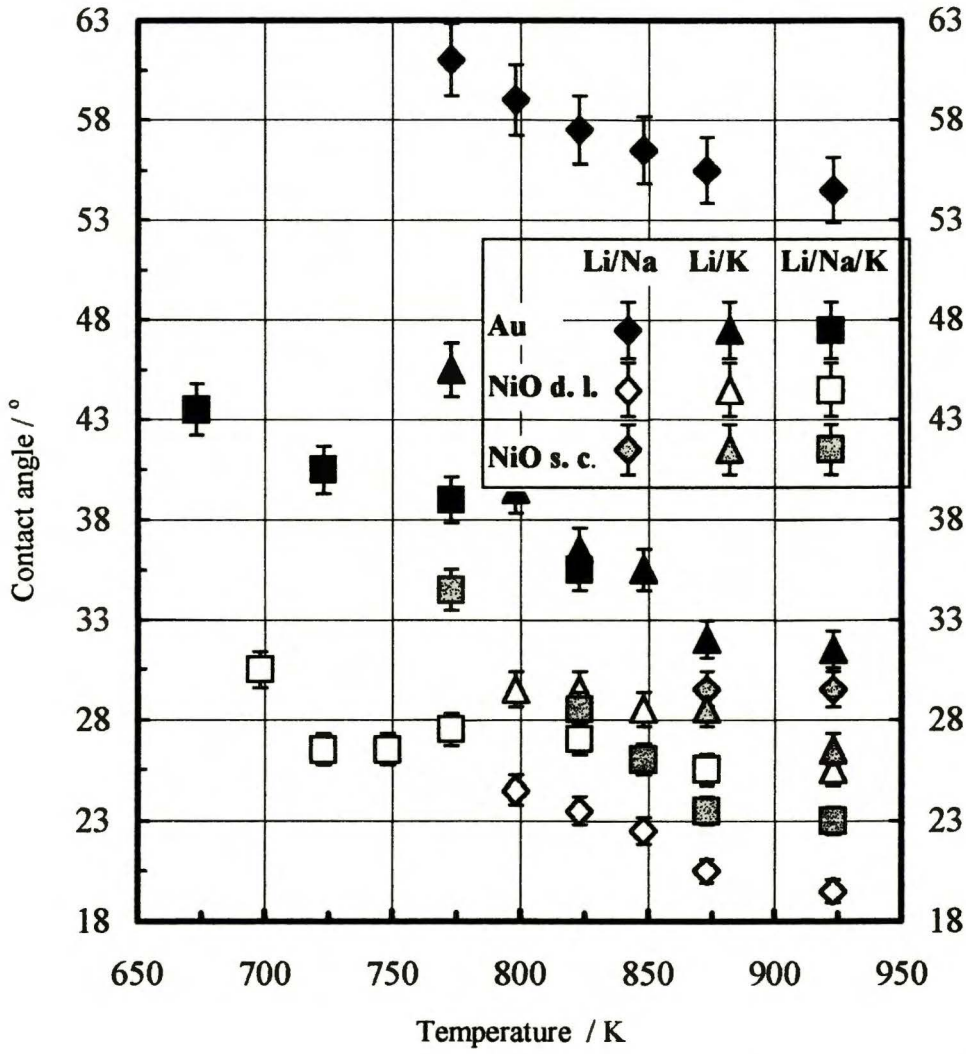

Fig. 22. Comparison of CA - temperature dependencies, determined by the sessile drop method on Au, with those determined by the vertical plate method on NiO deposited layers and on NiO single crystal, under CO_2 atmosphere, in three carbonate eutectic melts.

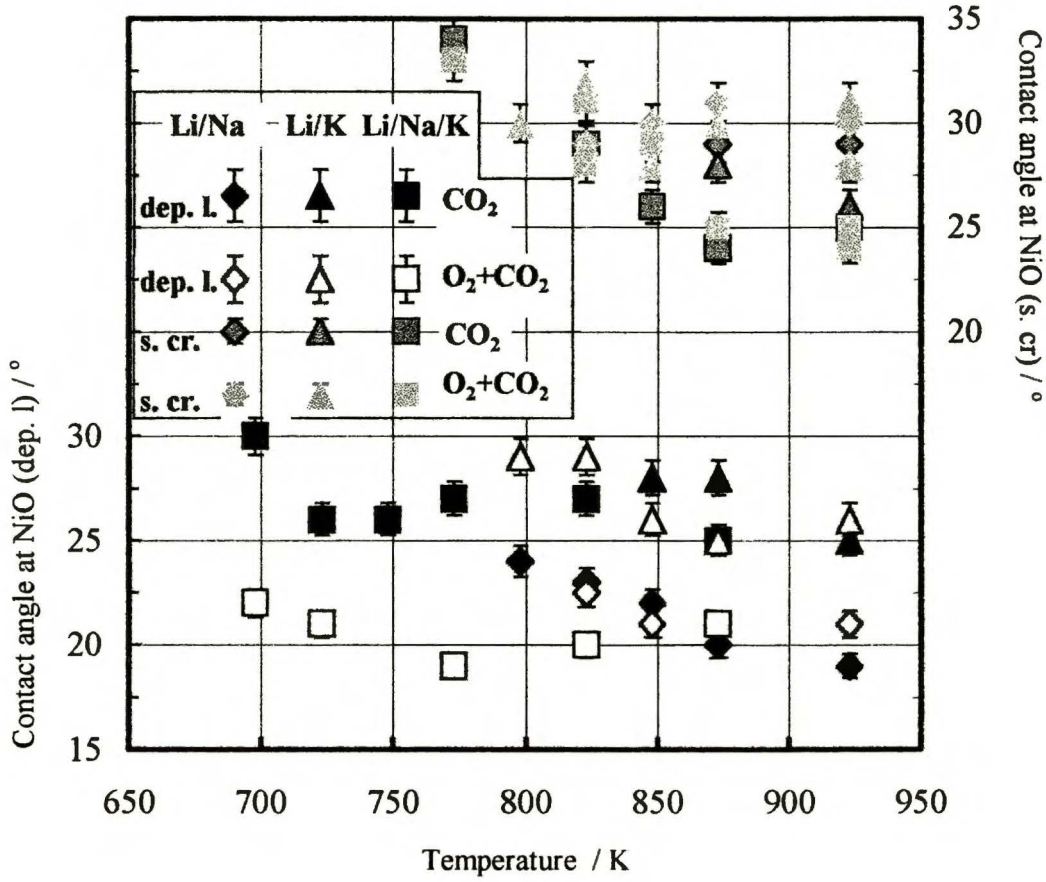

Fig. 23. Comparison of CA - temperature dependencies, determined by the vertical plate method on NiO deposited layers and on NiO single crystal, under CO_2 atmosphere with those determined by under $0.33O_2 + 0.67\ CO_2$ atmosphere, in three carbonate eutectic melts.

Dependencies for Au (Fig. 22) show the same typical trends of the melt composition influence on CA values on this metal. Values for Li/Na carbonates are the highest, whereas for Li/K and Li/Na/K are nearly equal and lower. Behavior of the NiO surface does not reproduce this sequence. Values of CA determined on NiO deposited layer in three melts lie within the 19 - 30°, whereas on NiO single crystal - within 23 - 34°. It is difficult to find some regularity from these scattered data, however one can conclude that CA of Li/Na carbonate are not higher of those of two other melts. Analysis of data presented in Fig. 23 give rise to analogous conclusion. Addition of O_2 to the CO_2 atmosphere does not change, within the limits of experimental error and reproducibility, the values of CA in three melts studied. One can conclude only that in presence of CO_2, CA on NiO in three eutectic melts are very near, with only remark, that on NiO single crystal these parameters are a little bit higher than those on NiO layers, deposited on Au by ion sputtering.

Temperature dependencies of CA on Ni and on NiO. As it results from all the data reported in this chapter, the CA values on Ni and NiO are less dependent on temperature, than

those on Au. On base of these results only small decrease of the CA values with temperature may be concluded. Another words, a small increase of NiO/molten carbonates wettability properties with temperature, analogous to the Au case, results from this study. Moreover, it may be supposed that the temperature measured by the thermocouple is, in some extent, higher than the real temperature of the wetted surface, due to the heat capacity of the vertical plate. Possibly, a heat flow may take place, due to some temperature gradient through this plate. If so, eliminating this effect, even larger decrease of CA values would be obtained. Therefore, I am unable to confirm the results for Li/K carbonate melt by Kamping *et al.* [16,17], who claim the increase of CA values with temperature.

Qualitative interpretation of experimental results. Equilibrium basicities of three melts under study follows sequence Li/K<Li/Na/K<Li/Na [4]. This sequence is projected on the CA values of these melts at metallic gold: these values are the highest in case of the most basic Li/Na carbonate melt, whereas near values determined for both other melts do not deny such a regularity, which has been shown in O_2, H_2 and CO_2 atmospheres as well.

However, metallic gold (like Ni in reducing atmosphere) is a material chemically inert in molten carbonates, whereas NiO is not. The reactivity of NiO in three carbonate eutectic melts seems to be manifested in CA values determined at NiO thin layers, deposited on Au by ion sputtering. In pure O_2 atmosphere, at the lowest CO_2 partial pressures, oxide ion concentrations in three melts are the highest possible and the Ni^{2+} ion equilibrium concentrations are the lowest. Therefore, the process of nickel elution from the NiO deposited layer influences in the lowest extent its wettability by carbonate melts. Another are circumstances under CO_2 atmosphere, where the oxide ion concentrations are the lowest and those of Ni^{2+} ions - the highest. In these cases the nickel elution from NiO thin layers seems to make the Au background increasing the CA values. This effect should be the most intensive when the least basic is the melt. In fact, the CA values at NiO deposited layers in Li/Na melt are the lowest and those of Li/K - the highest. This behavior has been shown in both pure CO_2 and O_2+CO_2 standard mixture, whereas it not evident in diagrams concerning NiO single crystal, the surface of which is very poorly reactive. Therefore, CA values determined on it are practically, in the limit of experimental points scattering, independent of the melt composition.

IX.1.4. Conclusions

(1) For the first time, CA at Ni and NiO / molten carbonate interfaces have been measured in three eutectic systems, under both oxidizing and reducing atmospheres, in temperature range from melting points to 650° C. These parameters have been compared to the respective ones, measured on Au as reference material. Some conclusions, important for MCFC developers, may be formulated.

(2) Wettability of solid surfaces by molten carbonates is not only depending on their nature, but is also a physical property characteristic for a given molten carbonate system. Dependence on the melt basicity is evident. At Au, Li/Na carbonate eutectic shows the highest CA values (the lowest ability of wetting) in all gas atmospheres studied - in O_2, CO_2 and in H_2 containing gas mixtures. Data for Li/K and Li/Na/K carbonate melts are lower but very near each other. The same is behavior of metallic Ni under reducing atmosphere.

(3) Important conclusions concern the wettability of NiO. Till now, qualitative results reported in the literature have indicated a perfect wettability of this substance by molten carbonates (0° CA value), probably because a smooth surface of NiO was not attainable for the researches. My results, consistent for both NiO deposited layers and for single crystal, show, that the CA, characteristic for a smooth surface of this compound, are a well determined values, even higher than for Ni. Influence of melt compositions on CA at NiO in O_2 follows the melt basicity sequence, like in the Au case. In CO_2 containing atmosphere, the Ni^{2+} ion elution processes seems to make melt composition dependencies more complicated. All determined data have shown decreasing of CA with temperature. In general, the influence of the electrolyte composition seems to be more important at the MCFC anodic material (Ni) in reducing atmosphere than on the cathodic one (NiO) in oxidant atmosphere. In reducing atmosphere the Li/Na electrolyte shows evidently higher CA values, however more temperature dependent than the K^+ ion containing melts. It should be emphasized, however, that these conclusions cannot be directly extended on the sintered powders of the materials studied.

IX.1.5. References

1. J. R. Selman, *Wetting and oxidation of metals by molten carbonates*, Workshop on MCFC – Stockholm – February 20-22, 1995, documentation from the lecture, Kungl Tekniska Hogskolan, Stockholm, 1995.
2. R. Weewer, *Study of electrochemical processes and wetting phenomena at the molten carbonate fuel cell anode*, Doctoral thesis, Delft Technical University, Delft, 1991.
3. G. K. Moiseev and G. K. Stepanov, *Trudy Inst. Elektrokhim. Akad. Nauk SSSR, Ural'sk. Filial.* nr 8, 103 (1966).
4. J. R. Selman and H. C. Maru, *Physical Chemistry of Alkali Carbonate Melts*, [in] *Advances in Molten Salt Chemistry*, Vol. 4, G. Mamantov, J. Braunstein, Eds. Plenum Press, N. Y., 1981, p. 159.
5. M. Fisher and P. S. Bennett, *J. Mater. Sci.*, **26**, 749 (1991).
6. R. Weewer, J. F. Vente, K. Hemmes and J. H.W. de Vitt, *Ber. Bunsenges., Phys. Chem.*, **94**, 967 (1990).
7. R. Weewer, J. F. Vente, K. Hemmes and J. H. W. De Vitt, *Proceedings of the Second Symposium on Molten Carbonate Fuel Cell Technology*, J. R. Selman, I. Uchida, D. A. Shores eds., The Electrochemical Society, Inc., Proceedings Volume 90-16, Pennington, N.J., 1990, p. 281.
8. J. M. Fisher, P. S. Bennett, J. F. Pignon, R. C. Makkus, R. Weewer and K. Hemmes, *J. Electrochem. Soc.*, **137**, 1493 (1990).
9. Y. Mugikura and J. R. Selman, *J. Electrochem. Soc.*, **143**, 2442 (1996).
10. Y. Mugikura and J. R. Selman, *Denki Kagaku*, **64**, 491 (1996).
11. A. Lundblad and B. Bergman, *J. Electrochem. Soc.*, **144**, 984 (1997).
12. A. W Adamson., *Physical Chemistry of Surfaces*, Fifth Edition, J. Wiley & Sons, Inc., N. Y., 1990.
13. A. Marmur, *Langmuir*, **12**, 5704 (1996).
14. A. Godula-Jopek and L. Suski, *Polish J. Chem.*, **72**, 1045 (1998).
15. M. Matsumura and J. R. Selman, *J. Electrochem. Soc.*, **139**, 1255 (1992).
16. H. Kamping, *Electrocapillary effect of gold in molten carbonate measured by Wilhelmy balance*, Delft University of Technology, Delft, 1994.
17. W. H. A. Peelen, K. Hemmes, H. Kamping, M. Bos and J. H. W. De Wit, *J. Solid State Electrochem.*, **2**, 334 (1998).
18. P. A. Kralchevsky and K. Nagayama, *Langmuir*, **10**, 23 (1994).
19. L. Suski, J. Obłąkowski and P. Tomczyk, *Ceramics Int.*, **13**, 197 (1987).
20. P. Tomczyk, *Oxygen Electrode Reaction in Molten Carbonates*, Institute of Physical Chemistry of the Polish Academy of Sciences, Warsaw, 1996.
21. A. W. Neumann, *Z. Phys. Chem., Neue Folge*, **41**, 339 (1964).
22. A. W. Neumann and D. Renzow, *Z. Phys. Chem., Neue Folge*, **68**, 11 (1969).

IX.2. Influence of the electrode overpotential

IX.2.1. Introduction

In molten carbonate fuel cells (MCFC) the electrolyte is distributed among three porous beds: two electrodes, Ni anode and NiO cathode, and ceramic ($LiAlO_2$) matrix tile. This distribution is dependent of the wetting phenomena at these interfaces. Mugikura and Selman[1] have shown that the force balance in porous anode/electrolyte matrix/porous cathode system may be described, with good approximation, by the equation

$$cos\Theta_a / cos\Theta_c = d_a / d_c, \qquad (IX.2.1.1)$$

where Θ_a and Θ_c are CA at anode/electrolyte and cathode/electrolyte interfaces, respectively, d_a and d_c are mean anode and cathode pore diameters, respectively. When the fuel cell is charged the contact angles (CA) are dependent on the electrode overpotentials and electrocapillary equilibria are shifted to new values. The electrolyte distribution among three porous beds, established in the not loaded cell (at open circuit potentials of the electrodes – OCP), changes when the current is generated. At given electrode overpotentials a part of the electrolyte is moving from one electrode to the other. Therefore, the porous size distribution of both electrodes should be optimized taking this effect into consideration. Equation (IX.2.1.1) gives me a possibility to calculate only the optimal ratio of the mean pore sizes for the Ni anode and lithiated NiO cathode, both at OCP and at given overpotential, using the respective CA values, experimentally determined. Mugikura and Selman [1] have calculated this ratio for the MCFC system with Li/K carbonate electrolyte at 650° C, for uncharged cell as well as for the cell under load. However, these authors have assumed a nearly 0° value of CA at NiO surface. Respective data for the alternative, Li/Na carbonate electrolyte have not been determined till now. In the chapter IX.1 I have presented results of CA values measurements at the interfaces: basic MCFC electrode materials / molten carbonate electrolytes [2]. In order to furnish comparative data concerning differences in wetting of Ni and NiO under reducing or oxidizing atmospheres, respectively, CA values for three molten alkali carbonate systems - binary (0.53 Li_2CO_3 + 0.47 Na_2CO_3 and 0.62 Li_2CO_3 + 0.38 K_2CO_3) and ternary (0.43 Li_2CO_3 + 0.32 Na_2CO_3 + 0.25 K_2CO_3) eutectic mixtures - have been measured. It has been shown that CA values at NiO surfaces, both at thin NiO layers deposited on Au and at lithiated NiO single crystal, are within 20-30° in all electrolytes studied. In this chapter, it has been determined the influence of electrode overpotentials, on CA values, both at Ni anode (under standard mixture

of 0.8 H_2 + 0.2 CO_2) and at NiO single crystal cathode (under standard mixture of 0.33 O_2 + 0.67 CO_2), at constant temperature. These gas mixtures correspond to commonly used in the MCFC, fuel and oxidant gases, respectively. Also the ranges of overpotentials applied to the electrodes have been limited to those adequate to MCFC polarization. Measurements have been carried out at 650° C – the usual MCFC operation temperature. In order to obtain comparative data, an analogous set of experiments has been carried out using Au as both cathodic and anodic reference materials.

CA values at Ni, NiO and Au under electrode overpotential, but only in Li/K eutectic carbonates electrolyte, have been extensively investigated by Selman *et al.*[1,3-5]. These authors have used the method of meniscus rise measurements at vertical plates, partially immersed in the melt. The Au electrode in Li/K carbonates melt has been used also in investigation, performed by Kamping *et al.*, who have applied the Wilhelmy balance method, under air atmosphere [6,7]. However, the results obtained at gold only, are far to be directly applied for modeling the MCFC processes. All the above studies have been done in order to determine the electrocapillary effects in the systems investigated, in a large range of both positive and negative overpotential values. In this chapter, a comparison of the respective behavior among three electrolytes is reported only within the range of electrode overpotentials (from 0 to +0.300V at the Ni and Au anodes and from 0 to –0.400V at the NiO and Au cathodes), at 550°C and 650°C temperatures. Determination of the respective full electrocapillary curves has not been the aim of this research, whereas the main parameters of the experiments, overpotential ranges, gas mixture compositions and temperature, were near of those of the operation of MCFC stacks.

IX.2.2. Experimental

As it results from data presented in the chapter IX.1 [2], the meniscus-rise determination method, used by Selman *et al.* [1,3-5] may be a source of unexpected difficulties. On the other hand, the more correct sessile-drop method consists in such a solid/liquid configuration, that impossible is the application of three electrodes system, required, when to the solid plates the electrode overpotential is applied. Therefore, in this investigation, it has been used a method of CA measurements at the meniscus formed by the electrolyte at the vertical electrode, partially submerged in the liquid. The correctness of such a CA determination method has been verified in the previous chapter [2]. Also in the present investigation, in all experiments, two vertical

plates, one of Ni (or NiO), the other one of Au, have been immersed in the melt, permitting us using, alternatively, one of them as working electrode, the other as the reference one. NiO has been used only under the form of the single crystal [2].

Experimental set-up. The heating chamber used in optical observation of CA measurements has been described in the chapter IX.1 [2]. Also in the present investigation it has been used the gold crucible (Ø 0.65 cm, 0.17 cm height), filled with the melt under study. In the electrolyte have been immersed the vertical, solid plates (Au 0.7x0.25x0.03 cm and Ni 1.0x0.25x0.03 cm or NiO single crystal 0.75x0.2x0.17 cm). The crucible has been placed on a golden plate (2.0x1.6x0.1 cm) to which the counter electrode overpotential has been applied. For direct determination of CA on vertical plates only external menisci have been used (as indicated in because those between two plates were deformed by superposition of different capillary forces [8]. Polarization of electrodes has been carried out using the EP-20A Potentiostat. The configuration of solid electrodes and the simple circuit for polarization measurements are presented in Fig. 24.

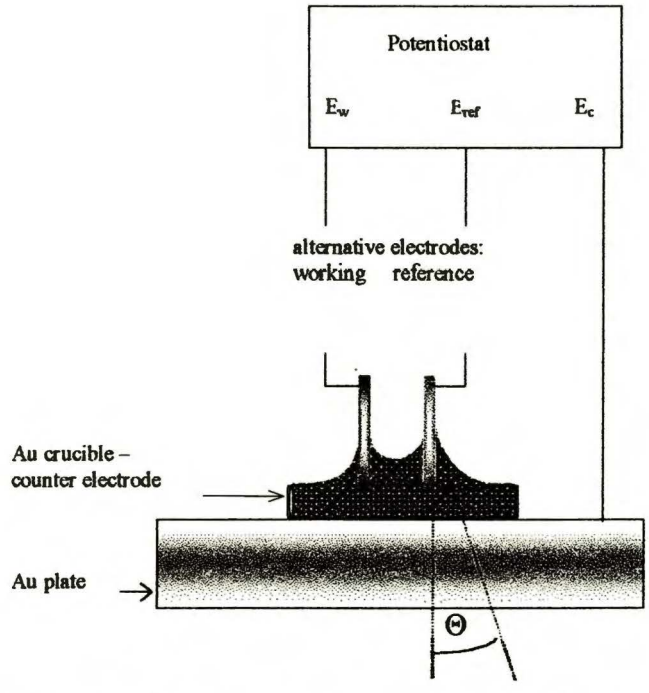

Fig. 24. Configuration of vertical electrodes in contact angle – electrode overpotential dependencies investigation.

Reagents and gases, preparation of the solid plates. Reagents, gases and preparation of metallic plates (Au and Ni) have been described in the chapter IX.1 [2]. The NiO single crystals, doped with 0.7 Li atom percent, have been prepared by the Verneuil method.

Experimental procedure. In order to establish the initial acid – base equilibrium in the melt before the CA measurements, weighted amounts of alkali carbonates were fused in an alundum crucible and flashed by CO_2 for few hours. Solid plates under investigation and samples of prepared melts were placed in the gold crucible, and inserted in the heated chamber. This chamber has been tightly closed and flashed by the given gas during 24 hours in the reducing gas (0.8 H_2 + 0.2 CO_2 mixture), or during few hours in the oxidizing gas (0.33 O_2 + 0.67 CO_2 mixture), in order to remove air and to obtain the gas atmosphere required. Then samples have been heated to the measurement temperatures – 550° and 650° C under reducing atmosphere, 650° C under oxidizing atmosphere. After fusing carbonates, the lower parts of the investigated plates were submerged in the melt. CA measurements have been performed at constant temperatures, within the limits of maximum ± 5°. Such a constancy of temperature was satisfying when taking into account the dependencies of CA on temperature, determined previously [2]. The overpotential has been applied to the given plate as working electrode, *vs.* the second plate as reference electrode, using the Au crucible as counter electrode. Before applying of the constant overpotential pulses, the potential differences between the working and the reference electrodes, the OCP value have been measured as long, as its constancy has been observed within the limits of ± 5mV. Then the constant-overpotential-pulse was applied and the CA value was determined. This procedure was repeated every 0.025 V, starting from +0.025 up to +0.3 V (reducing atmosphere), or from –0.025 up to –0.4 V (oxidizing atmosphere), and back. After every pulse, the system has been relaxed as long as the starting, stationary OCP value has been obtained. Every series of measurements have been repeated twice.

IX.2.3. Results and discussion.

All results of this investigation indicate a rather small influence of both anodic and cathodic overpotentials on CA values at Ni, NiO and Au. In order to make the determined effect more accented, increments of CA values under given overpotential in respect to the one corresponding to OCP values, defined as

$$\Delta\Theta(\eta) \equiv \Theta_\eta - \Theta_{OCP}, \qquad \text{(IX.2.3.1)}$$

(where Θ_η and $\Theta_{\eta=0}$ are CA values at given electrode overpotential η and at OCP potential, respectively,) are reported on diagrams.

Anodic process In Figs. 25 and 26 there are presented the increments of CA values at Ni under 0.8 H_2 + 0.2 CO_2 atmosphere, in three carbonate eutectic melts, at 550° and 650° C, respectively. In molten alkali carbonates, under hydrogen containing atmosphere, within the overpotential range of 0 to +0.30 V used in this investigation, at both Au and Ni electrodes, the hydrogen anodic oxidation takes place according to the overall reaction

$$H_2 + CO_3^{2-} \rightarrow H_2O + CO_2 + 2e \qquad \text{(IX.2.3.2)}$$

At higher overpotential the Ni electrode become unstable because of the anodic oxidation of this metal. It is not so in the case of Au electrode, which may be polarized up to the overpotential values corresponding to the next electrochemical reactions. Selman *et al.* [1,3-5] have detected the maximum on the electrocapillary curve at Au near the overpotential value of +0. 2 V. Comparison of results at the Ni electrode (Figs. 25 and 26) to those at the Au one may be done using the data in Figs. 27 and 28. Data obtained by Mugikura and Selman [1] for Ni and Au / Li/K carbonate interfaces, respectively, under reducing atmosphere with low hydrogen concentration, at 650° C, are also reported in Figs. 26 and 28. In spite of differences in hydrogen concentrations used by these authors and in this study, there is no an essential discrepancy between the results for both these metals. Analogous measurements have been carried out also at 550° C, however, the CA increments have shown to be negligibly low.

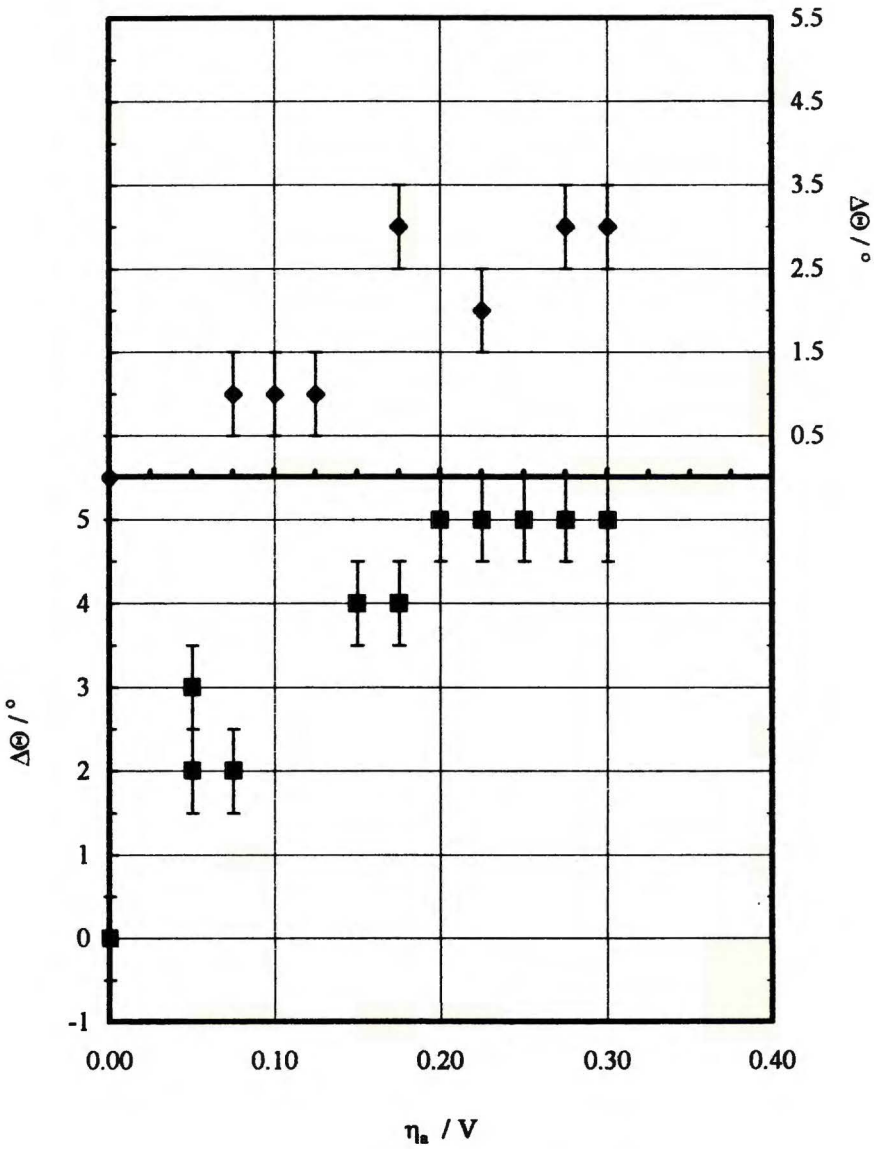

Fig. 25. Contact angle increment ($\Delta\Theta$) as dependent on Ni electrode overpotential (η_a), under 0.8 H_2 + 0.2 CO_2 atmosphere, at 650° C. Upper diagram – Li/Na carbonates electrolyte; lower diagram – Li/Na/K carbonates electrolyte.

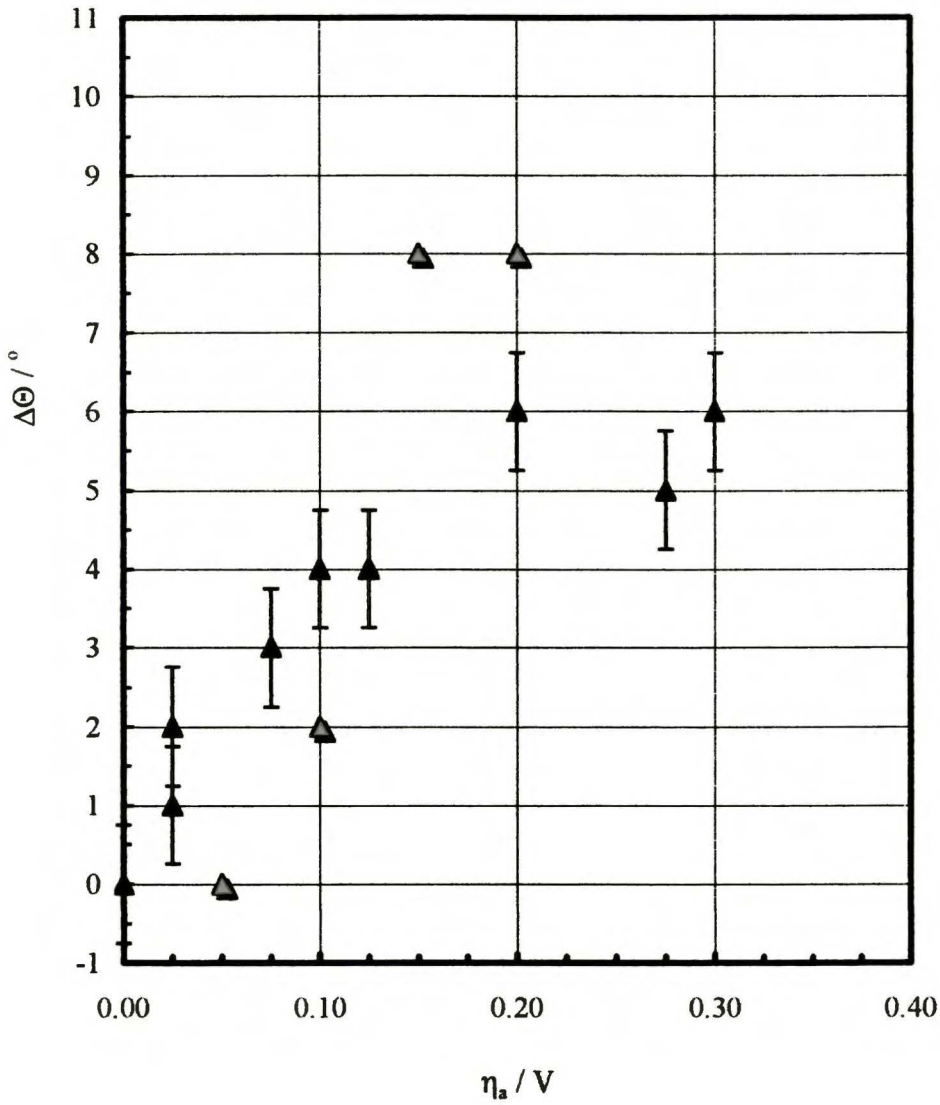

Fig. 26. Contact angle increment ($\Delta\Theta$) as dependent on Ni electrode overpotential (η_a), for Li/K carbonates electrolyte, under 0.8 H_2 + 0.2 CO_2 atmosphere, at 650° C.
Grey triangles – values according to ref. 1.

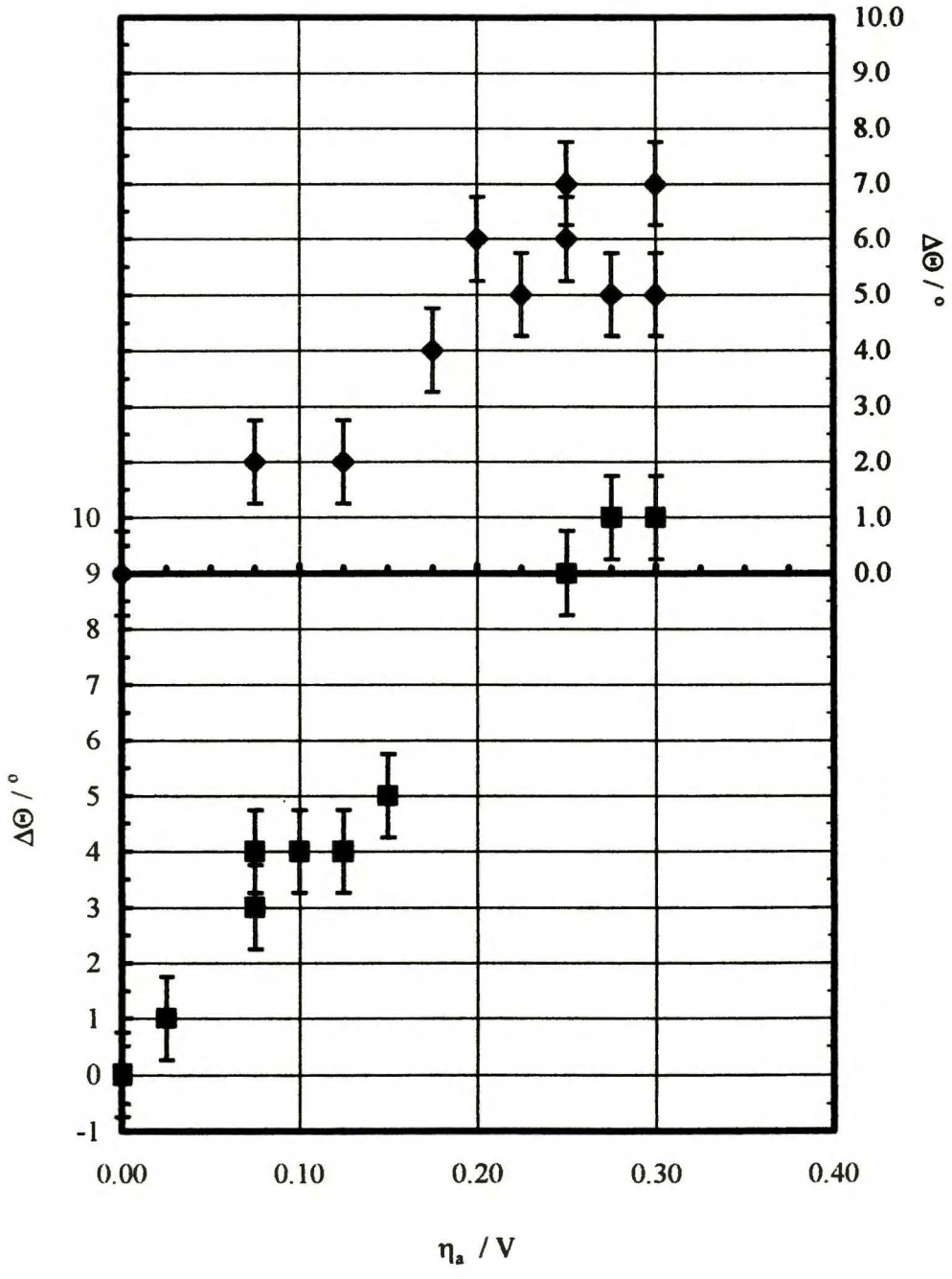

Fig. 27. Contact angle increment ($\Delta\Theta$) as dependent on Au electrode overpotential (η_a), under 0.8 H_2 + 0.2 CO_2 atmosphere, at 650° C. Upper diagram – Li/Na carbonates electrolyte; lower diagram – Li/Na/K carbonates electrolyte.

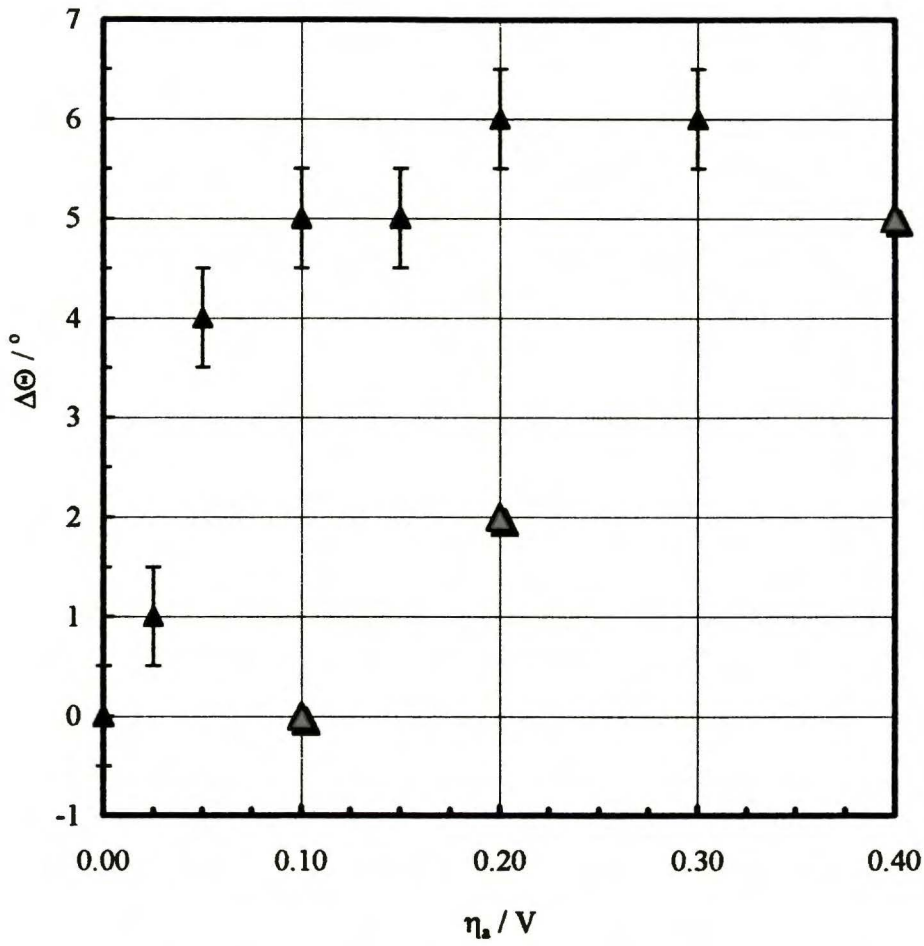

Fig. 28. Contact angle increment ($\Delta\Theta$) as dependent on Au electrode overpotential (η_a) for Li/K carbonates electrolyte, under 0.8 H_2 + 0.2 CO_2 atmosphere, at 650° C.
Grey triangles –values according to ref. 1.

From this study it results that in Li/Na carbonates the effect of anodic polarization of Ni is the lowest. Therefore it may be expected that in MCFC this electrolyte would show the more stable behavior in the porous structure of the Ni anode under cell operating conditions. This CA values stability should be even better at lower temperature of 550° C than at the normal MCFC operation temperature of 650° C. The effects in Li/K and Li/Na/K carbonates are higher and similar each other. As it may be seen in Figs. 27 and 28, such a difference among the effects in three melts studied does not repeat for Au electrode, where the CA increment in Li/Na/K carbonates system is distinctly higher, than this for both Li/Na and Li/K eutectics.

Cathodic process The overall cathodic process in the alkali carbonate melts, (and, therefore, also in the MCFC) is

$$0.5\,O_2 + CO_2 + 2\,e \rightarrow CO_3^{2-} \qquad \text{(IX.2.3.3)}$$

All mechanisms of this process, discussed till now in the literature, consider the electrochemical ionization of O_2, dissolved in the melt under the form of superoxide (O_2^-) and/or peroxide (O_2^{2-}) ions to oxide ion (O^{2-}), as it has been proposed for the first time by Appleby and Nicholson [9,10]. Establishing of the acid-base chemical equilibrium must follow this electrochemical process, according to the reaction

$$O^{2-} + CO_2 \leftrightarrow CO_3^{2-} \qquad \text{(IX.2.3.4)}$$

The oxygen ionization process takes place within the overpotential not exceeding –0.30 V values. At the cathode polarized to more negative potentials, other reactions occur, *e. g.* CO_2 direct reduction and solid carbon deposition at the electrode.

The lithiated NiO single crystal, semi-conducting electrode has its own ohmic resistance, which introduces a not negligible iR drop contribution to the measured overpotential values. Using the value of specific resistance for NiO single crystal with respective content of Li, reported by Austin *et al.* [12], the total resistance for the single crystal sample used in this investigation, has been evaluated equal 1.5 ohm. This is the maximum resistance corresponding to the crystal wetted by the melt only at its bottom surface. However, due to wetting of a fraction of the sample lateral faces, the potential distribution over the electrode, as well as the electrode *effective surface area* cannot be simply determined. Therefore, the effective electrode ohmic resistance is probably lower. For the same reason, the current density cannot be calculated using the measured current values. Nevertheless, at 650° C, *i. e.* at usual MCFC operation temperature, the electrode resistance correction may be evaluated at least semi-quantitatively.

In Figs. 29 – 32 there are presented the increments of CA values at NiO single crystal and at Au, under 0.33 O_2 + 0.67 CO_2 gas mixture, in three carbonate eutectics, at 650° C, respectively. For NiO single crystal, the overpotential values applied to this electrode have been corrected assuming its highest possible effective resistance value. As it results from the reported diagrams, (Figs. 29,30) the CA value - overpotential dependencies are practically independent of the electrolyte composition. It may be noted only that the maximum of the respective electrocapillary curves corresponds to the effective overpotential value of –0.3 V in three different melts.

At Au, data obtained by Selman *et al.* for Li/K carbonates, under 0.33 O_2 + 0.67 CO_2 atmosphere [1,4], as well as by Kamping *et al.* using the Wilhelmy balance method in air [6,7], at

650° C, are also reported in Fig. 32. In this case, the discrepancies among the results obtained in various laboratories are evident. The main differences are in the overpotential values corresponding to the maximum of the electrocapillary curves determined by the research teams. According to the data obtained in this study, this maximum would be shifted towards more negative overpotential values, than it results from the investigations of the cited authors. However, also data reported by Kamping *et al.* considerably differ from those by Selman *et. al.*

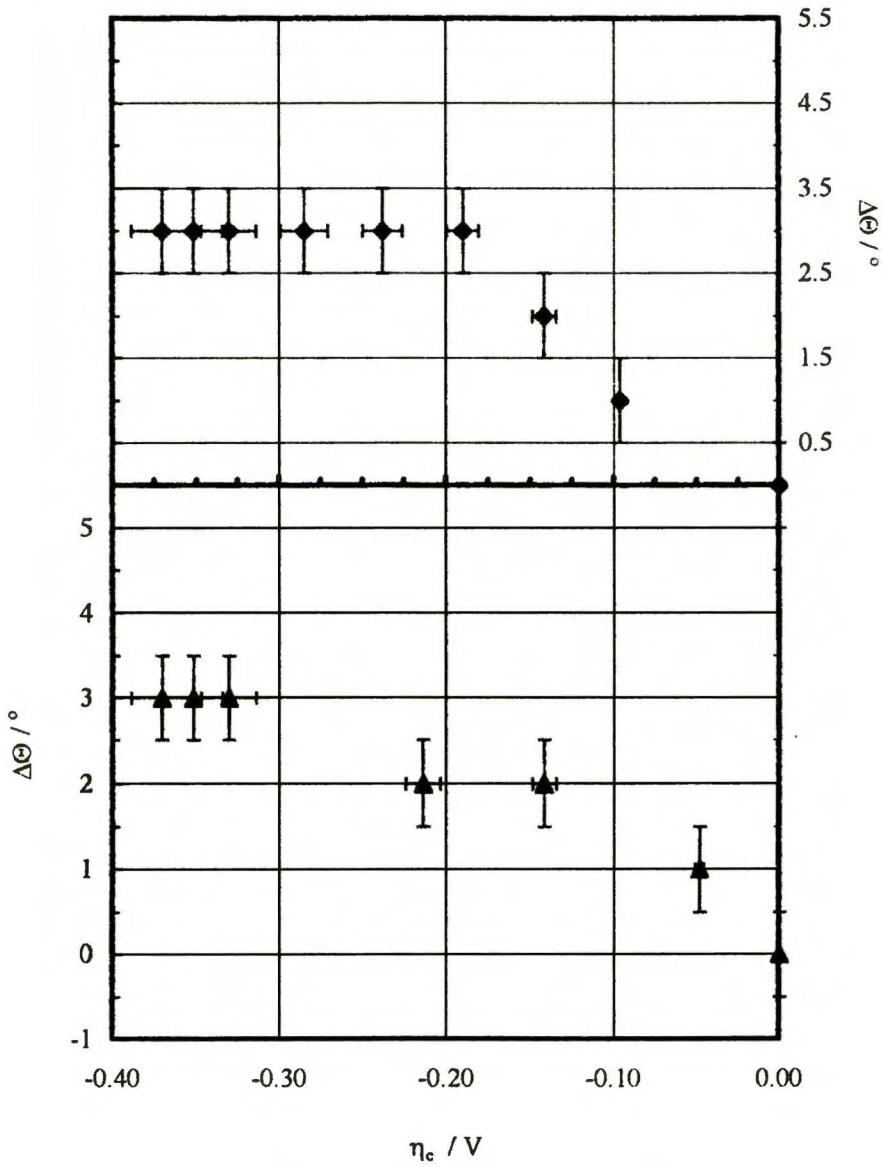

Fig. 29. Contact angle increment ($\Delta\Theta$) as dependent on lithiated NiO single crystal electrode overpotential (η_c), under 0.33 O_2 + 0.67 CO_2 atmosphere, at 650° C.
Upper diagram – Li/Na carbonates electrolyte; lower diagram – Li/K carbonates electrolyte.

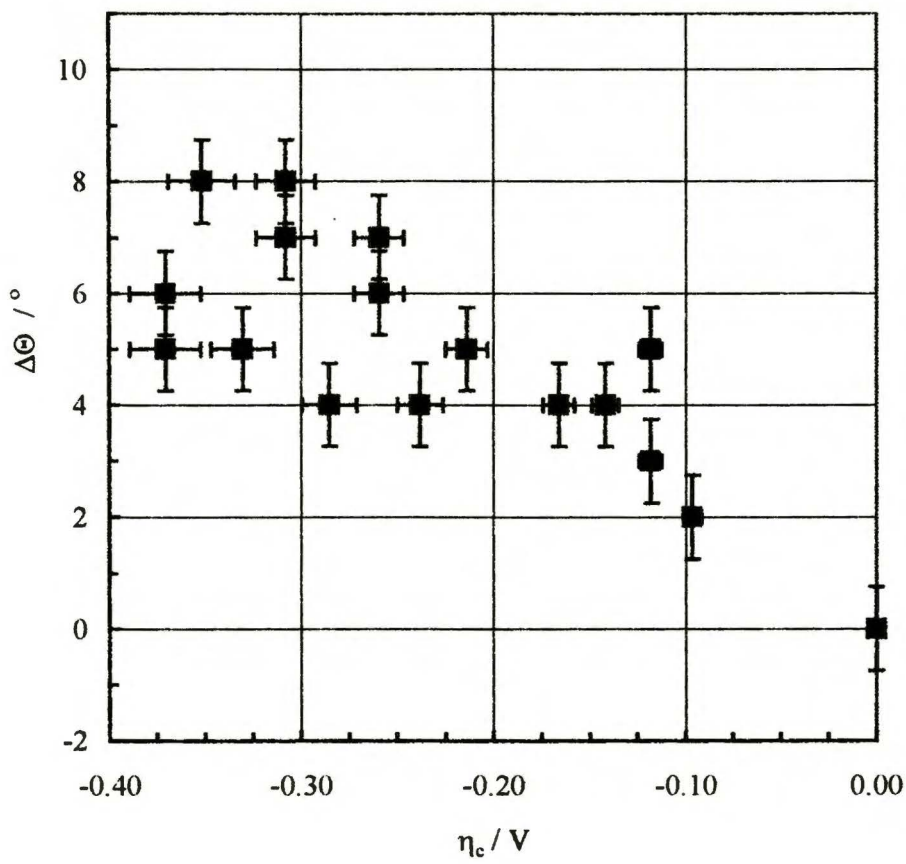

Fig. 30. Contact angle increment ($\Delta\Theta$) as dependent on lithiated NiO single crystal electrode overpotential (η_c), for Li/Na/K carbonates electrolyte, under 0.33 O_2 + 0.67 CO_2 atmosphere, at 650° C.

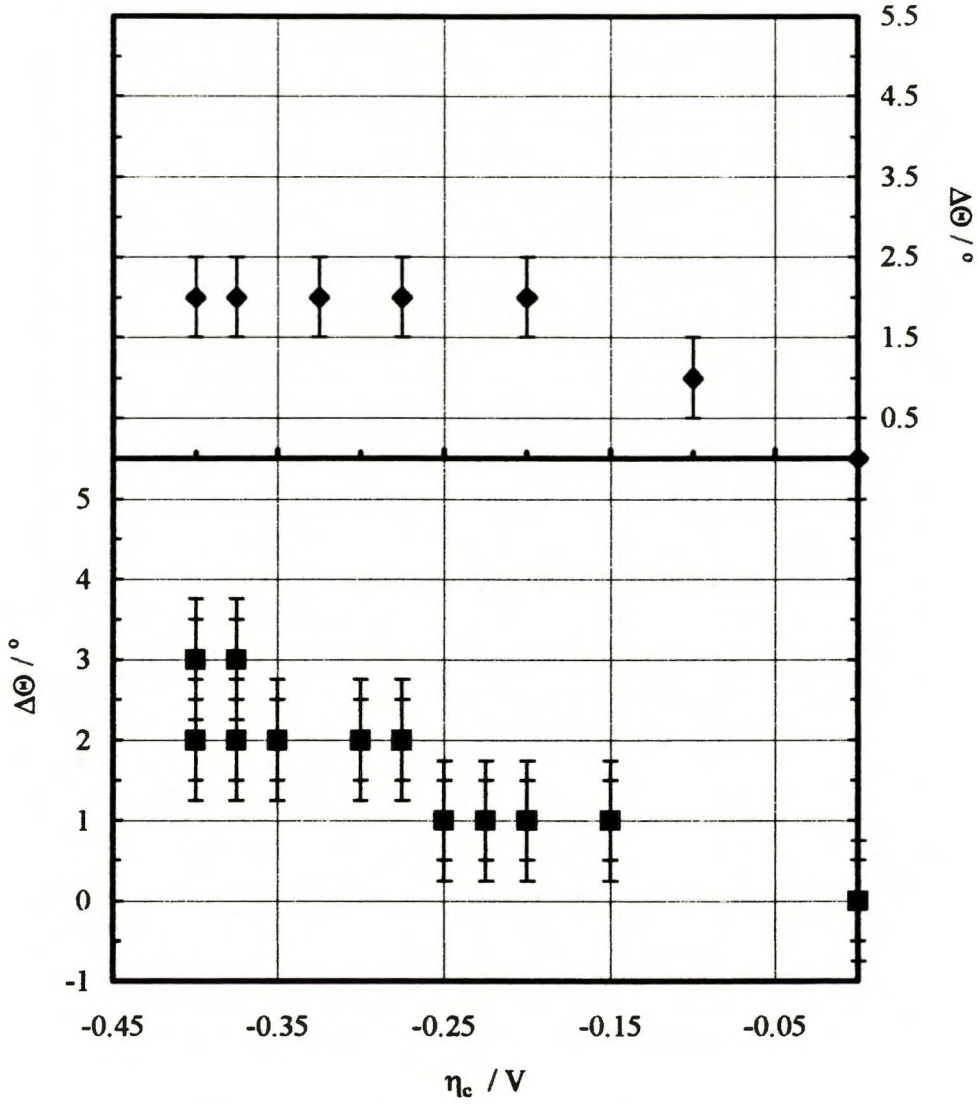

Fig. 31. Contact angle increment ($\Delta\Theta$) as dependent on Au electrode overpotential (η_c), under 0.33 O_2 + 0.67 CO_2 atmosphere, at 650° C. Upper diagram – Li/Na carbonates electrolyte; lower diagram – Li/Na/K carbonates electrolyte.

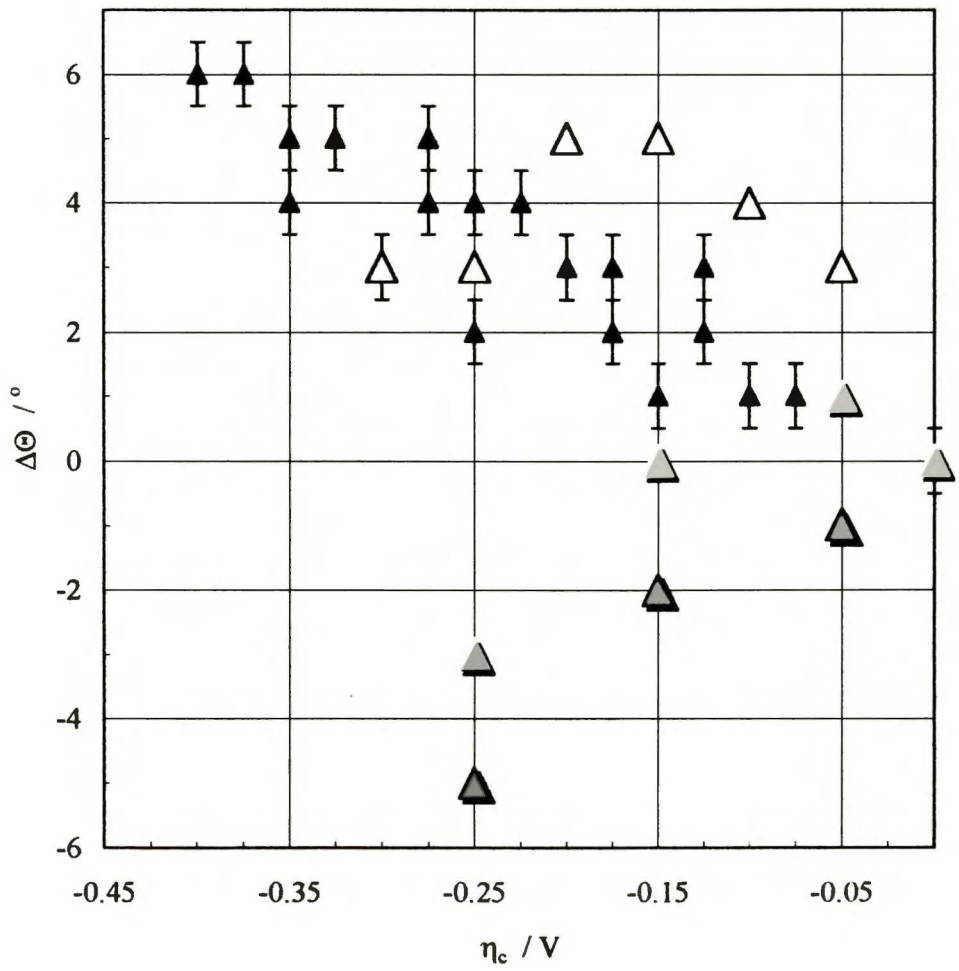

Fig. 32. Contact angle increment ($\Delta\Theta$) as dependent on Au electrode overpotential (η_c), for Li/K carbonates electrolyte, under 0.33 O_2 + 0.67 CO_2 atmosphere, at 650° C.
Empty triangles – values according to ref. 6,7; light grey triangles – values according to ref. 1; dark grey – values according to ref. 4.

Equilibrium of capillary forces in MCFC with various carbonate electrolytes. On base of results presented in both previous and present papers one can conclude about the electrocapillary equilibria in the fuel cells with alternative carbonate electrolytes. The value of the optimal ratio of anode to cathode pore size distribution for Li/K carbonate electrolyte at 650° C, is 0.6 as determined by Mugikura and Selman [1], very near to those applied in the state-of-the-art MCFC stacks. In our previous work it has been shown that CA at NiO surface have much higher values than 0°, as the above authors have assumed [2]. The values of this optimal ratio, when calculated on base of our results for three eutectic carbonate melts, are reported in Table 6.

Table 6. Optimal ratios of anodic to cathodic pore diameters calculated according to formula (IX.2.1.1) on base of CA values determined at OCP of MCFC electrodes (ref. [2]), as well as at anodic overpotential 0.2 V and cathodic overpotential –0.3 V (this study), for three eutectic carbonate melts, at temperatures of 550° and 650° C.

		$\cos\Theta$					
Carbonate eutectic melt		Li/Na		Li/K		Li/Na/K	
Temperature / ° C		550	650	550	650	550	650
Ni $0.8H_2+0.2\ CO_2$	OCP	0.88	0.93	0.94	0.96	0.93	0.96
	η_a = 0.2 V	0.88	0.90	0.94	0.90	0.93	0.89
NiO $0.33O_2+0.67CO_2$	OCP	0.92	0.93	0.87	0.90	0.89	0.92
	η_c = –0.3 V	0.92	0.89	0.87	0.85	0.89	0.83
d_a / d_c	OCP	0.95	1.00	1.08	1.03	1.04	1.04
	η_a = 0.2 V η_c = –0.3 V	0.95	1.01	1.08	1.05	1.04	1.07

At OCP (unloaded cell), the optimal ratios of anodic and cathodic pore diameters, reported in Table 6 for three different electrolytes, are very close to one, differently to those calculated by Mugikura and Selman for Li/K carbonate melt. The reason of these differences results from the different CA values for NiO considered in our and their investigations. For a cell with electrodes polarized as far as 0.2 V for the Ni anode and –0.3 V for the NiO cathode, the optimal pore diameters ratio would change for only few percent at 650° C. Under assumption that at 550° C, the overpotential influence on CA values is negligible. Therefore, also the optimal diameters ratio shows to be overpotential independent. This parameter calculated by Mugikura and Selman is only 20 percent higher than the one characterizing the state-of-the-art MCFC electrode, whereas these in three carbonate melts, reported in Table 6, are about twice (*ca* 100 percent) higher. Differences among three carbonate electrolytes are rather negligible.

The main conclusion resulting from the investigations at the surface of lithiated NiO single crystal is such the optimal ratio of anodic to cathodic pore diameters should be nearly one, not nearly 0.6, as it is admitted in *the state-of –the-art* MCFC stacks[1]. However, this conclusion would be correct only assuming the identity of wettability properties of smooth NiO

single crystals and NiO sintered powders. As yet, such an identity cannot be proved by carbonate melts contact angle investigations.

IX.2.4. Conclusions

(1) When using the CA values determined at the smooth NiO single crystal surface in three carbonate eutectic melts, one may conclude that the optimal ratio of mean pore size of MCFC porous anodes and cathodes should be nearly 1, not nearly 0.5 as it is admitted in the state-of-the-art MCFC electrodes. However, possible differences between smooth NiO surface and sintered NiO powder behavior must be taken into account.

(2) Assuming the CA values for the smooth NiO electrode as significant also to the NiO porous electrode, the above conclusion would have further consequence. Namely, as it results from the features of the cosine function, within the range of CA values for smooth NiO surface, the small effect of electrode overpotential does not change considerably this optimal ratio. It means, that in the loaded cell the depletion of electrolyte from one electrode to another should be not very significant.

(3) When the anodic overpotential is applied and hydrogen anodic oxidation occurs, the metallic nickel electrode shows the lowest increment of the CA value in Li/Na carbonates eutectic mixture, whereas in Li/K carbonates, - the highest one. At Au electrode, the effects at Li/Na and Li/K carbonates melts are very similar, but are higher in Li/Na/K carbonate eutectic.

(4) When the cathodic overpotential is applied and oxygen cathodic reduction occurs, the lithiated NiO single crystal electrode shows practically the same CA values increment in Li/Na and Li/K carbonate electrolytes. In Li/Na/K carbonate melt this effect is a little higher. At Au electrode the CA values increment is evidently higher in Li/K carbonate melt than in both other electrolytes.

IX.2.5. References

1. Y. Mugikura and J. R. Selman, *J. Electrochem. Soc.*, **143**, 2442 (1996).
2. L. Suski and A. Godula-Jopek, *J. Electrochem. Soc.*, (presented to publication).
3. J. R. Selman, *Wetting and oxidation of metals by molten carbonates*, Workshop on MCFC Stockholm – February 20-22, 1995, Kungl Tekniska Hogskolan, Stockholm, 1995.
4. M. Matsumura and J. R. Selman, *J. Electrochem. Soc.*, **139**, 1255 (1992).
5. Y. Mugikura and J. R. Selman, *Denki Kagaku*, **64**, 491 (1996).
6. H. Kamping, *Electrocapillary effect of gold in molten carbonate measured by Wilhelmy balance*, Delft University of Technology, Delft, 1994.
7. W. H. A. Peelen, K. Hemmes, H. Kamping, M. Bos and J. H. W. De Wit, *J. Solid State Electrochem.*, **2,** 334 (1998).
8. P. A. Kralchevsky and K. Nagayama, *Langmuir*, **10**, 23 (1994).
9. A. J. Appleby and S. B. Nicholson, *J. Electroanal. Chem.*, **53**, 105 (1974).
10. A. J. Appleby and S. B. Nicholson, *J. Electroanal. Chem.*, **83**, 309 (1977).
11. A. J. Appleby and S. B. Nicholson, *J. Electroanal. Chem.*, **112**, 71 (1980).
12. I. G. Austin, A. J. Springthorpe, B. A. Smith and C. E. Turner, *Proc. Phys. Soc.*, **90**, 157 (1967).

X. CONCLUDING REMARKS

In this work for the first time the contact angle values at the MCFC electrode materials (Ni and NiO)/molten carbonate interfaces have been measured in three eutectic systems, under both oxidizing and reducing atmospheres, from the melting point to 650°C (MCFC operating temperature). These parameters have been compared to the respective ones, measured on Au as reference material. The investigations embraces also the influence of the anodic and cathodic overpotential, applied to the solids under study.

Importance of the results obtained in this study consists first of all in the determination of the contact angle values at the NiO/molten alkali carbonate interfaces under oxidizing atmosphere using two forms of this compound, *i.e* NiO single crystal and NiO smooth, continuous layer deposited on Au by ion-sputtering method. Till now, a perfect wettability (0° of contact angle value) of this substance by molten carbonates was supposed in the literatureon basis of very doubtful experimental results.

Using the contact angle value data obtained in this investigation, the adhesion work parameters for Au/molten carbonate interfaces have been determined. Moreover, the optimal ratio of anodic to cathodic pore size values for porous MCFC electrodes have been calculated. As indicates from this study, the ratio should be nearly 1, not nearly 0.5 as it is admitted in the state- of- the-art MCFC devices. This results seems to be of essential importance for the development of these power sources.